

Philbrick

AFGL-TR-78-0195
AIR FORCE SURVEYS IN GEOPHYSICS, NO. 396



Atmospheric Properties From Measurements at Kwajalein Atoll on 5 April 1978

C. R. PHILBRICK
J. P. NOONAN
E. T. FLETCHER, Jr.
T. HANRAHAN
J. E. SALAH
D. W. BLOOD
R. O. OLSEN
B. W. KENNEDY

~~AD A057 743~~

AD-A061-083

11 August 1978

Approved for public release; distribution unlimited.

AERONOMY DIVISION PROJECT 627A
AIR FORCE GEOPHYSICS LABORATORY
HANSCOM AFB, MASSACHUSETTS 01731

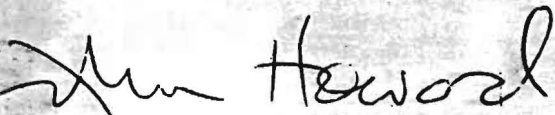
AIR FORCE SYSTEMS COMMAND, USAF



This report has been reviewed by the ESD Information Office (OI) and is releasable to the National Technical Information Service (NTIS).

This technical report has been reviewed and is approved for publication.

FOR THE COMMANDER

A handwritten signature in cursive script that reads "Jim Heword". The signature is written in dark ink and is positioned above a horizontal line.

Chief Scientist

Qualified requestors may obtain additional copies from the Defense Documentation Center. All others should apply to the National Technical Information Service.

Unclassified

SECURITY CLASSIFICATION OF THIS PAGE (When Data Entered)

REPORT DOCUMENTATION PAGE		READ INSTRUCTIONS BEFORE COMPLETING FORM
1. REPORT NUMBER AFGL-TR-78-0195	2. GOVT ACCESSION NO.	3. RECIPIENT'S CATALOG NUMBER
4. TITLE (and Subtitle) ATMOSPHERIC PROPERTIES FROM MEASUREMENTS AT KWAJALEIN ATOLL ON 5 APRIL 1978		5. TYPE OF REPORT & PERIOD COVERED Scientific. Interim.
		6. PERFORMING ORG. REPORT NUMBER AFSG No. 396
7. AUTHOR(s) C. R. Philbrick T. Hanrahan** R. O. Olsen† J. P. Noonan* J. E. Salah+ B. W. Kennedy† E. T. Fletcher, Jr. ** D. W. Blood+		8. CONTRACT OR GRANT NUMBER(s)
9. PERFORMING ORGANIZATION NAME AND ADDRESS Air Force Geophysics Laboratory (LKB) Hanscom AFB Massachusetts 01731		10. PROGRAM ELEMENT, PROJECT, TASK AREA & WORK UNIT NUMBERS Program Element 63311F Work Unit 627A5501
11. CONTROLLING OFFICE NAME AND ADDRESS Air Force Geophysics Laboratory (LKB) Hanscom AFB Massachusetts 01731		12. REPORT DATE 11 August 1978
		13. NUMBER OF PAGES 123
14. MONITORING AGENCY NAME & ADDRESS (If different from Controlling Office)		15. SECURITY CLASS. (of this report) Unclassified
		15a. DECLASSIFICATION/DOWNGRADING SCHEDULE
16. DISTRIBUTION STATEMENT (of this Report) Approved for public release; distribution unlimited.		
17. DISTRIBUTION STATEMENT (of the abstract entered in Block 20, if different from Report)		
18. SUPPLEMENTARY NOTES *RDP, Inc. **XONICS, Inc. +MIT Lincoln Laboratory †Army Atmos. Sciences Laboratory		
19. KEY WORDS (Continue on reverse side if necessary and identify by block number) Atmospheric density Atmospheric structure scales Atmospheric temperature Hypersonic sphere Atmospheric wind Mesosphere Lower thermosphere		
20. ABSTRACT (Continue on reverse side if necessary and identify by block number) Measurements of atmospheric density, temperature, and wind velocity were obtained in the altitude range from 0 to 130 km using several sensors flown during a six hour period on 5 April 1978 from Kwajalein Atoll. The results from rawinsonde, rocketsonde, robin sphere, accelerometer sphere, and hypersonic sphere techniques were analyzed and the error sources associated with each technique were investigated. The measurements have been used together with a study of atmospheric variability to calculate a "best profile" for each of		

Unclassified

SECURITY CLASSIFICATION OF THIS PAGE(When Data Entered)

20. Abstract (Continued)

the atmospheric parameters. A study of atmospheric scale sizes expected in the mesosphere was compared to the measurements and the vertical wavelengths measured were found in agreement with those predicted. These studies have also shown that regions of large atmospheric variability in the mesosphere are associated with turbulent, or unstable, layers based on the Richardson number stability criteria.

Unclassified

SECURITY CLASSIFICATION OF THIS PAGE(When Data Entered)

Preface

The authors acknowledge and appreciate the efforts of the several administrators, scientists, and engineers who have contributed to the gathering of the data and analysis of the results for the Density Measurements Program. These efforts have been in support of the SAMSO/ABRES program office, Maj. J. Christian, TREP Program Manager.

The discussions and comments of A. Cole, A. Kantor, S. P. Zimmerman, E. Murphy, K. S. W. Champion, A. C. Faire, R. Birch, J. Ellinwood, A. B. Bailey, and T. C. Lin are gratefully acknowledged. The computer programming support of N. Orrick, M. Hervey, J. D. de Clercq Zubli and B. J. Welch is acknowledged.

Contents

1. INTRODUCTION	9
2. MATHEMATICAL APPROACH	12
3. MEASUREMENTS AND ACCURACIES	15
3.1 Rawinsonde and Rocketsonde	16
3.2 Passive Spheres	17
3.3 Robin Spheres	22
3.4 Hypersonic Sphere	24
3.5 AFGL Accelerometer Sphere	28
4. BEST PROFILE RESULTS	32
REFERENCES	51
APPENDIX A: Derivation of Density "Best Profile" Estimates Equation	53
APPENDIX B: Summary of Sensor Measurements	59
APPENDIX C: Robin Sphere Analysis	101
APPENDIX D: Hypersonic Sphere Analysis	105

Illustrations

1.	Area Around Kwajalein Atoll Showing the Locations of the Measurements of Atmospheric Properties on 5 April 1978	10
2.	Estimates of Atmospheric Variability as a Function of Time	15
3.	Estimate of Rawinsonde and Rocketsonde RMS Errors From Cole ⁵	18
4.	Wavelengths of Propagating Modes Expected in the Mesosphere and Lower Thermosphere From a Reexamination of the Analysis of Hines ¹¹ With Inclusion of Eddy Viscosity Contribution	19
5.	Estimate of Standard Deviation Error for the Hypersonic Sphere, Accelerometer Instrumented Sphere and Robin Spheres	25
6a.	Drag Coefficient Versus Altitude for the Hypersonic Sphere With Error Estimates	26
6b.	Drag Coefficient Profiles for Various Reynolds Numbers as a Function of Mach Number From a Summary of Bailey ¹⁵ Using All Available Data	26
7a.	Ratio of Density Measured to the Model for the Hypersonic Sphere Data Analysis by XONICS and Lincoln Laboratory	29
7b.	Temperature Profiles Determined From the Density Profiles of Figure 7a	29
8a.	Hypersonic Sphere Density Results Compared to Model From the Lincoln Laboratory Analysis of the ALCOR Radar Data	30
8b.	Temperature Profile From Lincoln Laboratory Analysis of the Hypersonic Sphere Data	30
8c.	Comparison of the Temperature Measurements From Figure 8b to the Atmospheric Model in Order to See the Small Scale Structure in the Vertical Profile	31
9a.	Summary Plot From 0 to 130 km of all of the Density Measurements of 5 April 1978 Compared to the USSAS 1966 (15 ⁰ Annual) Model With the Calculated Best Profile Shown as a Line	34
9b.	Summary Plot From 0 to 130 km of all of the Temperature Measurements With "Best Profile" Line Shown	34
9c.	Summary Plot of all of the Wind Speed Measurements With "Best Profile" From 0 to 105 km	35
9d.	Summary Plot of Wind Azimuth Measurements With "Best Profile" Shown as the Line	35
10a.	Expanded Plot of the Density Data From all Sensors in the 50-100 km Range Compared to the Model	36
10b.	Expanded Plot of the Temperature Data From all Sensors in the 50-100 km Range	36
10c.	Expanded Plot of the Wind Speed Data From all Sensors in the 50-100 km Range	37
10d.	Expanded Plot of the Wind Azimuth Data From all Sensors in the 50-100 km Range	37
11a.	Density Measurements From Sensors Most Significant in Weighting the Best Profile are Shown as Ratio to Model Between 50 and 100 km	38

Illustrations

11b.	Temperature Measurements Corresponding to the Density Measurements of Figure 11a	38
11c.	Wind Speed Measurements From the Rocketsonde and the two Robin Spheres Launched 1 hr Before and 1 hr After the Reference Time	39
11d.	Wind Azimuth Corresponding to the Wind Speed Measurements of Figure 11c	39
12a.	"Best Profile" Density Ratio to the Model From the Analysis With Weights Dependent on Sensor Accuracy and Atmospheric Variability	49
12b.	"Best Profile" Temperature From Unweighted Average of all Data	49
12c.	"Best Profile" of Wind Speed From the Unweighted Average of the 2019A and 2021 Robin Spheres Above 40 km and all Measurements Below 40 km	50
12d.	"Best Profile" of Wind Azimuth Corresponding to Figure 12c	50
C1.	Comparison of the Density Measurements for the 2018 Robin From the XONICS and ASL Analysis	102
C2.	Comparison of the Temperature Measurements for the 2018 Robin From the XONICS and ASL Analysis	102
C3.	Comparison of the Wind Speed Measurements for the 2018 Robin From the XONICS and ASL Analysis	103
C4.	Comparison of the Wind Azimuth Measurements for the 2018 Robin From the XONICS and ASL Analysis	103
D1.	Comparison of the Hypersonic Sphere Determined Density to Model Atmosphere for the Three Cases of Drag Coefficient Presented in Figure 6a	107
D2.	Temperature Profiles From Analysis of the Hypersonic Sphere Data Corresponding to the Density Profiles of Figure D1	107

Tables

1.	Summary List of Atmospheric Measurements Obtained on 5 April 1978	10
2.	Estimates of Atmospheric Density Variation With Distance and Time* (See Figure 2)	14
3.	List of the Instrument Errors Assigned as a Function of Altitude	17
4.	Density Errors in Percent Associated With XONICS Processed Robin Sphere Data	23
5.	Density Errors in Percent Associated With Standard Robin Data Processing (ASL)	24
6.	Density Errors in Percent Associated With XONICS Processed Hypersonic Sphere Data	27

Tables

7. Density Errors in Percent Associated With Lincoln Laboratory Processed Hypersonic Sphere Data	28
8. Errors Associated With the Low Sensitivity Accelerometer Data Obtained on 5 April 1978	31
9. Experiment Weights Used in Calculating the Best Density Profile	40
10. "Best Profiles" of Density and From Analysis of Data Collected on 5 April 1978	43
11. "Best Profile" From Analysis of the Wind Speed and Azimuth Measurements on April 1978	46
B1. Rawinsonde R0022 at 0825 GMT	60
B2. Rawinsonde R0023 at 1240 GMT	62
B3. Rawinsonde K0129 at 1233 GMT	64
B4. Rocketsonde 2022A at 1429 GMT	66
B5. Robin Sphere (XONICS) 2018 at 0855 GMT From XONICS Analysis	70
B6. Robin Sphere (XONICS) 2019A at 1041 GMT From XONICS Analysis	76
B7. Robin Sphere (XONICS) 2021 at 1243 GMT From XONICS Analysis	81
B8. Robin Sphere (ASL) 2018 at 0855 GMT From ASL Analysis	87
B9. Robin Sphere (ASL) 2019A at 1041 GMT From ASL Analysis	88
B10. Robin Sphere (ASL) 2021 at 1243 GMT From ASL Analysis	89
B11. AFGL Accelerometer Sphere at 1226 GMT	90
B12. Hypersonic Sphere at 1142 GMT From MIT Lincoln Laboratory Analysis	95
D1. Drag Coefficient for Hypersonic Flow as a Function of Mach and Reynolds Numbers From Study of Bailey ³	106
D2. Calculated Parameters From Analysis of the Hypersonic Sphere Lincoln Laboratory Using the Drag Coefficient of Lin ¹ for $T_w/T_\infty = 3$	108
D3. The Hypersonic Sphere Results From XONICS Analysis Using the Bailey Drag Coefficient	114
D4. The Hypersonic Sphere Results From XONICS Analysis Using the Lin [$T_w/T_\infty = 3$]	118

Atmospheric Properties From Measurements at Kwajalein Atoll on 5 April 1978

1. INTRODUCTION

Several measurements of atmospheric properties were made on 5 April 1978 in the vicinity of Kwajalein Atoll to properly characterize the atmospheric conditions during the reentry of the SAMSO/ABRES sponsored TREP mission. In this report, a summary of the atmospheric measurements obtained is presented together with an analysis of the results combined into a single "best profile" of the atmospheric conditions appropriate to the reentry mission. The approach has been to perform a straightforward weighted average of the measurements by weighting each data set according to its RMS (or standard deviation) error and its proximity in time to the period of interest. Table 1 lists the measurements and pertinent information on data collected on 5 April 1978. In Figure 1, the locations of the atmospheric measurements in the vicinity of Kwajalein Atoll are shown. The measurement techniques used in obtaining the data included the standard rawinsonde (0 to 30 km) and rocketsonde (20 to 65 km) techniques which are presently in routine use for meteorological data collection. In addition, an accelerometer instrumented

(Received for publication 11 August 1978)

Table 1. Summary List of Atmospheric Measurements Obtained on 5 April 1978

Time (GMT)	I.D. Number *	Sensor	Data Interval (km)	Relative Time (min)
0825	R0022	Rawinsonde	0-32	T-197
0825	K0128	Rawinsonde	0-11	T-197
0855	2018	Robin Sphere	40-100	T-167
1041	2019A	Robin Sphere	40-100	T-61
1142		Hypersonic Sphere	50-120	T-0
1226	788A	AFGL Sphere	40-68	T+44
1233	K0129	Rawinsonde	0-29	T+51
1240	R0023	Rawinsonde	0-26	T+58
1243	2021	Robin Sphere	40-100	T+61
1429	2022A	Rocketsonde	20-67	T+167

*K and R denote release from Kwajalein or Roi-Namur respectively.

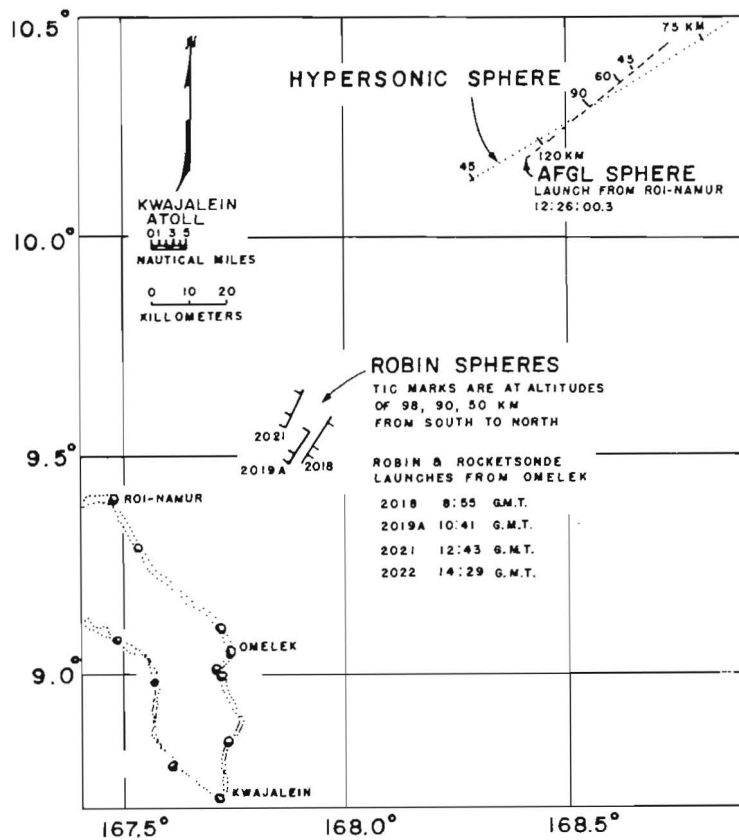


Figure 1. Area Around Kwajalein Atoll Showing the Locations of the Measurements of Atmospheric Properties on 5 April 1978 (see Table 1 for other details)

sphere,¹ several inflatable passive falling spheres (Robin spheres),^{*, 2, 3} and a hypersonic passive sphere,⁴ released from the reentry vehicle, were used to measure the atmospheric properties at higher altitudes, above 50 km. In each case attention has been given to assigning appropriate errors (standard deviations) to each data set as a function of altitude.

The primary attention has been given to determining the appropriate density profile. The temperature structure is less important and has been calculated as an unweighted average of the data sets; however, the same analysis which has been performed for the density profile could be applied. The other important parameter is the wind structure. Since the primary sensor providing this data in the 50 to 100 km region is the inflatable sphere, the result is the unweighted average profile obtained from Robin Sphere ID Numbers 2019A and 2021. These measurements were made at times ± 1 hr from the reentry and because of its smaller smoothing interval, the XONICS analysis was chosen.

The general approach to the density calculations has been performed in these complementary analyses. "Method 1" calculates a "best profile" using the data weighted only by the instrument errors. This approach has the inherent assumption that the measurements were all performed at the same time and place. "Method 2" calculates a "best profile" with weights determined from the instrument error and makes an estimate of the variability of the atmosphere based on the data collected at times relative to the reentry time. With such a small data base as obtained here, the results from this approach are not expected to be very significant but can provide some indication of the atmospheric variation for altitudes above 70 km where no statistical studies have been performed. In fact, this approach did provide information on atmospheric variability when applied to the TDV-1 data set which contained more measurements, but did not provide significant information when applied to the present data set. "Method 3" calculates a "best profile" using the weights from instrument errors and from the temporal variability determined

*The robin sphere results from two independent radar systems, ALCOR and TPQ-18, have been analyzed and will be referred to as XONICS and ASL data analysis respectively.

1. Philbrick, C.R., Faire, A.C., and Fryklund, D.H. (1978) AFGL-TR-78-0058, Measurements of Atmospheric Density.
2. Olsen, R.O. and Kennedy, B.W. (1977) ASL-TR-0005, ABRES Pretest Atmospheric Measurements.
3. Martin, L. and Azzarelli, T. (1977) XONICS Report, Wind and Density Measurements on Four Robin Spheres.
4. Salah, J.E. (1967) J. Geophys. Res. 72:5389.

by Cole,⁵ and Cole and Kantor⁶ from 0 to 70 km. Above 70 km, the temporal variability is estimated using the results of "Method 2" applied to the TDV-1 program data^{1, 7, 8} together with the Cole table to extrapolate the variation to higher altitude regions. Specifically, above 70 km the table is extrapolated by the ratio of the environment σ estimates obtained from "Method 2." If no estimate is available the next two lower altitude entries in the table are used for extrapolation, but no extrapolation was necessary in the case of the TDV-1 data set. While both of the first two methods provide some insight to the problem, it is "Method 3" which is used to perform the analysis finally reported as the "best profile." The distance variability would normally be expected to be less than the variation with time when comparing distances of a few hundred kilometers to time periods of hours. The average variation with distance was taken from the study of Cole⁵ for altitudes between 0 and 70 km. Above these altitudes, the spatial variability was extrapolated by comparison to the temporal variation. For altitudes below 70 km, the effect of 400 km in distance was found to be approximately the same as 1 hr of time. This model for temporal and spatial variability, although somewhat crude, allows the data to be weighted for time and space differences.

2. MATHEMATICAL APPROACH

Estimators can be chosen to be the minimum variance unbiased estimates under the assumption that the data are of a form,

$$X_i = \mu + \epsilon_i \quad (1)$$

where X_i is the measured value, μ is the desired parameter, and ϵ_i is the random noise with a zero mean and a standard deviation σ_i . The estimator equation is,

$$\hat{\mu} = \bar{X} = \sum_{i=1}^N \omega_i X_i \quad (2)$$

5. Cole, A.E. (1977) Private communication of unpublished report, Time and Space Variability of Density at Kwajalein.
6. Cole, A.E. and Kantor, A.J. (1975) AFCRL-TR-75-0527, Tropical Atmospheres, 0 to 90 km.
7. Fletcher, E.T., Jr. (1977) Private communication of Robin sphere results from the TDV-1 program.
8. Kennedy, B.W. and Hackerson, L.D. (1977) Private communication of unpublished ASL report, Analysis of Meteorological Data at Kwajalein Missile Range.

where $\hat{\mu}$ is the estimate of the true value of the parameter μ and ω_i are the weights. In the case of unweighted data, $\omega_i = 1/N$ and in the case of weighted data,

$$\omega_i = \frac{\frac{1}{\sigma_i^2}}{\sum_{j=1}^N \frac{1}{\sigma_j^2}} \quad (3)$$

and in all cases considered here the data is treated as unbiased, thus,

$$\sum_{i=1}^N \omega_i = 1 \quad (4)$$

The details of the derivation of the minimum variance weights are given in Appendix A (also, see for example Deutsch⁹).

"Method 1" calculates the best profile by setting σ_i equal to the instrument standard deviation at each altitude. All of the instruments errors assigned to the data sets are assumed to be randomly distributed, thus RMS errors are to be referred to as standard deviations.

"Method 2" includes both instrument effects and an "average environment" effect due to the separation in distance and time as,

$$\sigma_i^2 = (\sigma_{\text{Instrument}})^2 + (\sigma_{\text{Time/Distance}})^2 \quad (5)$$

The data for each instrument type was used to estimate an overall variance $(\sigma_{\text{Total}})^2$ and the $(\sigma_{\text{Instrument}})^2$ was subtracted from each of the calculations to estimate $(\sigma_{\text{Time/Distance}})^2$ for each instrument type. The averages of these variances were then used as an estimate of the "atmospheric variance" or average effect of the environment.

"Method 3" calculates a "best profile" from weights determined by the instrument effects together with an environment effect for each measurement. The environment effect is considered to be that due to time and distance changes from the study of Cole,⁵ see Table 2. The study of Cole⁵ only provides information up to 70 km, and above this altitude the results were extrapolated by comparison to the results of "Method 2" from the earlier TDV-1 data set in estimating the environment

9. Deutsch, R. (1965) Estimation Theory, Prentice-Hall, Inc., Englewood Cliffs, N.J.

Table 2. Estimates of Atmospheric Density Variation With Distance and Time*
 (See Figure 2)

ALT (km)	Distance [†]	Time (hours)			
		1	2	4	6
10	.13	0.2	0.2	<1	<1
20	.41	0.6	0.8	1.0	1.2
30	.47	0.7	1.0	1.4	1.8
40	.73	1.1	1.2	1.6	2.0
50	.85	1.8	1.9	3.0	4.3
60	1.2	1.9	2.1	3.0	4.0
70	1.3	1.9	2.1	3.2	4.0
80	1.6	2.8	3.1	4.7	5.9
90	1.9	3.8	4.2	6.3	7.9
100	2.5	5.0	5.5	8.4	10
110	2.7	5.3	5.8	8.9	11

*Values up to 70 km are based on study by Cole⁵ and above 70 are estimates based on analysis of a set of high altitude measurements extrapolated from the 70 km level.

†The separation distances for the rawinsonde releases and launches of the robin and rocketsonde are shown in Figure 1; these distances are of the order of 200 km. No distance effect was applied to the hypersonic or AFGL spheres.

effect, see Figure 2. These estimates of the environmental effects have been compared to several other data sets and appear to be reasonable estimates. One special point of interest was noted in these comparisons, however. In the altitude region between 60 to 100 km, the cases where the atmospheric variation was largest occurred about strong wind shear regions. At these altitudes, wind shear would be expected to be the principal destabilizing force. In regions of strong wind shear, several cases of large atmospheric variability with changes comparable to 2 and 3 times these σ 's were found in layers a few kilometers thick.

The analysis of each method was performed at 1 km height intervals using data from the region ± 500 m. The number of data samples used from each data set were chosen to reflect approximately the number of independent samples. The "best profile" is calculated for the time 1142 GMT and the atmospheric variability for the various measurements is referred to that time.

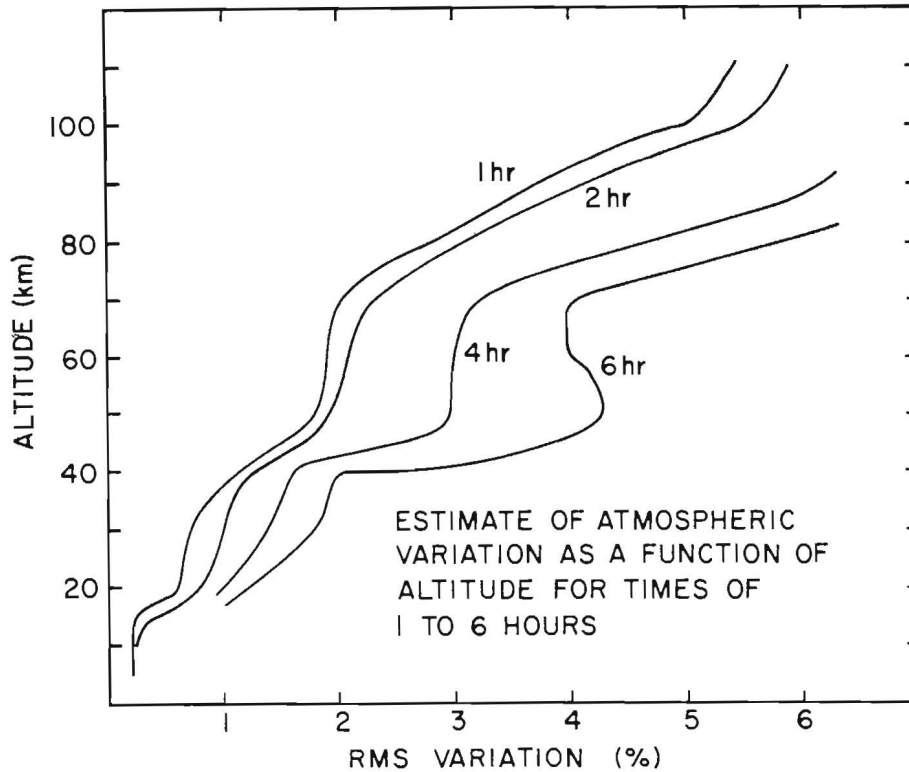


Figure 2. Estimates of Atmospheric Variability as a Function of Time. Values up to 70 km are from study of Cole⁵ and the higher altitude values are extrapolated based on the analysis of an earlier data set (see Table 2)

3. MEASUREMENTS AND ACCURACIES

One of the most important, yet most difficult, steps in any experiment is to assign the proper accuracy to the data. Frequently, a certain amount of judgment is involved because of lack of sufficient information to apply valid statistical determinations. Uncertainties have been applied to each of the measurements based on estimates of the various errors affecting each technique. The low altitude rawinsonde and rocketsonde have been studied statistically using a large data set.^{5, 6} The other techniques depend on measuring drag acceleration on a falling sphere and determining atmospheric density from the relation

$$\rho = \frac{2 a_D m}{v^2 C_D A} \quad (6)$$

where a_D is the drag acceleration of a sphere of mass, m , and cross section, A , which is moving at velocity, v . The drag coefficient, C_D , is determined from wind tunnel studies.¹⁰ The standard deviation of the density measurement is,

$$\sigma_\rho = \left[\sum_{j=1}^J \left(\frac{\partial \rho}{\partial X_j} \right)^2 \sigma_{X_j}^2 \right]^{1/2}$$

$$= \left[\sigma_{a_D}^2 + \sigma_m^2 + 4\sigma_v^2 + \sigma_{C_D}^2 + \sigma_A^2 \right]^{1/2} \quad (7)$$

Since the temperature profile from the sphere techniques is determined from integration of the density profile under the assumption of hydrostatic equilibrium and the ideal gas law,¹ the error will be related to that determined for the density profile. An additional error will be incurred near the top of the profile due to the initial assumption of a starting temperature.

3.1 Rawinsonde and Rocketsonde

The rawinsonde and rocketsonde techniques have been used for routine meteorological studies for many years. The instrument errors for the rawinsonde and rocketsonde measurements are taken from previous studies^{5, 6} and are listed in Table 3. The data used includes profiles from three rawinsondes, two of which were released from Roi-Namur (R0022 and R0023) and one released from Kwajalein (K0129). The earlier release from Kwajalein (K0128) only provided data to about 11 km and was not included in the analysis. Figure 3 shows the RMS error which has been taken to be the percent standard deviation of the measurement. The values below 30 km apply to the rawinsonde and above 30 km, near the tie-on point, the values apply to the rocketsonde data (2022). Since the rawinsonde provides a near continuous data output, the data, as provided, with samples approximately 300 m apart were used as independent samples. The rocketsonde data provides unique measurements with a resolution of only about 1.5 km and one sample per each kilometer interval was selected from the data set. The data obtained from the rawinsondes and rocketsonde are listed in Appendix B.

10. Bailey, A. B. and Hiatt, J. (1971) AEDC-TR-70-291, Free-Flight Measurements of Sphere Drag.

Table 3. List of the Instrument Errors Assigned as a Function of Altitude. The rawinsonde and rocketsonde are from study of Cole⁵ and the other instruments are discussed in the text (see Figure 5)

Alt. (km)	Rawinsonde	Rocketsonde	Robin (XONICS)	Robin (ASL)	Accelerometer (AFGL)	Hypersonic (XONICS)	Hypersonic (Lincoln Lab)
5	0.12						
10	0.20						
15	0.25						
20	0.30	0.30					
25	0.36	0.36					
30	0.42	0.42					
35		0.63					
40		1.0	3.5	5.0	2.5		
45		1.4	3.4	4.8	2.5		
50		1.6	3.5	5.1	2.5	3.2	3.0
55		1.7	3.6	5.1	2.6	3.2	3.0
60		1.8	3.7	5.4	3.0	3.2	3.0
65		2.2	3.1	5.5	3.7	3.2	3.0
70		3.0	3.3	6.5	5.0	3.2	3.0
75			3.5	6.5		3.2	3.5
80			3.7	6.3		4.1	4.0
85			4.4	6.2		5.1	5.0
90			6.2	10.7		7.1	7.0
95			8.8	22.0		7.1	7.1
100			16.6			7.1	7.1
105						7.3	7.1
110						6.8	7.1
115						9.9	9.6
120						13.6	12.1

3.2 Passive Spheres

The determination of density from the drag acceleration measured by radars requires some degree of smoothing to remove noise so that derivatives of position and velocity data can be obtained. Thus, the Robin and hypersonic sphere data have been subjected to filters that can affect the results when the bandpass of the filter is smaller than the scales of atmospheric variations. In order to estimate the magnitude of the effect, the minimum wavelength of atmospheric structure must be

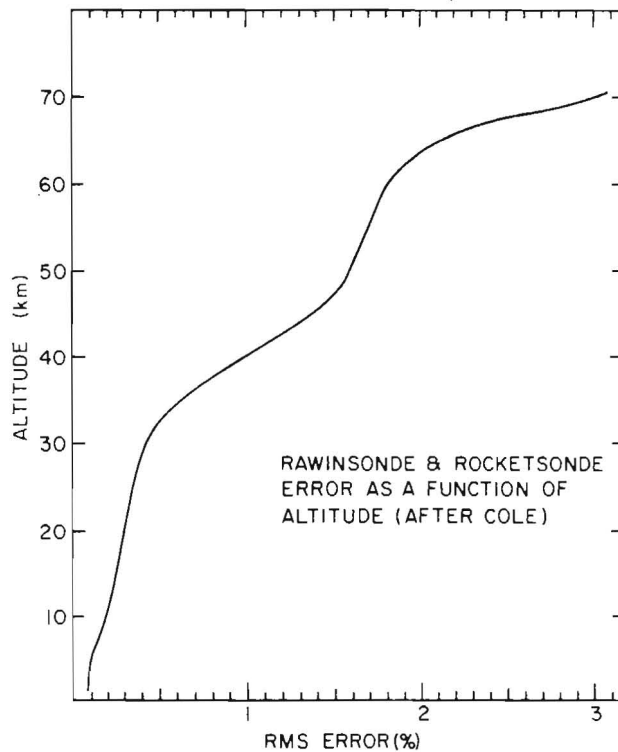


Figure 3. Estimate of Rawinsonde and Rocketsonde RMS Errors From Cole⁵ (see Table 3)

known. Our present knowledge of these scales is poor; however, it is possible to roughly estimate the vertical scales from the work of Hines.¹¹ Hines study indicates the wavelength for propagating modes which lie in the range between those long wavelengths that are reflected to the ground in the middle atmosphere, and those short wavelengths which are dissipated by viscosity. In the original work, only damping resulting from molecular viscosity was included. It is now known that eddy viscosity must also be considered, and following the suggestion of Hines in his later supplementary notes, a correction to his curves has been made for the present purposes. The eddy diffusion from the work of Zimmerman (Philbrick, et al¹²), was selected to correct the curves. With these considerations, the results in Figure 4, indicate that the range of significant minimum vertical

11. Hines, C.O. (1974) American Geophysical Union Monograph 18, The Upper Atmosphere in Motion.
12. Philbrick, C.R., Narcisi, R.S., Good, R.E., Hoffman, H.S., Keneshea, T.J., MacLeod, M.A., Zimmerman, S.P., and Reinisch, B.W. (1973) Space Research XIII, 441.

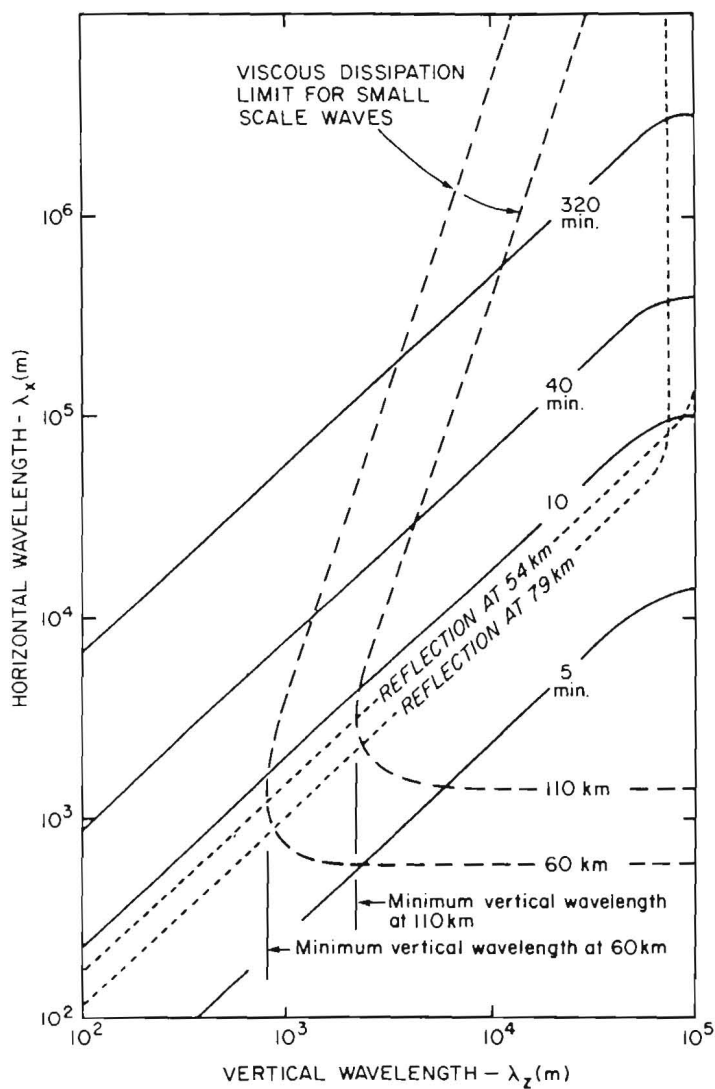


Figure 4. Wavelengths of Propagating Modes Expected in the Mesosphere and Lower Thermosphere From a Reexamination of the Analysis of Hines¹¹ With Inclusion of Eddy Viscosity Contribution. The periods in minutes are shown as constant period contours (solid lines). The viscous dissipation limit for small scale waves at 60 and 110 km are shown (dash lines) and represent the limits of the permitted spectrum from effects of viscous damping (modes lying to the left and below these curves are excluded). Modes subject to reflection back toward the ground at heights of 54 and 79 km are indicated (dot lines) and modes lying to the right of these curves cannot proceed from the lower atmosphere

wavelengths at 60 km altitude should lie between 1 and 4 km. At 110 km, the vertical scales probably range from 2.5 to 12 km. Since we are interested in the minimum scale size that may significantly affect the structure, the values of 1 km at 60 km and 2.5 km at 110 km are used with an assumed linear interpolation between. These wavelengths are then used to provide a basis of comparison to the filter scales of the various measurements. While this analysis was developed for gravity waves propagating from sources in the lower atmosphere, it is reasonable to expect that the dissipative forces would also be effective on acoustical waves. In general, acoustical waves would be expected to have much shorter wavelengths and would therefore require large energy input to produce significant density variations. Thus, it is reasonable to expect that the range of waves indicated in Figure 4 are the ones of concern for atmospheric variations in the mesosphere. The scale sizes indicated here are also in good agreement with the structure observed in the 90 to 110 km region from chemical trails studied by Zimmerman and Champion¹³ and Zimmerman and Rosenberg.¹⁴ There are obviously many other factors that should be included in a careful treatment. However, for the present purpose of roughly estimating atmospheric scales, this argument allows a basis for proceeding. As we will see later, the data indicate general agreement with this choice.

The smoothing of the radar data amounts to subjecting the measurements to a low pass filter, thus the standard deviation of the results should be increased to represent the noise at the input. The following argument shows that the standard deviation should be increased by a factor \sqrt{W} to account for the smoothing of the measurements. Basically, the idea is that the smoothing may be viewed as averaging a number of independent input samples to obtain one output sample. The standard deviation is thus decreased by the averaging (as the square root of the number of independent samples averaged). Furthermore, the number of independent input samples averaged is approximately given by the ratio of the filter input to output bandwidths (denoted W).

The argument that the standard deviation should be increased by \sqrt{W} may be demonstrated as follows: The input to the filter is a measurement taken at a given altitude h_i and may be represented as,

$$\hat{\rho}(h_i) = \hat{\rho}_i = \rho_i + \epsilon_i \quad (8)$$

13. Zimmerman, S. P. and Champion, K. S. W. (1963) J. Geophys. Res. 68:3049.

14. Zimmerman, S. P. and Rosenberg, N. W. (1972) Space Research XII, 623.

where ϵ_i is the random noise with a standard deviation equal to σ_i . The output is considered as a continuous analog measurement where the estimate $\hat{\rho}_i$ is a filtered value of the density as a function of altitude. Then,

$$\hat{\rho}_i = [\rho(h) + \epsilon(h)] * I R(h) \quad (9)$$

where * stands for the convolution integral, and

$$\hat{\rho}_i = \int_{h_1}^{h_2} I R(h_i - \tau) [\rho(\tau) + \epsilon(\tau)] d\tau \quad (10)$$

where $I R(h)$ is the impulse response of the filter. This integral may be approximated by an appropriate sum of samples of the input,

$$\hat{\rho}(h_i) \cong \sum_{\tau=h_1}^{h_2} [\rho(\tau) + \epsilon(\tau)] \Delta\tau \quad (11)$$

in steps of $h_2 - h_1 / \Delta\tau$, where $\Delta\tau$ and the number of points, $W = h_2 - h_1 / \Delta\tau$ depend on the filter bandwidth, $I R(h)$. That is, the filter may be viewed as approximately a running average of N input data points. Choosing the appropriate sum, the $\epsilon(\tau)$'s may be considered as approximately independent identically distributed random variables. In this case the standard deviation of $\hat{\rho}$ is $\sqrt{1/W}$ times the standard deviation of the input random variables $\epsilon(\tau)$. That is,

$$\sigma_{\hat{\rho}} = \sigma_I = \frac{\sigma}{\sqrt{W}} \quad (12)$$

Thus the measurement standard deviation σ should be estimated as,

$$\hat{\sigma} = \sqrt{W} \sigma_I \quad (13)$$

This relationship shows that the standard deviation at the input is increased by the effective bandwidth reduction caused by the filter. The Nyquist Theorem states, "A signal with bandwidth, BW , is determined by (and requires) $2 BW$ independent samples per second (to describe the signal uniquely)." A similarity theorem may be stated, "A filter generating a signal (at output) of bandwidth BF_F is essentially given by $2BF_F$ samples per second." Thus, approximately $2BW/2BF_F$ independent samples are averaged in the filter, and therefore

$$\begin{aligned}
 W &\cong \frac{BW}{BW_F} = \frac{\text{Input Bandwidth}}{\text{Filter Bandwidth}} \\
 &= \frac{\lambda(\text{Filter})}{\lambda(\text{Atmosphere})} \quad (14)
 \end{aligned}$$

Thus, we can now estimate the standard deviation associated with the density profiles which have been obtained from filtered radar observations.

3.3 Robin Spheres

The Robin spheres are 1 m diameter inflated spheres which are tracked by radars to determine the drag acceleration and wind velocity. The results from different analysis techniques using data from two independent radar systems are included in this study. One analysis (made by XONICS) uses the measurements from the ALCOR radar and the second analysis (made by ASL) uses the TPQ-18 radar data. The ASL analysis is the standard technique presently used for routine soundings (a revision of the technique described by Luers¹⁵). The smoothing interval used in the XONICS analysis is significantly smaller than that used by ASL, see Tables 4 and 5. The smaller smoothing interval used in processing the ALCOR data makes the error estimate significantly smaller than those of the TPQ-18 radar data, see Figure 5. The results from the Robin sphere analyses are listed in Appendix B. A comparison of the Robin sphere results from the ALCOR and TPQ 18 radar measurements is given in Appendix C.

Data sets were obtained for three Robin sphere flights, 2018, 2019A and 2021. The 2019A and 2021 flights were approximately 1 hr before and 1 hr after the reference time. The wind measurements were only obtained from the Robin spheres above 70 km and these measurements should also be more reliable than the rocket-sonde parachute measurements below this altitude. Therefore, the ALCOR radar data from the 2019A and 2021 Robins were used to determine the best wind profile above 40 km.

15. Luers, J. K. (1970) University of Dayton Contract Report, A Method for Computing Winds, Density, Temperature, Pressure and Their Associated Error from Robin Spheres.

Table 4. Density Errors in Percent Associated With XONICS Processed Robin Sphere Data

Alt. (km)	$\sigma(a_D)^1$	$\sigma(C_D)^2$	$\sigma(T_o)^3$	$\sigma(\text{Other})^4$	$\lambda(\text{Filter})^5$ (km)	$\lambda(\text{Atm})^6$ (km)	σ_ρ^7
40	1.0	3		1	1.0	0.4	3.5
45	1.0	3		1	1.0	0.6	3.4
50	1.1	3		1	1.2	0.7	3.5
55	1.2	3		1	1.5	0.8	3.6
60	1.3	3		1	2.4	1.0	3.7
65	1.4	2		1	3.0	1.2	3.1
70 ⁸	1.6	2		1	3.0	1.3	3.3
75	1.8	2		1	3.0	1.4	3.5
80	2.0	2		1	3.6	1.6	3.7
85	2.3	2		1	4.5	1.7	4.4
90	3.0	3	1	1	5.7	1.9	6.2
95	4.5	3	3	1	6.0	2.1	8.8
100	9.0	4	6	1	6.0	2.2	16.6

¹Error in determination of drag acceleration from XONICS estimates based on studies of radar simulations and residuals from several Robin sphere flights.

²Error in drag coefficient based on wind tunnel studies. ¹⁰ The increase at the higher altitudes is due to consideration of flow conditions at low Reynolds Numbers. The increase at lower altitudes is associated with possible errors in assigning drag coefficients in the Mach 0.5 range and possible effects associated with vertical motion.

³Error in drag coefficient due to errors in calculating Mach and Reynolds Numbers from temperatures near the top of density profile.

⁴General allowance for errors associated with mass, area, dynamical motion or wind.

⁵Filter wavelength in kilometers response estimated at 3 dB point from XONICS analysis.

⁶Estimate of minimum significant propagating wavelength in atmosphere.

$$\sigma_\rho = [(\sqrt{W} \times \sigma_{a_D})^2 + \sigma_{C_D}^2 + \sigma_T^2 + \sigma_o^2]^{1/2}, \quad W = \lambda_F / \lambda_A$$

⁸The error near 70 km may be 2 to 3 percent larger due to difficulty in assigning the proper drag coefficient near the Mach 1 transition.

179 27
Baker

*Weight acc
 determined by velocity error*

Table 5. Density Errors in Percent Associated With Standard Robin Data Processing (ASL)

Alt. (km)	$\sigma(a_D)^1$	$\sigma(\text{Bias})^1$	$\sigma(C_D)^2$	$\sigma(T_o)^2$	$\sigma(\text{Other})^2$	$\lambda(\text{Filter})^3$	$\lambda(\text{Atm})^2$	σ_ρ^4
40	2	-	3	-	1	1.5	.4	5.0
45	2	-	3	-	1	2.0	.6	4.8
50	2	-	3	-	1	2.8	.7	5.1
55	2	-	3	-	1	3.3	.8	5.1
60	2	1	3	-	1	3.8	1.0	5.4
65	2	1	2	-	1	6.0	1.2	5.5
70	2	1	2	-	1	9.8	1.3	6.5
75	2	1	2	-	1	10.5	1.4	6.5
80	2	1	2	-	1	11.0	1.6	6.3
85	2	1	2	-	1	11.2	1.7	6.2
90	4	1	3	1	1	11.5	1.9	10.7
95	8	1	3	3	1	15	2.1	22

¹Error in drag acceleration determination from radar data from study of Luers¹⁵.

²See notes on Table 4.

³Filter wavelength in kilometers at 3 dB point from study of Luers¹⁵.

$$\sigma_\rho^4 = \{[\sqrt{W} \times (\sigma_{a_D}^2 + \sigma_{BIAS}^2)^{1/2}]^2 + \sigma_{C_D}^2 + \sigma_T^2 + \sigma_o^2\}^{1/2}$$

3.4 Hypersonic Sphere

The hypersonic sphere data obtained by the ALCOR radar have been independently analyzed by XONICS and MIT Lincoln Laboratory. The data processing techniques are different but the results are very similar. The dominate error in this data is due to uncertainty in the drag coefficient. Profiles have been generated using three different determinations of drag coefficient. Drag coefficients from a study by Lin¹⁶ (with T_W/T_∞ of 1 and 3) and a recent summary by Bailey,¹⁷ have been used to generate density profiles, see Figures 6a and 6b and the material in Appendix D. In Tables 6 and 7 the error estimates for the XONICS and Lincoln Laboratory processing of the hypersonic sphere data are given. Over most of the

16. Lin, T.C. (1975) Private communication of unpublished AVCO report, Sphere-Drag in Rarefied Flow Regime.
 17. Bailey, A.B. (1978) Private communication of results of recent study of drag coefficients at high Mach numbers.

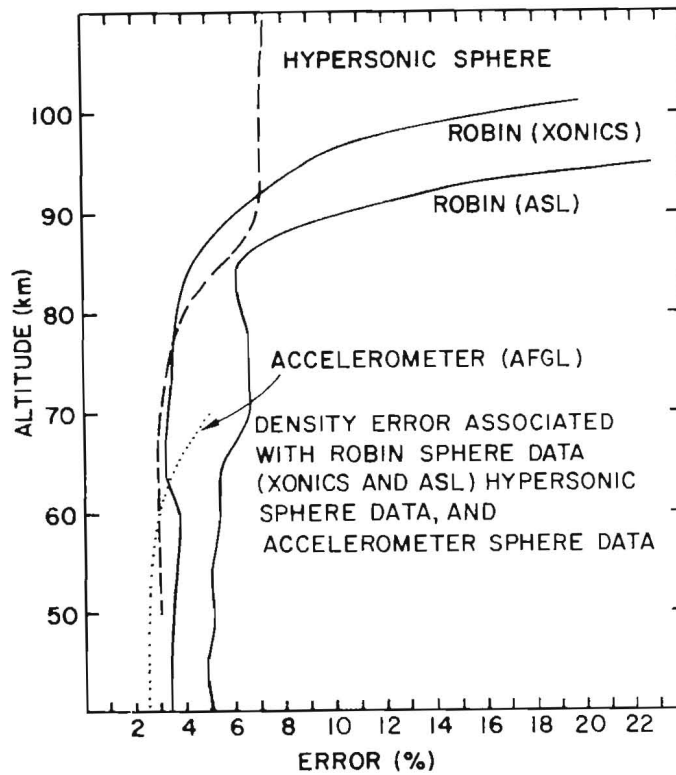


Figure 5. Estimate of Standard Deviation Error for the Hypersonic Sphere, Accelerometer Instrumented Sphere and Robin Spheres. The curve for the robin sphere labelled XONICS is from the ALCOR radar data and the curve labelled ASL is from the TPQ-18 radar data (see Tables 3 to 8)

altitude range the filter wavelength is comparable or smaller than the expected atmospheric wavelength, and no additional error due to the filter is assigned in these regions. The structure in the hypersonic sphere density profile, Figures 7a and 7b, and Figures 8a to 8c indicate that the argument made with regard to atmospheric wavelength scales may be quite reasonable. The structure is also similar to that observed in high resolution accelerometer data.¹

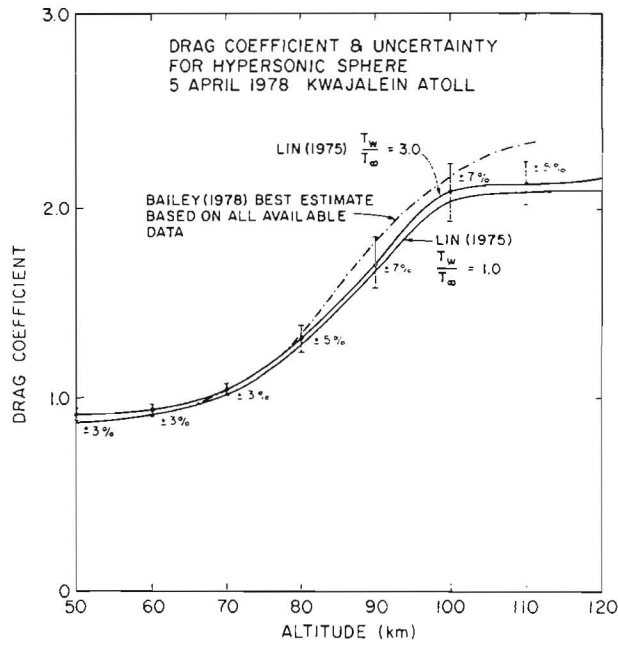


Figure 6a. Drag Coefficient Versus Altitude for the Hypersonic Sphere With Error Estimates. The three cases shown represent the conditions for the summary of Lin¹⁶ with wall to free-stream temperature ratios of 1 and 3 and for the best estimate summary of Bailey¹⁷

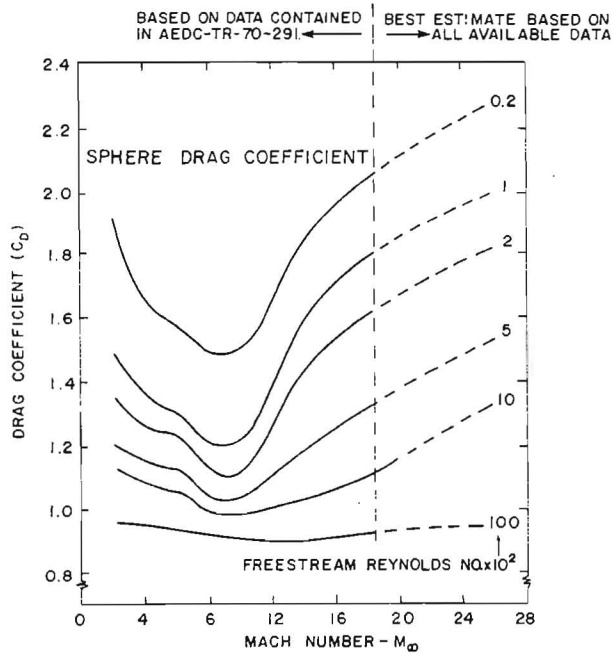


Figure 6b. Drag Coefficient Profiles for Various Reynolds Numbers as a Function of Mach Number From a Summary of Bailey¹⁵ Using all Available Data

1. D.
2. E.
be
lo
3. A.
M
4. T.
fo
5. σ
σ_β

Table 6. Density Errors in Percent Associated With XONICS Processed Hypersonic Sphere Data

Alt. (km)	$\sigma(a_D)^1$	$\sigma(C_D)^2$	$\sigma(\text{Other})^3$	$\lambda(\text{Filter})^4$ (km)	$\lambda(\text{Atm})^5$ (km)	σ_ρ^5
120	6.1	5	1	12	2.8	13.6
115	4.2	5	1	11	2.7	9.9
110	3.0	5	1	5.5	2.5	6.8
105	1.8	7	1	2.7	2.3	7.3
100	.96	7	1	2.2	2.2	7.1
95	.63	7	1	1.9	2.0	7.1
90	.48	7	1	1.2	1.8	7.1
85	.33	5	1	1.0	1.7	5.1
80	.22	4	1	.8	1.6	4.1
75	.15	3	1	.8	1.5	3.2
70	.10	3	1	.8	1.3	3.2
65	.09	3	1	.7	1.2	3.2
60	.08	3	1	.7	1.0	3.2
55	.08	3	1	.6	0.8	3.2
50	.08	3	1	.6	0.6	3.2

¹ Drag acceleration error based on analysis by XONICS.

² Estimate of drag coefficient error which is not well known for low Reynolds numbers. The values between 90-105 km have largest error due to uncertainties at low Reynolds Numbers.

³ At higher altitudes this number represents uncertainty in Reynolds number and Mach number. At lower altitudes there is an uncertainty due to surface heating.

⁴ The filter bandwidth is larger than the expected atmospheric scales, thus $W = 1$, for altitudes below 100.

⁵ $\sigma_\rho = \left[\sigma_{a_D}^2 + \sigma_{C_D}^2 + \sigma_o^2 \right]^{1/2}$ for altitudes less than 100 km.

$\sigma_\rho = \left[(\sqrt{W} \times \sigma_{a_D})^2 + \sigma_{C_D}^2 + \sigma_o^2 \right]^{1/2}$ for altitudes above 100 km.

Table 7. Density Errors in Percent Associated With Lincoln Laboratory Processed Hypersonic Sphere Data

Alt. (km)	$\sigma(a_D)^1$	$\sigma(C_D)^2$	$\sigma(\text{Other})$	$\lambda(\text{Filter})^2$ (km)	$\lambda(\text{Atm})^2$ (km)	σ_ρ
120	11	5	<1	4.2	2.8	12.1
110	5	5	<1	2.1	2.5	7.1
100	1	7	<1	2.1	2.2	7.1
90	.5	7	<1	2.1	1.8	7.0
80	.2	4	<1	1.0	1.6	4.0
70	.05	3	<1	<1	1.3	3.0
60	.03	3	<1	<1	1.0	3.0

¹ Drag acceleration error based on Lincoln Laboratory analysis.

² See Table 6 notes.

3.5 AFGL Accelerometer Sphere

The high sensitivity accelerometer did not provide high altitude data due to a pyrotechnique circuit failure, but low altitude data was obtained from a low sensitivity single axis accelerometer. The errors associated with the profile are given in Table 8. The large errors at the top of the profile are due to the quantization error of the data by the PCM encoder and the assignment of an estimated bias error. Since only one component of acceleration was available, the angle of the sphere spin axis in space was determined based on comparison to the other measurements at 60 km where the general agreement of all the profiles is good. With the position in space determined at one time, the complete profile can be generated.¹ Most of the same structural features are also observed in the hypersonic sphere and Robin sphere profiles.

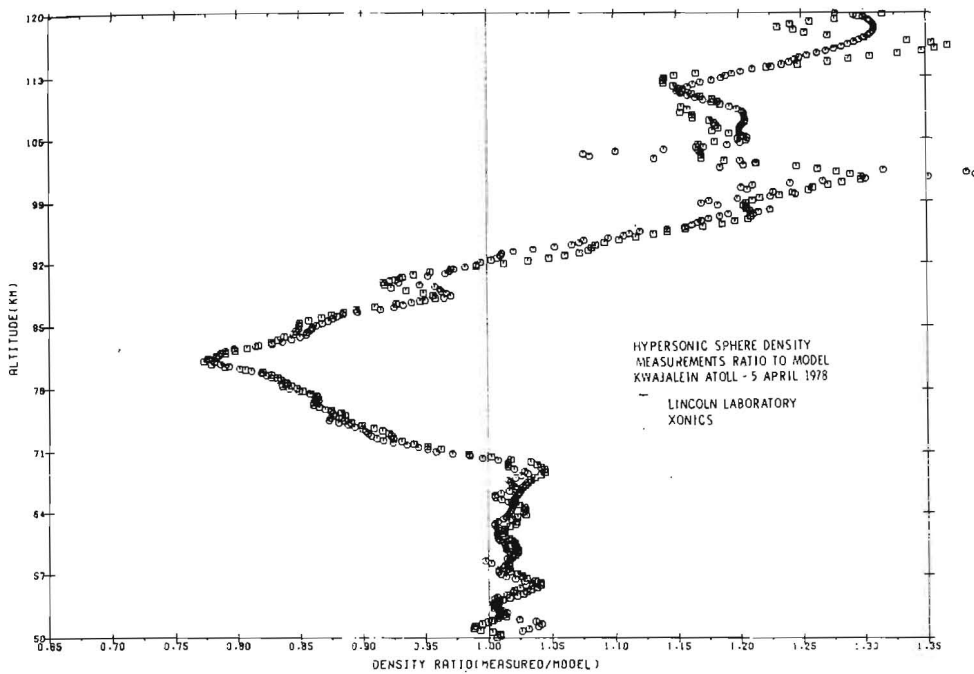


Figure 7a. Ratio of Density Measured to the Model for the Hypersonic Sphere Data Analysis by Xonics and Lincoln Laboratory

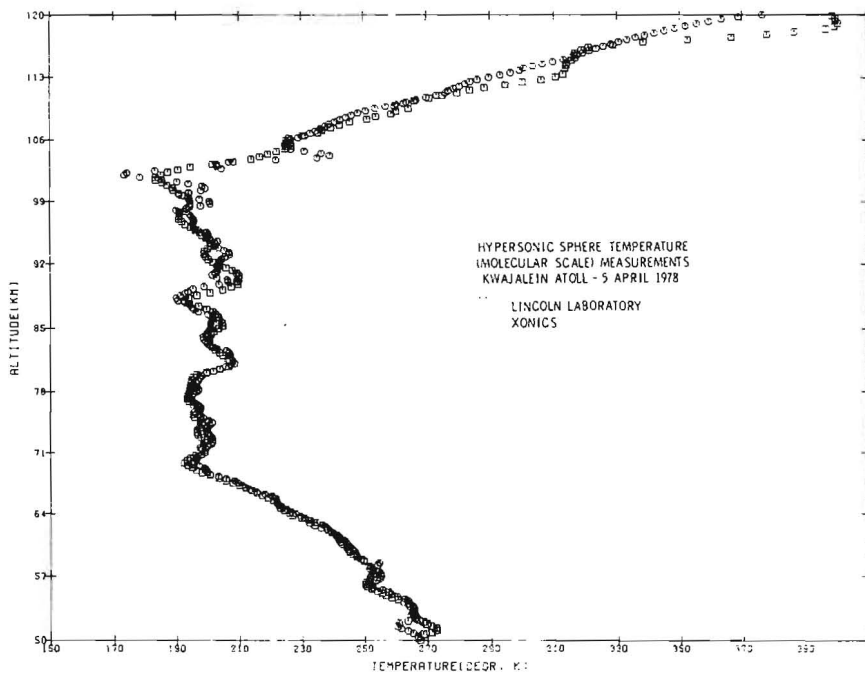


Figure 7b. Temperature Profiles Determined From the Density Profiles of Figure 7a

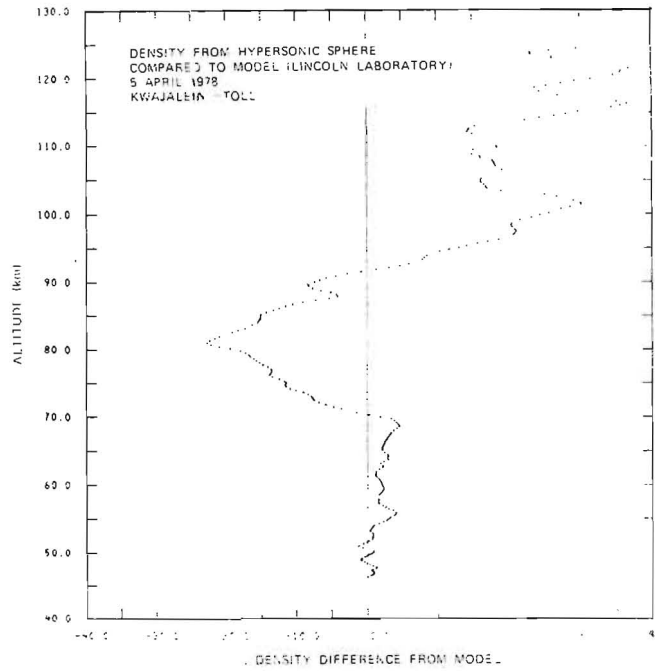


Figure 8a. Hypersonic Sphere Density Results Compared to Model From the Lincoln Laboratory Analysis of the ALCOR Radar Data. Note the scale sizes of the vertical structure compared to the scales expected based on arguments presented in the text

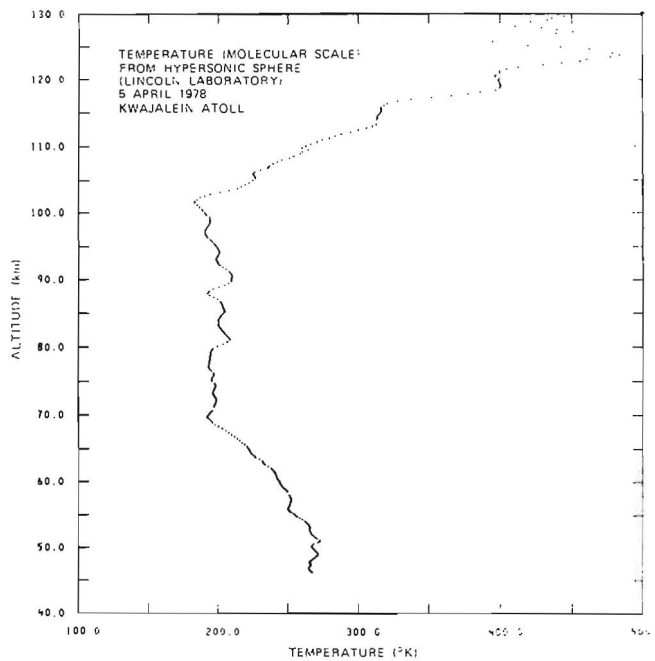


Figure 8b. Temperature Profile From Lincoln Laboratory Analysis of the Hypersonic Sphere Data

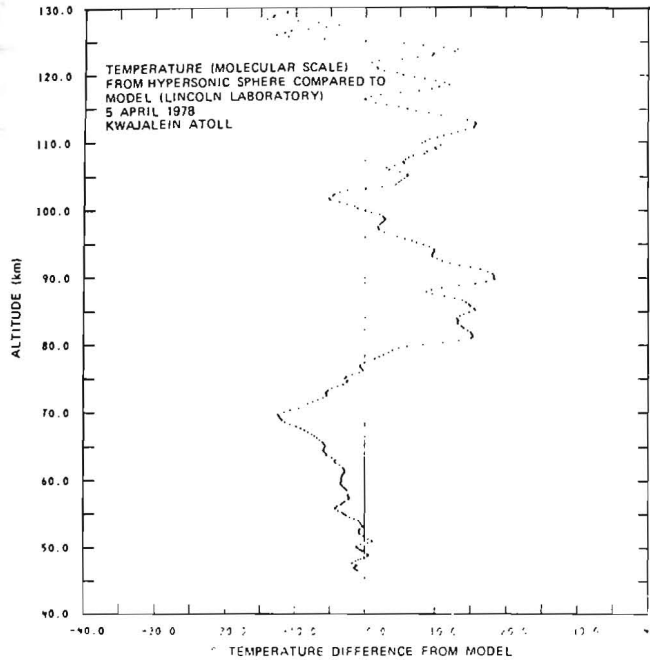


Figure 8c. Comparison of the Temperature Measurements From Figure 8b to the Atmospheric Model in Order to see the Small Scale Structure in the Vertical Profile

Table 8. Errors Associated With the Low Sensitivity Accelerometer Data Obtained on 5 April 1978

Altitude (km)	Bit Quantization and Bias Error (Percent)	Drag Coefficient Error (Percent)	Calibration Errors† (Percent)	Other Errors*‡ (Percent)	Total Error (Percent)
75	9.3	2.0	1.0	1.0	9.6
70	4.4	2.0	1.0	1.0	5.0
65	2.8	2.0	1.0	1.0	3.7
60	1.7	2.0	1.0	1.0	3.0
55	0.92	2.0	1.0	1.0	2.6
50	0.50	2.0	1.0	1.0	2.5
45	0.26	2.0	1.0	1.0	2.5
40	0.13	2.0	1.0	1.0	2.5

*The errors due to mass, area, velocity and position are $\ll 1$ percent.

†The standard deviation of calibration data was 0.4 percent and with other sources considered the absolute value error is estimated at 1 percent

‡The angle error of the mean spin axis is probably 1° and was selected based on a data comparison at 60 km. A 1° error would produce a density error just under 1 percent and the error due to C_g and C_p misalignment could add about 0.1 percent at the lower altitudes.

4. BEST PROFILE RESULTS

The individual profiles from the various sensors are plotted in Figures 9a to d and the data are listed in Appendix B. The listed data includes all points reported for each profile but the number of samples used in the analysis from each profile were chosen to approximate the sampling requirements based on the structure scales. The density measurements of Figure 9a are shown as a ratio to the model to allow the variations over the altitude range to be visualized. The model used for all comparisons in this report is the USSAS 1966 model corresponding to 15°N Annual (KMR standard). The temperature data shown in Figure 9b clearly indicates a split mesopause structure. The temperature profiles listed and plotted for the Robin spheres, accelerometer sphere, and hypersonic sphere are molecular scale temperatures from integration along the density profile. The molecular scale and gas kinetic temperatures are equivalent up to about 90 km and then differ as the mean molecular weight of the atmosphere changes. The molecular scale temperature, T_M , is related to the gas kinetic temperature, T , by

$$T_M = \frac{M_o}{M} T ,$$

where M_o is the ground level value of mean molecular weight. Several strong wind-shear regions are seen in the results of Figures 9c and d. The set of Figures 10a to d allow better detail to be seen in the profiles between 50 and 100 km. A brief study of the atmospheric stability has been made using the rocketsonde (2022) and both the ASL and Xonics analyses of Robin 2021. This examination followed the procedure outlined by Zimmerman and Murphy¹⁸ in determining the Richardson number from the wind and temperature data. The Richardson number is defined by the equation,

$$R_i = \frac{g}{T} \left(\frac{\partial T}{\partial Z} + \Gamma \right) \frac{1}{\left(\frac{\partial V}{\partial Z} \right)^2} \quad (15)$$

where g is the acceleration of gravity, Γ is the adiabatic lapse rate ($\sim 9.8^\circ\text{K}/\text{km}$), T is the atmospheric temperature, and V is the total wind speed. When used as a stability criteria, $R_i \leq 1/4$ is generally accepted as defining an unstable or turbulent region and for $R_i \leq 1$, instability is likely. The analysis indicates a strong turbulent

18. Zimmerman, S.P. and Murphy, E.A. (1977) Stratosphere and Mesospheric Turbulence, in Dynamical and Chemical Coupling Between the Neutral and Ionized Atmosphere, NATO Advanced Study Institute, D. Reidel Publishing Company.

layer in the region 72 to 78 km. The unstable condition in this region is primarily due to the strong wind shear, see Figures 10c and d. Several other regions indicate some instability, but none as strong. Examination of the density profiles indicates that this region (~75 km) also exhibits the strongest density variability. Comparison of the Robin sphere, hypersonic sphere and accelerometer sphere results in Figures 10 and 11 shows that many of the same structural features are found in each of the profiles. The analysis that was shown in Figure 4 would be consistent with this observation. The separation of the Robin and hypersonic sphere profiles was about 200 km. From Figure 4, horizontal scales of structural features of 100 to 1000 km with periods of an hour or more should be expected.

Because of the strong variability in the 75 km region, the two Robin sphere flights closest to the reference time were chosen for the analysis. The XONICS analysis was used because of the better resolution of the ALCOR radar. The hypersonic sphere profile from the Lincoln Laboratory analysis using the Lin ($T_w/T_\infty = 3$) drag coefficient was used for the calculation. In Figures 11a to d the measurements which will weight the calculation of the "best profile" in the 50 to 100 km region are shown.

As previously discussed, the results from "Method 3" which weights the data based on instrument error and atmospheric variability estimates are used for the "best profile." The weights calculated from the instrument error and the atmospheric variability are given in Table 9. The shift of profile weight from one instrument to another as a function of altitude can be followed in the table. The lines shown on Figures 9, 10 and 11 are the results from the analysis. The calculated profiles are shown in the important region from 50 to 100 km in Figures 12a to d and the results are listed in Tables 10 and 11. The density profile was calculated based on the weights of Table 9 and its standard deviation is determined from the instrument errors and atmospheric variability. The temperature profile is calculated from an unweighted average of the data and its standard deviation is that of the data set. Since the only instrument that measures between 32 and 38 km is the rocketsonde, no standard deviation can be obtained. An estimate of about 4°K is inserted into the table for this altitude region. In other regions of the profile no standard deviation is given. The wind speed and azimuth standard deviation are also calculated from the data sets. The best profile obtained here is probably the most accurate representation for the atmospheric properties that can be reasonably expected from this data set. The profile σ indicates that the density profile has a very high confidence (2 or 3 σ) of being better than 5 percent in the primary region of interest between 50 and 90 km.

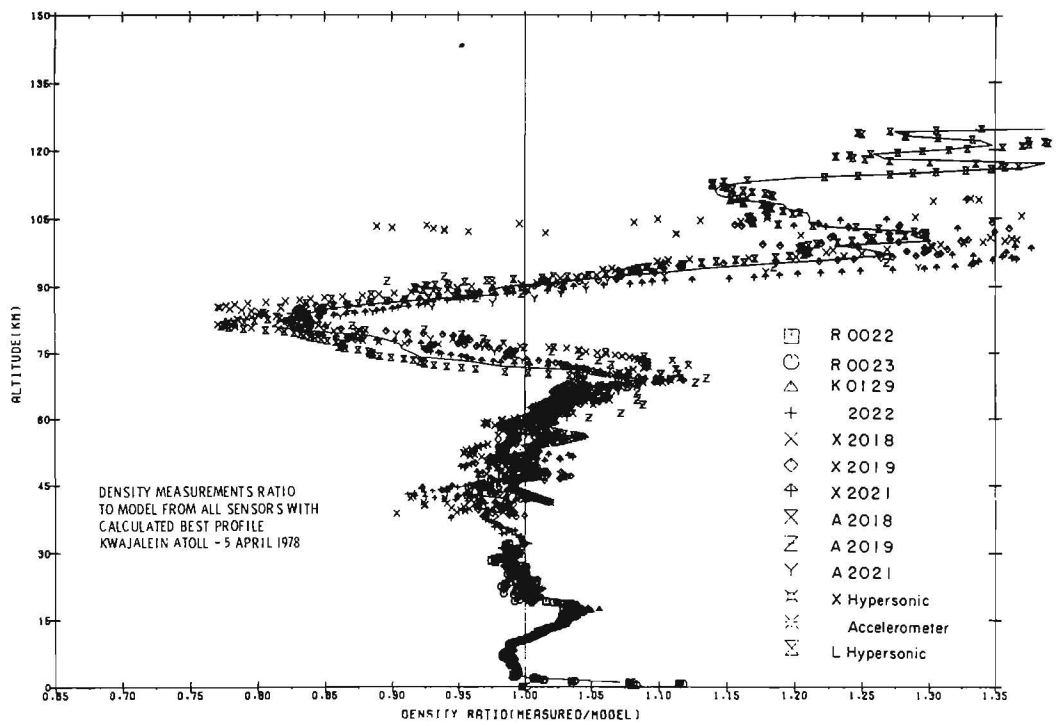


Figure 9a. Summary Plot From 0 to 130 km of all of the Density Measurements of 5 April 1978 Compared to the USSAS 1966 (15^o Annual) Model With the Calculated Best Profile Shown as a Line. The flight identification numbers are shown (see Table 1) and the X, A and L denote data processed by XONICS, ASL and Lincoln Laboratory, respectively

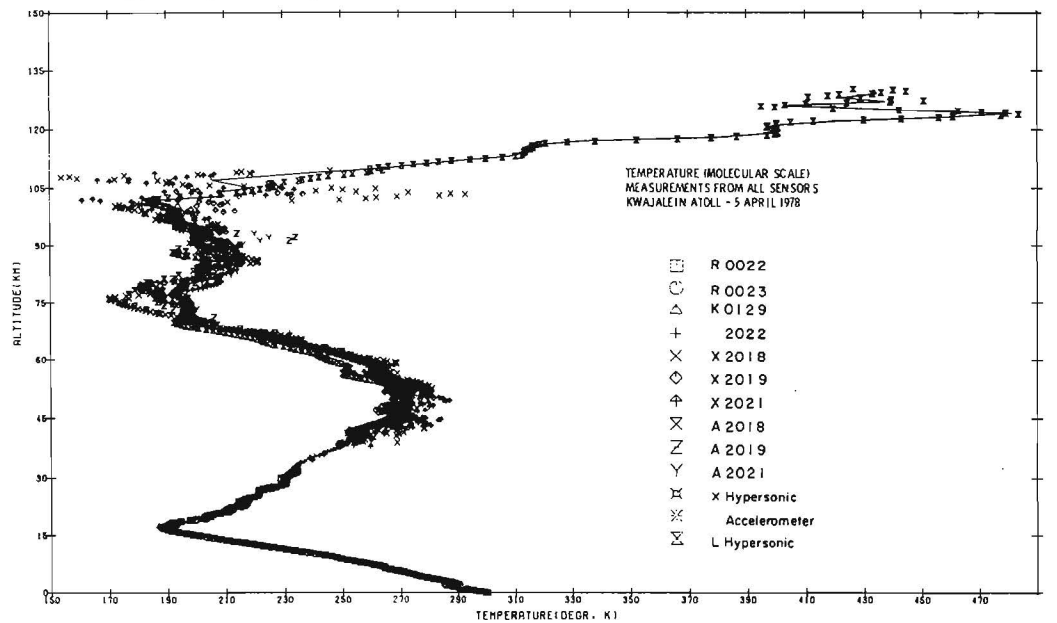


Figure 9b. Summary Plot From 0 to 130 km of all of the Temperature Measurements With "Best Profile" Line Shown

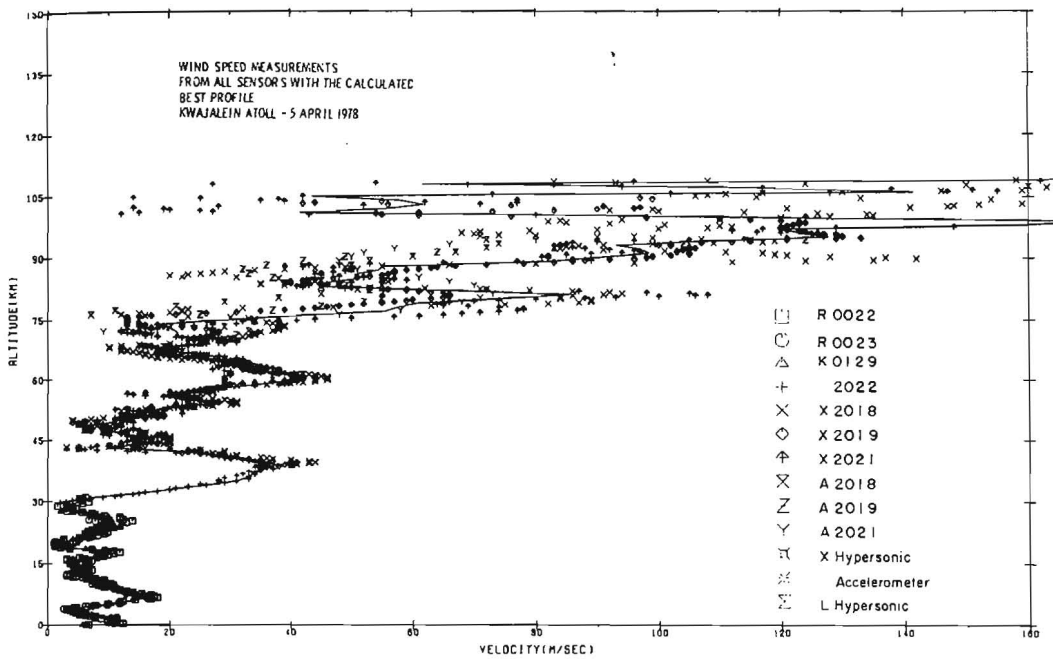


Figure 9c. Summary Plot of all of the Wind Speed Measurements With "Best Profile" From 0 to 105 km

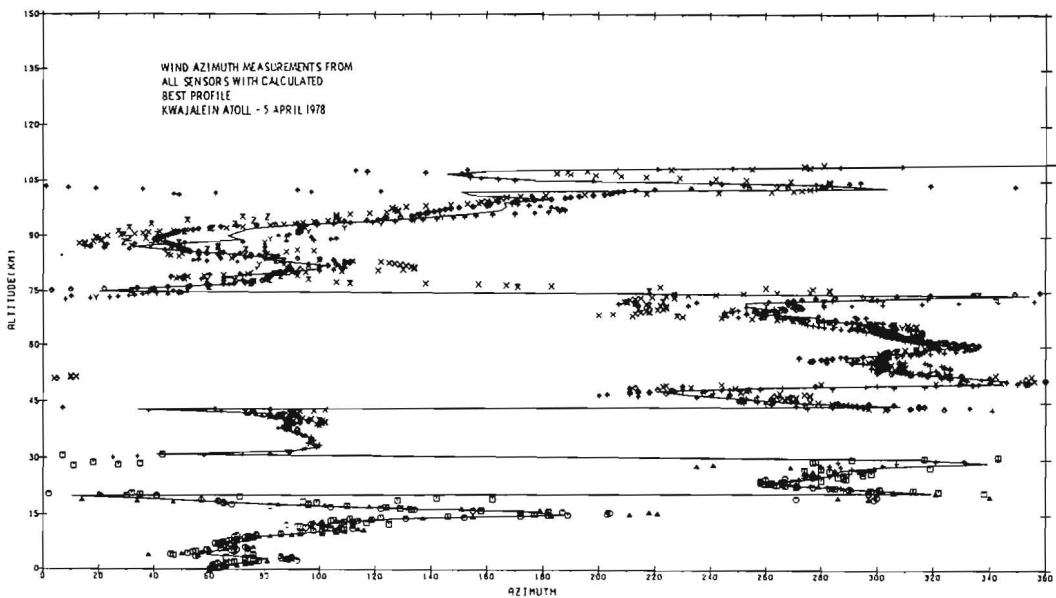


Figure 9d. Summary Plot of Wind Azimuth Measurements With "Best Profile" Shown as the Line

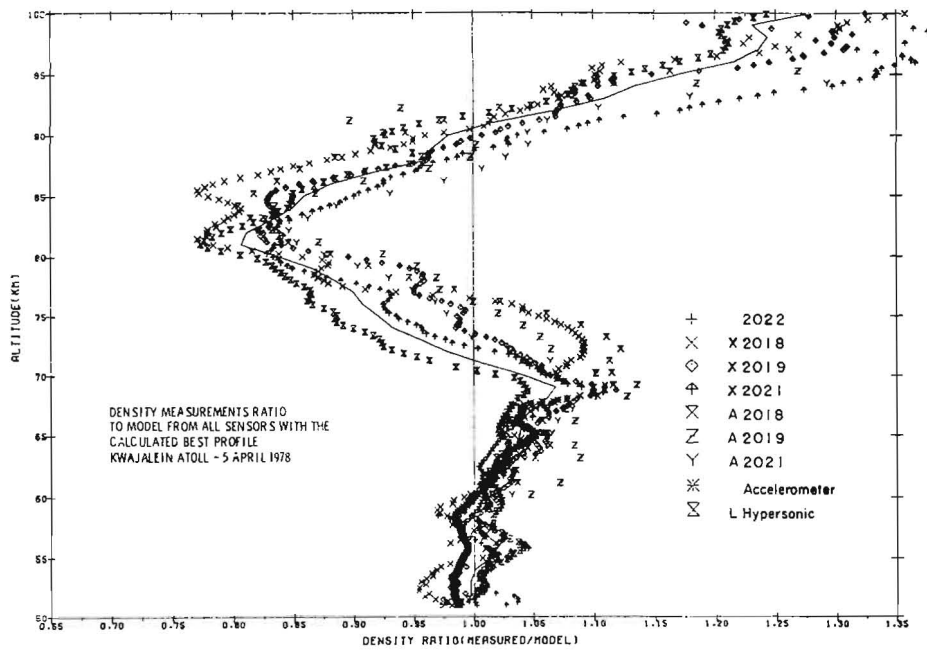


Figure 10a. Expanded Plot of the Density Data From all Sensors in the 50-100 km Range Compared to the Model

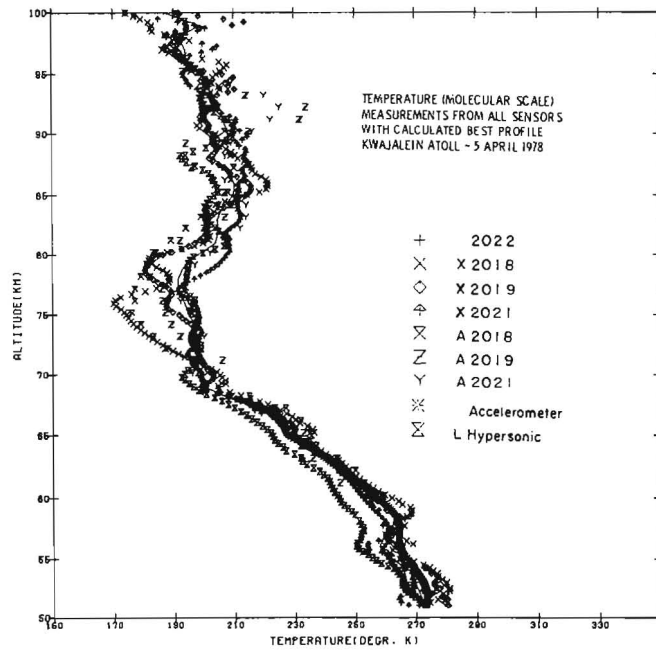


Figure 10b. Expanded Plot of the Temperature Data From all Sensors in the 50-100 km Range

Altitude (km)

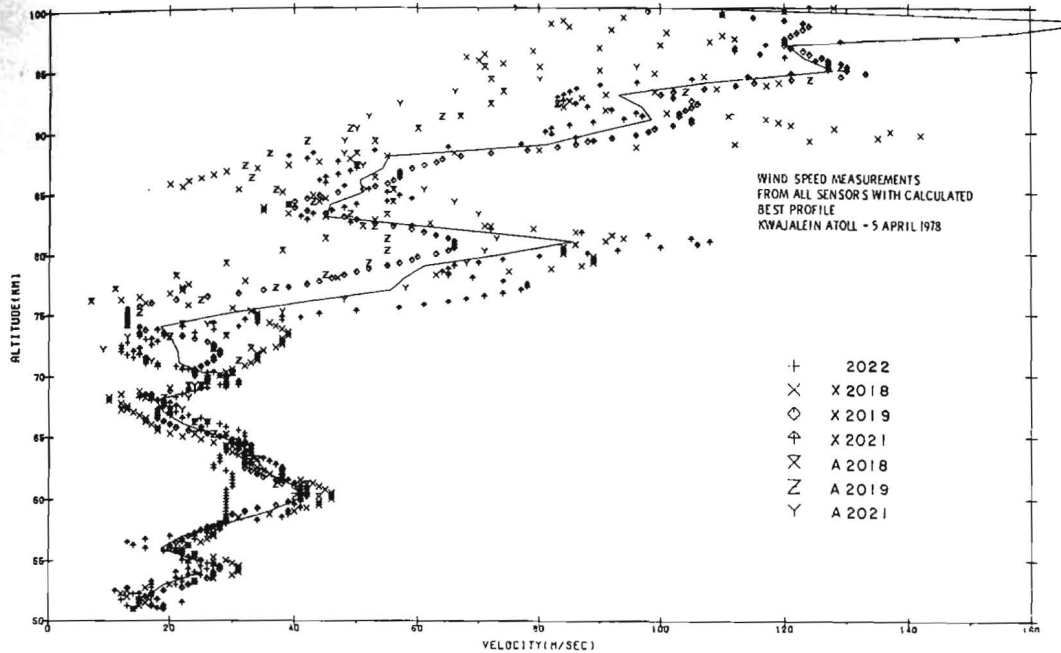


Figure 10c. Expanded Plot of the Wind Speed Data From all Sensors in the 50-100 km Range

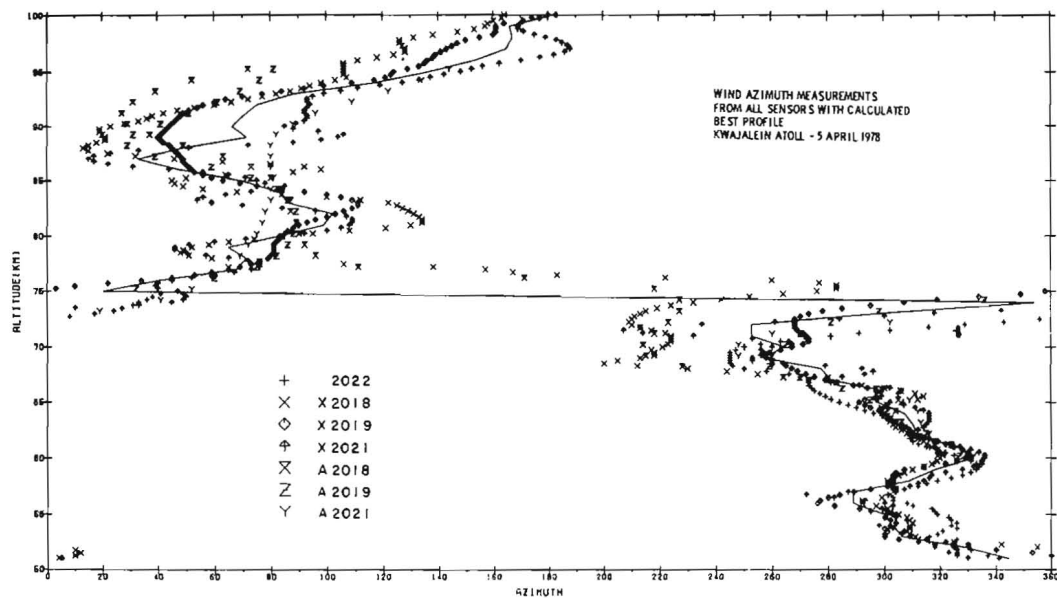


Figure 10d. Expanded Plot of the Wind Azimuth Data From all Sensors in the 50-100 km Range

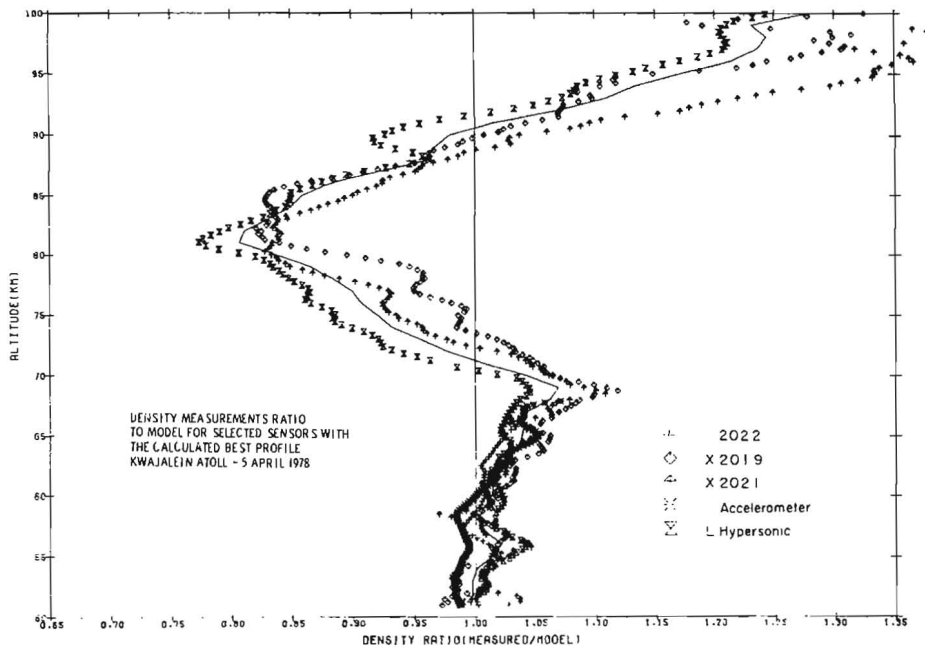


Figure 11a. Density Measurements From Sensors Most Significant in Weighting the Best Profile are Shown as Ratio to Model Between 50 and 100 km

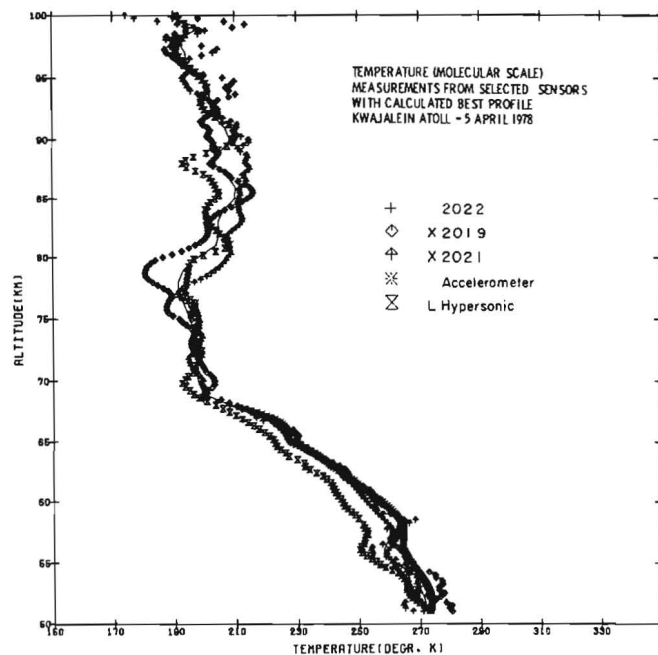


Figure 11b. Temperature Measurements Corresponding to the Density Measurements of Figure 11a

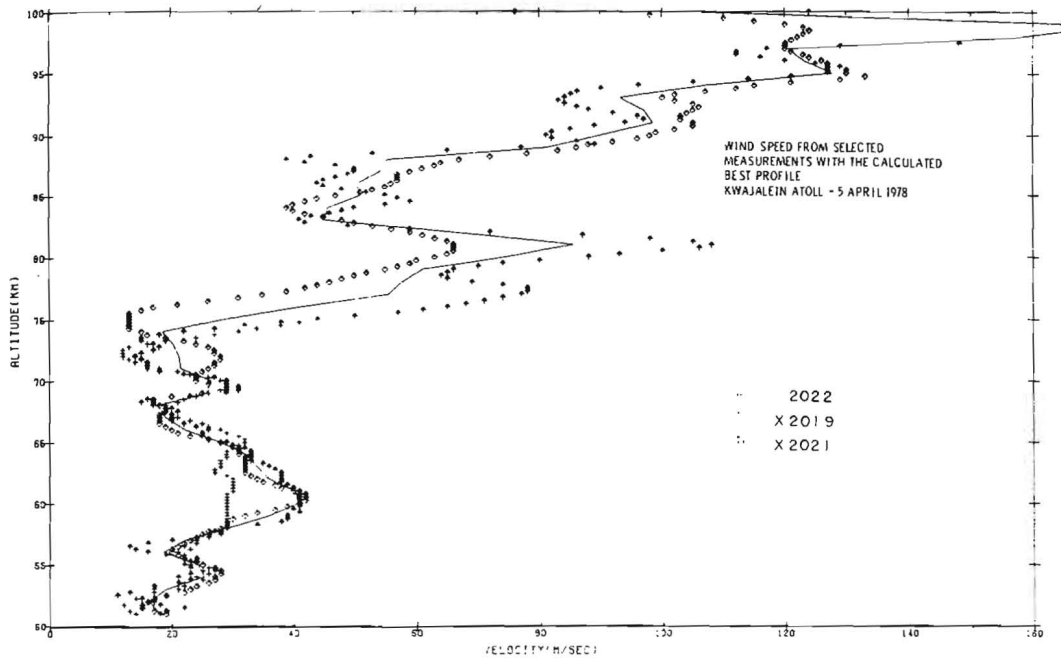


Figure 11c. Wind Speed Measurements From the Rocketsonde and the Two Robin Spheres Launched 1 hr Before and 1 hr After the Reference Time

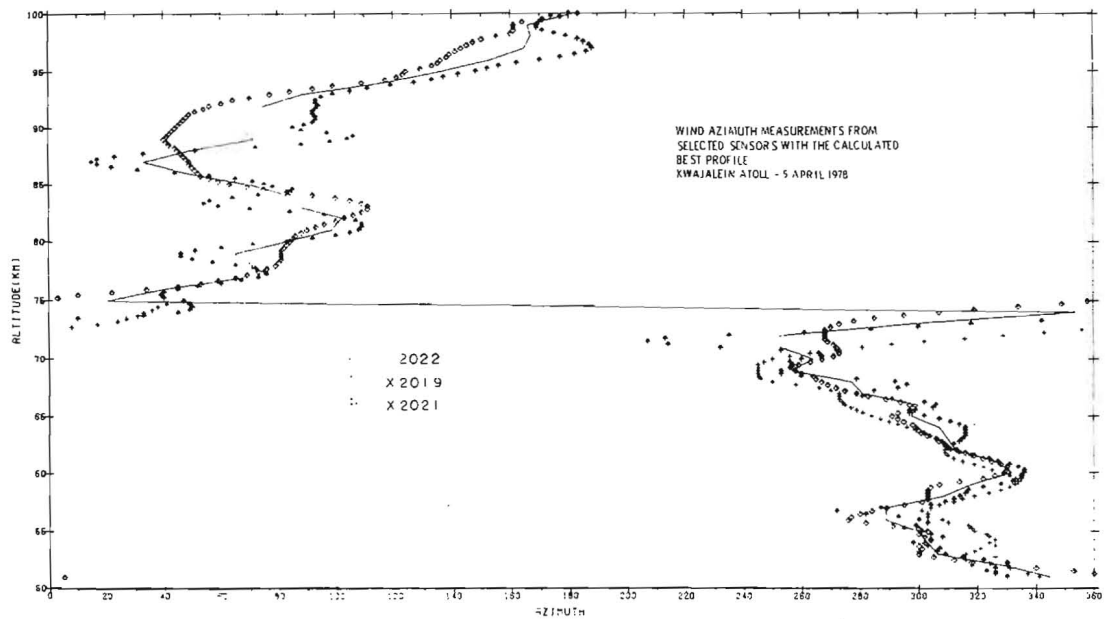


Figure 11d. Wind Azimuth Corresponding to the Wind Speed Measurements of Figure 11c

Table 9. Experiment Weights Used in Calculating the Best Density Profile

Altitude (km)	Rawinsondes			Rocket- sonde 2022A	Robin		Accel- erometer	Hyper- sonic
	R0022	K0129	R0023		X2019A	X2021		
1	.309	.316	.374	0.000	0.000	0.000	0.000	0.000
2	.311	.318	.372	0.000	0.000	0.000	0.000	0.000
3	.312	.319	.369	0.000	0.000	0.000	0.000	0.000
4	.313	.320	.367	0.000	0.000	0.000	0.000	0.000
5	.315	.321	.365	0.000	0.000	0.000	0.000	0.000
6	.316	.321	.363	0.000	0.000	0.000	0.000	0.000
7	.317	.322	.361	0.000	0.000	0.000	0.000	0.000
8	.318	.323	.359	0.000	0.000	0.300	0.000	0.000
9	.319	.324	.358	0.000	0.000	0.000	0.000	0.000
10	.320	.324	.356	0.000	0.000	0.000	0.000	0.000
11	.314	.328	.358	0.000	0.000	0.000	0.000	0.000
12	.310	.331	.359	0.000	0.000	0.000	0.000	0.000
13	.305	.334	.361	0.000	0.000	0.000	0.000	0.000
14	.302	.336	.362	0.000	0.000	0.000	0.000	0.000
15	.298	.339	.363	0.000	0.000	0.000	0.000	0.000
16	.263	.351	.385	0.000	0.000	0.000	0.000	0.000
17	.239	.360	.401	0.000	0.000	0.000	0.000	0.000
18	.223	.365	.412	0.000	0.000	0.000	0.000	0.000
19	.211	.369	.420	0.000	0.000	0.000	0.000	0.000
20	.202	.372	.426	0.000	0.000	0.000	0.000	0.000
21	.178	.338	.387	.097	0.000	0.000	0.000	0.000
22	.175	.340	.390	.096	0.000	0.000	0.000	0.000
23	.171	.342	.392	.094	0.000	0.000	0.000	0.000
24	.168	.344	.395	.093	0.000	0.000	0.000	0.000
25	.165	.346	.397	.092	0.000	0.000	0.000	0.000
26	.197	.210	.482	.110	0.000	0.000	0.000	0.000
27	.248	0.000	.614	.139	0.000	0.000	0.000	0.000
28	.246	0.000	.616	.138	0.000	0.000	0.000	0.000
29	.244	0.000	.619	.137	0.000	0.000	0.000	0.000
30	.639	0.000	0.000	.361	0.000	0.000	0.000	0.000
31	.642	0.000	0.000	.358	0.000	0.000	0.000	0.000
32	.477	0.000	0.000	.523	0.000	0.000	0.000	0.000
33	0.000	0.000	0.000	1.000	0.000	0.000	0.000	0.000
34	0.000	0.000	0.000	1.000	0.000	0.000	0.000	0.000
35	0.000	0.000	0.000	1.000	0.000	0.000	0.000	0.000
36	0.000	0.000	0.000	1.000	0.000	0.000	0.000	0.000
37	0.000	0.000	0.000	1.000	0.000	0.000	0.000	0.000
38	0.000	0.000	0.000	.541	.229	.229	0.000	0.000
39	0.000	0.000	0.000	.523	.238	.238	0.000	0.000
40	0.000	0.000	0.000	.506	.247	.247	0.000	0.000
41	0.000	0.000	0.000	.374	.204	.204	.218	0.000
42	0.000	0.000	0.000	.285	.172	.172	.372	0.000
43	0.000	0.000	0.000	.264	.176	.176	.384	0.000
44	0.000	0.000	0.000	.246	.179	.179	.396	0.000
45	0.000	0.000	0.000	.230	.162	.162	.407	0.000
46	0.000	0.000	0.000	.188	.159	.159	.364	.130
47	0.000	0.000	0.000	.139	.126	.126	.294	.316
48	0.000	0.000	0.000	.130	.125	.125	.298	.322
49	0.000	0.000	0.000	.122	.124	.124	.303	.327
50	0.000	0.000	0.000	.114	.123	.123	.307	.333

Table 9. Experiment Weights Used in Calculating the Best Density Profile (Cont.)

r-c	Altitude (km)	Rawinsondes			Rocket-sonde	Robin		Accel-erometer	Hyper-sonic
		R0022	K0129	R0023	2022A	X2019A	X2021		
00	51	0.000	0.000	0.000	.114	.123	.123	.305	.336
00	52	0.000	0.000	0.000	.112	.123	.123	.303	.339
00	53	0.000	0.000	0.000	.113	.122	.122	.301	.342
00	54	0.000	0.000	0.000	.112	.122	.122	.299	.345
00	55	0.000	0.000	0.000	.111	.122	.122	.297	.348
00	56	0.000	0.000	0.000	.111	.124	.123	.286	.356
00	57	0.000	0.000	0.000	.110	.125	.125	.277	.364
00	58	0.000	0.000	0.000	.109	.126	.126	.267	.372
00	59	0.000	0.000	0.000	.108	.127	.127	.258	.379
00	60	0.000	0.000	0.000	.107	.129	.128	.250	.387
00	61	0.000	0.000	0.000	.105	.137	.137	.231	.391
00	62	0.000	0.000	0.000	.103	.145	.145	.214	.394
00	63	0.000	0.000	0.000	.100	.154	.153	.196	.395
00	64	0.000	0.000	0.000	.098	.162	.162	.183	.395
00	65	0.000	0.000	0.000	.095	.171	.171	.169	.395
00	66	0.000	0.000	0.000	.081	.153	.152	.135	.479
00	67	0.000	0.000	0.000	.090	.176	.175	.139	.420
00	68	0.000	0.000	0.000	0.000	.208	.208	.075	.508
00	69	0.000	0.000	0.000	0.000	.223	.223	0.000	.554
00	70	0.000	0.000	0.000	0.000	.221	.221	0.000	.559
00	71	0.000	0.000	0.000	0.000	.223	.223	0.000	.554
00	72	0.000	0.000	0.000	0.000	.225	.224	0.000	.551
00	73	0.000	0.000	0.000	0.000	.227	.226	0.000	.547
00	74	0.000	0.000	0.000	0.000	.228	.228	0.000	.544
00	75	0.000	0.000	0.000	0.000	.230	.229	0.000	.541
00	76	0.000	0.000	0.000	0.000	.231	.231	0.000	.538
00	77	0.000	0.000	0.000	0.000	.233	.232	0.000	.535
00	78	0.000	0.000	0.000	0.000	.234	.233	0.000	.533
00	79	0.000	0.000	0.000	0.000	.235	.235	0.000	.530
00	80	0.000	0.000	0.000	0.000	.236	.236	0.000	.528
00	81	0.000	0.000	0.000	0.000	.245	.244	0.000	.511
00	82	0.000	0.000	0.000	0.000	.253	.252	0.000	.495
00	83	0.000	0.000	0.000	0.000	.260	.259	0.000	.481
00	84	0.000	0.000	0.000	0.000	.266	.265	0.000	.469
00	85	0.000	0.000	0.000	0.000	.272	.271	0.000	.457
00	86	0.000	0.000	0.000	0.000	.271	.270	0.000	.459
00	87	0.000	0.000	0.000	0.000	.270	.270	0.000	.460
00	88	0.000	0.000	0.000	0.000	.269	.269	0.000	.462
00	89	0.000	0.000	0.000	0.000	.269	.268	0.000	.463
00	90	0.000	0.000	0.000	0.000	.268	.267	0.000	.465
00	91	0.000	0.000	0.000	0.000	.252	.251	0.000	.497
00	92	0.000	0.000	0.000	0.000	.237	.236	0.000	.527
00	93	0.000	0.000	0.000	0.000	.222	.222	0.000	.555
00	94	0.000	0.000	0.000	0.000	.209	.209	0.000	.582
00	95	0.000	0.000	0.000	0.000	.197	.197	0.000	.607
30	96	0.000	0.000	0.000	0.000	.166	.166	0.000	.668
16	97	0.000	0.000	0.000	0.000	.141	.141	0.000	.718
22	98	0.000	0.000	0.000	0.000	.120	.120	0.000	.759
27	99	0.000	0.000	0.000	0.000	.104	.103	0.000	.793
33	100	0.000	0.000	0.000	0.000	.090	.090	0.000	.821

Table 9. Experiment Weights Used in Calculating the East Density Profile (Cont.)

Altitude (km)	Rawinsondes			Rocket- sonde 2022A	Robin		Accel- erometer	Hyper- sonic
	R0022	K0129	R0023		X2019A	X2021		
101	0.000	0.000	0.000	0.000	.078	.078	0.000	.843
102	0.000	0.000	0.000	0.000	.069	.069	0.000	.862
103	0.000	0.000	0.000	0.000	.061	.061	0.000	.878
104	0.000	0.000	0.000	0.000	.054	.054	0.000	.892
105	0.000	0.000	0.000	0.000	0.000	.051	0.000	.949
106	0.000	0.000	0.000	0.000	0.000	.045	0.000	.955
107	0.000	0.000	0.000	0.000	0.000	.041	0.000	.959
108	0.000	0.000	0.000	0.000	0.000	.037	0.000	.963
109	0.000	0.000	0.000	0.000	0.000	.017	0.000	.983
110	0.000	0.000	0.000	0.000	0.000	0.000	0.000	1.000
111	0.000	0.000	0.000	0.000	0.000	0.000	0.000	1.000
112	0.000	0.000	0.000	0.000	0.000	0.000	0.000	1.000
113	0.000	0.000	0.000	0.000	0.000	0.000	0.000	1.000
114	0.000	0.000	0.000	0.000	0.000	0.000	0.000	1.000
115	0.000	0.000	0.000	0.000	0.000	0.000	0.000	1.000
116	0.000	0.000	0.000	0.000	0.000	0.000	0.000	1.000
117	0.000	0.000	0.000	0.000	0.000	0.000	0.000	1.000
118	0.000	0.000	0.000	0.000	0.000	0.000	0.000	1.000
119	0.000	0.000	0.000	0.000	0.000	0.000	0.000	1.000
120	0.000	0.000	0.000	0.000	0.000	0.000	0.000	1.000
121	0.000	0.000	0.000	0.000	0.000	0.000	0.000	1.000
122	0.000	0.000	0.000	0.000	0.000	0.000	0.000	1.000
123	0.000	0.000	0.000	0.000	0.000	0.000	0.000	1.000
124	0.000	0.000	0.000	0.000	0.000	0.000	0.000	1.000
125	0.000	0.000	0.000	0.000	0.000	0.000	0.000	1.000
126	0.000	0.000	0.000	0.000	0.000	0.000	0.000	1.000
127	0.000	0.000	0.000	0.000	0.000	0.000	0.000	1.000
128	0.000	0.000	0.000	0.000	0.000	0.000	0.000	1.000
129	0.000	0.000	0.000	0.000	0.000	0.000	0.000	1.000
130	0.000	0.000	0.000	0.000	0.000	0.000	0.000	1.000

Table 10. "Best Profiles" of Density and Temperature From Analysis of Data Collected on 5 April 1978

ALTITUDE (KM)	TEMPERATURE (DEG. K)	SIGMA (DEG. K)	DENSITY (KG/M**3)	PROFILE SIGMA (%)
1.0	291.7	2.0	1.070E+00	.09
2.0	287.9	2.1	9.695E-01	.10
3.0	285.5	2.0	8.702E-01	.10
4.0	278.7	1.9	7.904E-01	.10
5.0	273.4	1.6	7.126E-01	.11
6.0	266.7	2.1	6.443E-01	.11
7.0	252.4	1.7	5.760E-01	.11
8.0	255.5	2.1	5.189E-01	.12
9.0	248.8	1.6	4.656E-01	.12
10.0	241.7	2.5	4.174E-01	.12
11.0	233.0	2.3	3.752E-01	.13
12.0	224.7	2.4	3.355E-01	.13
13.0	216.6	2.4	2.986E-01	.14
14.0	208.1	2.2	2.647E-01	.14
15.0	200.4	2.3	2.329E-01	.15
16.0	192.7	1.9	2.038E-01	.19
17.0	138.3	.7	1.747E-01	.22
18.0	191.7	1.5	1.436E-01	.26
19.0	198.9	3.2	1.162E-01	.30
20.0	204.0	.9	9.587E-02	.34
21.0	209.1	1.6	7.930E-02	.33
22.0	212.2	1.9	6.654E-02	.33
23.0	215.7	1.1	5.589E-02	.34
24.0	216.4	1.3	4.764E-02	.34
25.0	219.3	1.3	4.031E-02	.35
26.0	221.1	.3	3.438E-02	.40
27.0	224.5	2.3	2.904E-02	.46
28.0	228.0	1.4	2.469E-02	.47
29.0	230.3	.7	2.110E-02	.48
30.0	229.4	1.0	1.821E-02	.79
31.0	232.5	1.0	1.553E-02	.81
32.0	232.4	4.0*	1.350E-02	1.00
33.0	234.3	4.0*	1.155E-02	1.42
34.0	236.8	4.0*	9.905E-03	1.45
35.0	238.6	4.0*	8.536E-03	1.49
36.0	243.2	4.0*	7.285E-03	1.55
37.0	246.8	4.0*	6.255E-03	1.61
38.0	249.2	7.4	5.448E-03	1.23
39.0	253.3	2.4	4.702E-03	1.26
40.0	255.3	1.9	4.075E-03	1.29
41.0	255.6	3.4	3.565E-03	1.18
42.0	258.9	+.8	3.109E-03	1.09
43.0	266.8	7.4	2.661E-03	1.11
44.0	271.7	7.5	2.319E-03	1.13
45.0	272.2	4.5	2.045E-03	1.14
46.0	268.9	3.1	1.812E-03	1.08
47.0	267.6	4.7	1.611E-03	.97
48.0	270.2	5.1	1.413E-03	.98
49.0	273.2	5.9	1.237E-03	.99
50.0	273.7	6.0	1.094E-03	1.00

Table 10. "Best Profiles" of Density and Temperature From Analysis of Data Collected on 5 April 1978 (Cont.)

ALTITUDE (KM)	TEMPERATURE (DEG. K)	SIGMA (DEG. K)	DENSITY (KG/M**3)	PROFILE SIGMA (%)
51.0	272.2	4.3	9.677E-04	1.00
52.0	271.2	4.4	8.592E-04	1.01
53.0	269.9	4.4	7.639E-04	1.01
54.0	257.5	4.4	6.807E-04	1.02
55.0	261.8	4.5	6.121E-04	1.02
56.0	257.5	5.3	5.469E-04	1.03
57.0	259.0	5.0	4.783E-04	1.05
58.0	259.4	5.9	4.206E-04	1.06
59.0	256.5	6.2	3.738E-04	1.07
60.0	252.4	5.7	3.331E-04	1.08
61.0	248.7	4.9	2.960E-04	1.08
62.0	243.9	3.9	2.631E-04	1.09
63.0	239.4	5.0	2.340E-04	1.09
64.0	232.8	4.8	2.088E-04	1.09
65.0	227.1	3.5	1.848E-04	1.09
66.0	223.7	4.5	1.628E-04	1.04
67.0	218.3	5.5	1.433E-04	1.12
68.0	207.7	4.6	1.280E-04	1.24
69.0	198.5	2.4	1.126E-04	1.29
70.0	197.5	4.5	9.598E-05	1.29
71.0	197.5	1.7	8.090E-05	1.33
72.0	197.3	1.6	6.823E-05	1.37
73.0	197.1	1.2	5.783E-05	1.41
74.0	197.2	1.1	4.884E-05	1.45
75.0	195.3	3.3	4.164E-05	1.49
76.0	193.9	4.3	3.534E-05	1.52
77.0	191.7	2.4	3.011E-05	1.56
78.0	191.7	6.2	2.536E-05	1.60
79.0	193.3	9.5	2.121E-05	1.64
80.0	197.6	9.0	1.749E-05	1.68
81.0	204.5	5.4	1.431E-05	1.77
82.0	204.7	3.1	1.219E-05	1.87
83.0	204.4	5.2	1.040E-05	1.96
84.0	205.4	5.0	8.810E-06	2.06
85.0	208.8	5.0	7.387E-06	2.15
86.0	209.2	5.4	6.289E-06	2.27
87.0	206.0	6.2	5.441E-06	2.39
88.0	201.9	9.3	4.724E-06	2.51
89.0	205.7	5.1	3.933E-06	2.63
90.0	208.4	4.9	3.305E-06	2.76
91.0	207.0	4.4	2.825E-06	2.85
92.0	203.1	2.1	2.446E-06	2.94
93.0	201.4	2.4	2.091E-06	3.02
94.0	201.8	5.3	1.765E-06	3.10
95.0	199.1	5.5	1.510E-06	3.17
96.0	194.1	1.4	1.297E-06	3.33
97.0	193.4	5.2	1.098E-06	3.46
98.0	191.5	1.8	9.192E-07	3.56
99.0	190.2	7.4	7.584E-07	3.65
100.0	187.6	8.2	6.591E-07	3.71

Table 10. "Best Profiles" of Density and Temperature From Analysis of Data Collected on 5 April 1978 (Cont.)

ALTITUDE (KM)	TEMPERATURE (DEG. K)	SIGMA (DEG. K)	DENSITY (KG/M**3)	PROFILE SIGMA (%)
101.0	191.4	11.0	5.572E-07	3.76
102.0	182.2	12.5	4.745E-07	3.81
103.0	217.8	17.2	3.690E-07	3.84
104.0	219.4	12.6	2.925E-07	3.87
105.0	220.1	13.1	2.396E-07	3.99
106.0	211.6	0.0*	2.075E-07	4.00
107.0	211.4	0.0*	1.729E-07	4.01
108.0	227.8	0.0*	1.439E-07	4.02
109.0	241.0	0.0*	1.202E-07	4.06
110.0	262.3	0.0*	1.044E-07	4.10
111.0	275.8	0.0*	8.812E-08	4.39
112.0	291.7	0.0*	7.446E-08	4.68
113.0	319.6	0.0*	6.308E-08	4.97
114.0	313.6	0.0*	5.623E-08	5.25
115.0	315.9	0.0*	5.046E-08	5.54
116.0	318.2	0.0*	4.534E-08	5.83
117.0	342.1	0.0*	3.833E-08	6.12
118.0	383.3	0.0*	3.135E-08	6.41
119.0	400.3	0.0*	2.770E-08	6.70
120.0	399.4	0.0*	2.566E-08	6.99
121.0	338.9	0.0*	2.374E-08	7.27
122.0	417.1	0.0*	2.102E-08	7.56
123.0	459.2	0.0*	1.777E-08	7.85
124.0	478.8	0.0*	1.594E-08	8.14
125.0	435.2	0.0*	1.640E-08	8.43
126.0	400.6	0.0*	1.650E-08	8.72
127.0	440.0	0.0*	1.395E-08	9.01
128.0	421.2	0.0*	1.356E-08	9.30
129.0	429.9	0.0*	1.235E-08	9.58
130.0	440.6	0.0*	1.132E-08	10.00

*Insufficient data available to calculate a value, estimates have been substituted in some cases.

Table 11. "Best Profile" From Analysis of the Wind Speed and Azimuth Measurements on 5 April 1978

ALTITUDE (KM)	WIND SPEED (M/SEC)	SIGMA (M/SEC)	WIND AZIMUTH (DEG.)	SIGMA (DEG.)
1.0	10.6	.5	65.	4.58
2.0	8.4	2.3	74.	9.21
3.0	5.6	.3	82.	3.55
4.0	3.9	.7	59.	15.93
5.0	9.4	1.9	61.	6.97
6.0	13.7	2.0	70.	4.26
7.0	16.6	1.2	64.	1.04
8.0	13.3	.9	70.	3.24
9.0	10.4	1.0	76.	5.15
10.0	9.0	1.2	93.	11.01
11.0	3.0	1.0	108.	5.76
12.0	4.8	1.5	39.	9.57
13.0	5.8	1.2	108.	7.37
14.0	5.4	1.0	127.	17.56
15.0	4.6	1.1	190.	21.25
16.0	4.8	1.5	175.	25.00
17.0	8.9	1.0	117.	15.39
18.0	3.0	1.7	76.	19.84
19.0	3.0	1.6	42.	97.17
20.0	2.1	1.4	17.	73.29
21.0	3.0	1.7	331.	42.32
22.0	7.3	1.1	292.	11.12
23.0	7.8	1.2	269.	6.01
24.0	9.6	1.5	264.	5.96
25.0	10.2	1.9	277.	9.37
26.0	10.0	1.4	285.	10.10
27.0	7.0	1.1	285.	13.17
28.0	3.4	1.0	282.	48.85
29.0	1.9	1.6	327.	46.79
30.0	5.1	1.3	322.	35.71
31.0	5.7	3.0	46.	22.50
32.0	15.0	3.0*	90.	0.00*
33.0	20.0	3.0*	99.	0.00*
34.0	25.0	3.0*	96.	0.00*
35.0	31.0	3.0*	97.	0.00*
36.0	33.0	3.0*	95.	0.00*
37.0	34.0	3.0*	90.	0.00*
38.0	35.4	1.1	88.	2.55
39.0	37.2	2.6	89.	1.30
40.0	33.6	3.7	91.	3.54
41.0	28.2	1.3	83.	4.30
42.0	22.4	3.3	81.	6.52
43.0	9.6	7.5	23.	56.48
44.0	14.2	3.2	301.	20.35
45.0	15.4	.9	266.	19.20
46.0	14.2	3.4	253.	11.03
47.0	11.2	2.9	233.	27.90
48.0	10.0	2.6	225.	10.48
49.0	9.0	3.7	262.	42.28
50.0	11.2	4.1	341.	11.52

Table 11. "Best Profile" From Analysis of the Wind Speed and Azimuth Measurements on 5 April 1978 (Cont.)

ALTITUDE (KM)	WIND SPEED (M/SEC)	SIGMA (M/SEC)	WIND AZIMUTH (DEG.)	SIGMA (DEG.)
51.0	17.2	2.0	344.	15.72
52.0	15.2	1.3	326.	9.21
53.0	13.4	4.4	308.	6.88
54.0	25.0	2.3	307.	9.64
55.0	24.0	1.7	304.	9.18
56.0	19.0	2.9	293.	13.24
57.0	22.4	3.8	292.	13.73
58.0	23.0	3.1	311.	7.37
59.0	34.6	5.3	321.	12.23
60.0	38.4	5.4	331.	4.21
61.0	38.2	4.8	324.	6.12
62.0	34.8	3.4	311.	3.33
63.0	32.8	3.4	309.	5.54
64.0	31.6	1.7	305.	9.44
65.0	20.0	2.7	295.	8.72
66.0	23.4	3.5	295.	11.32
67.0	13.4	1.3	279.	5.19
68.0	13.0	2.0	272.	17.08
69.0	25.8	4.4	254.	5.72
70.0	26.8	1.9	261.	8.44
71.0	20.8	4.9	258.	26.85
72.0	19.4	7.5	268.	41.22
73.0	19.4	4.5	313.	45.22
74.0	21.0	7.6	2.	51.16
75.0	20.5	18.6	20.	28.81
76.0	41.3	27.1	40.	12.52
77.0	55.5	24.0	68.	6.39
78.0	57.8	14.2	71.	10.05
79.0	61.0	8.0	65.	10.87
80.0	74.5	15.0	83.	8.73
81.0	85.5	23.1	99.	9.88
82.0	65.8	14.3	102.	5.19
83.0	45.0	3.5	86.	28.48
84.0	45.8	7.2	83.	14.73
85.0	51.0	5.4	69.	7.85
86.0	50.5	5.4	48.	11.35
87.0	54.3	5.7	33.	18.19
88.0	55.3	15.1	49.	16.52
89.0	81.3	11.1	72.	35.37
90.0	89.8	9.0	66.	25.71
91.0	98.5	7.2	70.	25.71
92.0	97.0	3.5	75.	20.93
93.0	93.0	10.4	89.	15.02
94.0	107.0	13.1	117.	13.95
95.0	127.8	5.1	137.	13.03
96.0	123.0	4.8	153.	20.05
97.0	120.5	7.1	165.	25.17
98.0	150.8	43.2	167.	14.81
99.0	172.3	61.7	160.	4.24
100.0	103.0	49.1	182.	7.32

Table 11. "Best Profile" From Analysis of the Wind Speed and Azimuth Measurements on 5 April 1978 (Cont.)

ALTITUDE (KM)	WIND SPEED (M/SEC)	SIGMA (M/SEC)	WIND AZIMUTH (DEG.)	SIGMA (DEG.)
101.0	41.5	27.3	155.	72.47
102.0	55.3	44.3	151.	65.00
103.0	61.8	17.5	304.	78.38
104.0	57.8	28.6	279.	32.51
105.0	43.5	41.7	181.	24.04
106.0	141.5	0.0*	154.	0.00*
107.0	116.0	0.0*	146.	0.00*
108.0	61.5	0.0*	167.	0.00*
109.0	162.0	0.0*	287.	0.00*

* Insufficient data available to calculate a value.

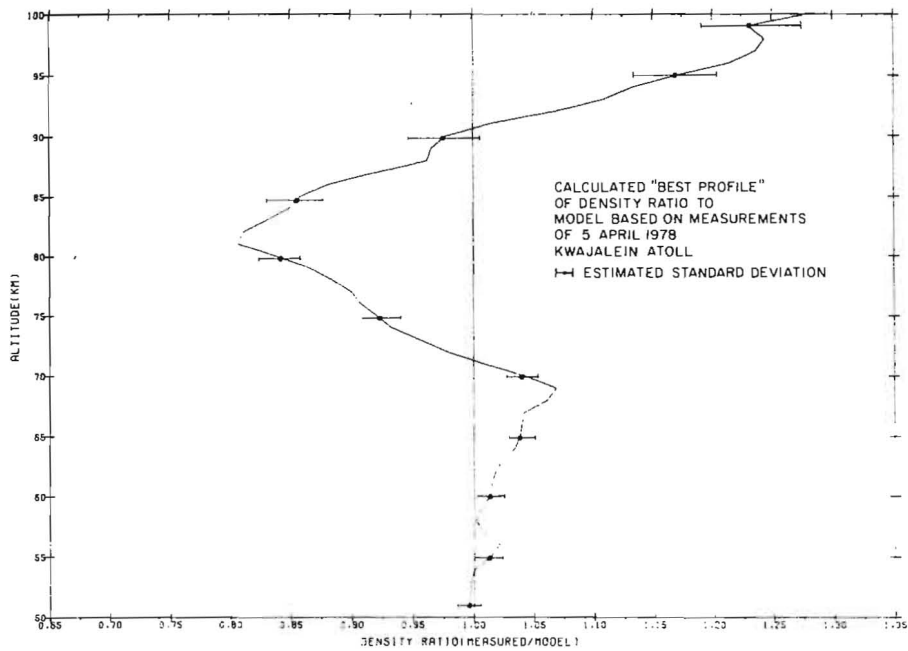


Figure 12a. "Best Profile" Density Ratio to the Model From the Analysis With Weights Dependent on Sensor Accuracy and Atmospheric Variability

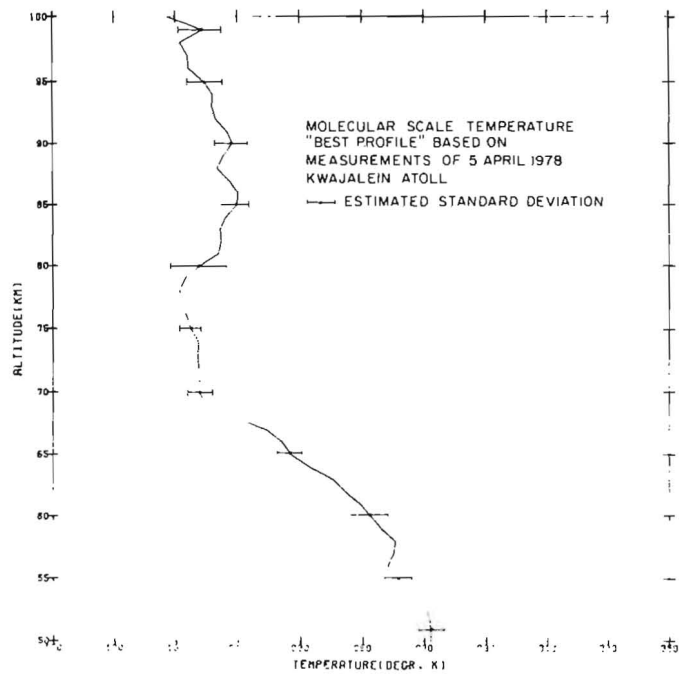


Figure 12b. "Best Profile" Temperature From Unweighted Average of all Data

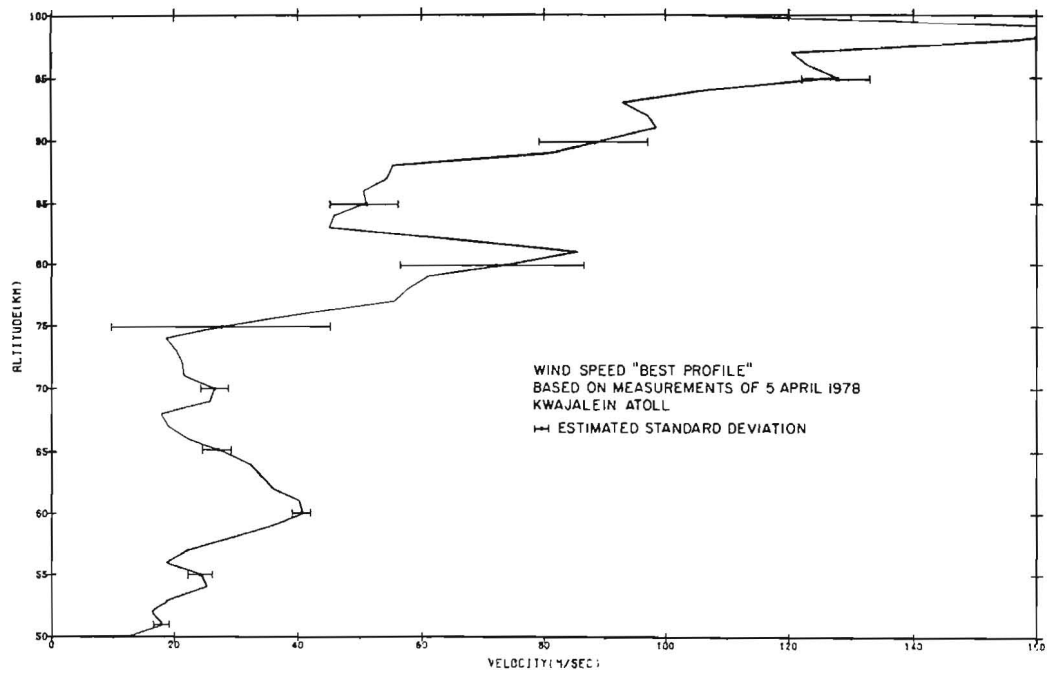


Figure 12c. "Best Profile" of Wind Speed From the Unweighted Average of the 2019A and 2021 Robin Spheres Above 40 km and all Measurements Below 40 km

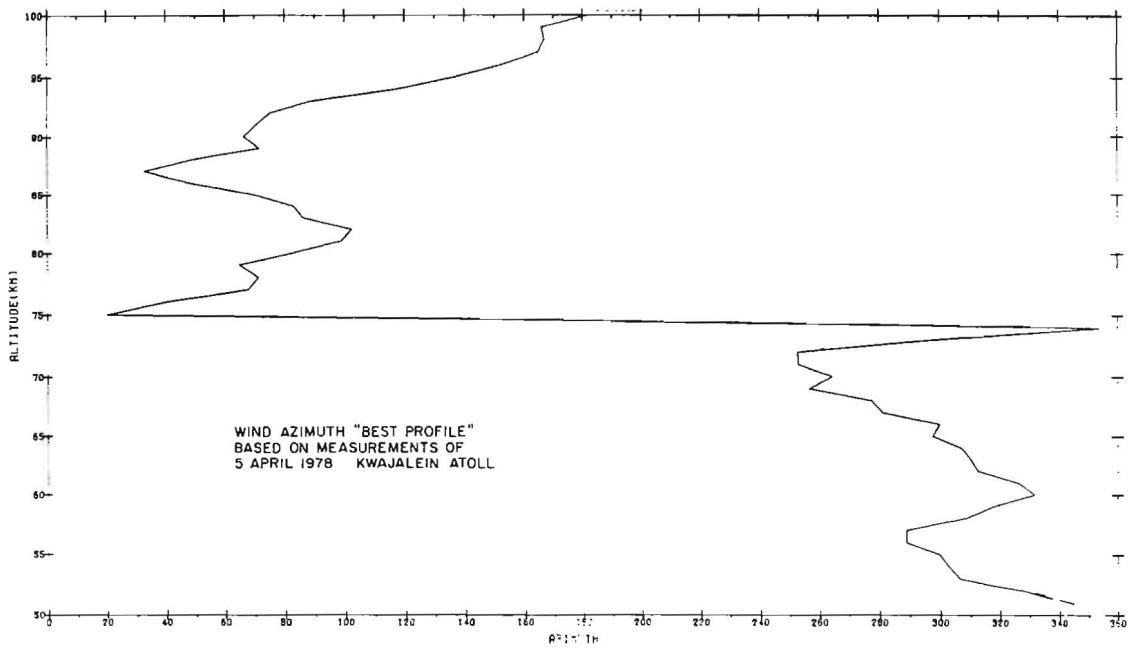


Figure 12d. "Best Profile" of Wind Azimuth Corresponding to Figure 12c

1.
2.
3.
4.
5.
6.
7.
8.
9.
10.
11.
12.
13.
14.

References

1. Philbrick, C.R., Faire, A.C., and Fryklund, D.H. (1978) AFGL-TR-78-0058, Measurements of Atmospheric Density.
2. Olsen, R.O. and Kennedy, B.W. (1977) ASL-TR-0005, ABRES Pretest Atmospheric Measurements.
3. Martin, L. and Azzarelli, T. (1977) XONICS Report, Wind and Density Measurements on Four Robin Spheres.
4. Salah, J.E. (1967) J. Geophys. Res. 72:5389.
5. Cole, A.E. (1977) Private communication of unpublished report, Time and Space Variability of Density at Kwajalein.
6. Cole, A.E. and Kantor, A.J. (1975) AFCRL-TR-75-0527, Tropical Atmospheres, 0 to 90 km.
7. Fletcher, E.T., Jr. (1977) Private communication of Robin sphere results from the TDV-1 program.
8. Kennedy, B.W. and Hackerson, L.D. (1977) Private communication of unpublished ASL report, Analysis of Meteorological Data at Kwajalein Missile Range.
9. Deutsch, R. (1965) Estimation Theory, Prentice-Hall, Inc., Englewood Cliffs, N.J.
10. Bailey, A.B. and Hiatt, J. (1971) AEDC-TR-70-291, Free-Flight Measurements of Sphere Drag.
11. Hines, C.O. (1974) American Geophysical Union Monograph 18, The Upper Atmosphere in Motion.
12. Philbrick, C.R., Narcisi, R.S., Good, R.E., Hoffman, H.S., Keneshea, T.J., MacLeod, M.A., Zimmerman, S.P., and Reinisch, B.W. (1973) Space Research XIII, 441.
13. Zimmerman, S.P. and Champion, K.S.W. (1963) J. Geophys. Res. 68:3049.
14. Zimmerman, S.P. and Rosenberg, N.W. (1972) Space Research XII, 623.

ed

rag

.c
nd
ing

Appendix A

Derivation of Density "Best Profile" Estimates Equation

One would like to determine a technique for combining multiple measurements (from different instruments) to obtain a "best" estimate of density when the relative accuracies (measurement errors) are taken into account.

We derive here an approach which yields a "best" profile in the sense of minimizing the variance.

Assuming the data is of the form

$$X_i = \mu + \epsilon_i \quad (A1)$$

where X_i is the measured value, μ is the desired parameter, and ϵ_i is the random noise with a zero mean and a standard deviation σ_i . That is,

$$E[\epsilon_i] = 0$$

$$\sigma^2[\epsilon] = \sigma_i^2 \quad (A2)$$

Let the estimate of μ be denoted $\hat{\mu}$ and be a weighted average of the independent data points available (at a given altitude). Thus,

$$\hat{\mu} = \sum_{i=1}^N \omega_i X_i \quad (A3)$$

We wish to choose the ω_i 's so that $\hat{\mu}$ is a minimum variance unbiased estimate of μ . (If the ϵ_i 's are gaussian, the estimate will also be the maximum likelihood estimate.)

(a) Now for unbiased case we require:

$$E[\hat{\mu}] = \mu$$

from Eq. (A3) we have

$$E[\hat{\mu}] = \sum_{i=1}^N \omega_i E[X_i]$$

and from Eq. (A1) we have

$$E[X_i] = \mu$$

Thus,

$$E[\hat{\mu}] = \mu \sum_{i=1}^N \omega_i$$

and for an unbiased estimate we have

$$\sum_{i=1}^N \omega_i = 1 \quad . \quad (A4)$$

(b) Minimum Variance:

The variance of the estimate is given by

$$\begin{aligned} \sigma_{\hat{\mu}}^2 &= \sigma^2 \left(\sum_{i=1}^N \omega_i X_i \right) \\ &= \sum_{i=1}^N \omega_i^2 \sigma_i^2 \quad . \end{aligned} \quad (A5)$$

(Trick to include unbiased assumption using Eq. (A4)).

$$\begin{aligned}\sigma_{\hat{\mu}}^2 &= \sum_{i=1}^{N-1} \omega_i^2 \sigma_i^2 + \omega_N^2 \sigma_N^2 \\ &= \sum_{i=1}^{N-1} \omega_i^2 \sigma_i^2 + \left(1 - \sum_{i=1}^{N-1} \omega_i^2\right) \sigma_N^2.\end{aligned}$$

Now for minimum variance we require

$$\frac{\partial \sigma_{\hat{\mu}}^2}{\partial \omega_j} = 0 \quad \text{for all } j \tag{A6}$$

yielding

$$\frac{\partial \sigma_{\hat{\mu}}^2}{\partial \omega_j} = 2\omega_j \sigma_j^2 - 2 \left(1 - \sum_{i=1}^{N-1} \omega_i^2\right) \sigma_N^2. \tag{A7}$$

Thus, using Eqs. (A6) and (A7)

$$\omega_j = \omega_N \frac{\sigma_N^2}{\sigma_j^2} \quad j = 1, 2 \dots N. \tag{A8}$$

Using Eqs. (A4) and (A8) we find,

$$1 = \sum_{j=1}^N \omega_j = \omega_N \sigma_N^2 \sum_{j=1}^N \frac{1}{\sigma_j^2}.$$

Therefore,

$$\omega_N = \frac{\frac{1}{\sigma_N^2}}{\sum_{j=1}^N \frac{1}{\sigma_j^2}}$$

But this must be true for any weight ω_i (we could have isolated any one weight in Eq. (A5), we just happen to choose ω_N). Thus we require

$$\omega_i = \frac{\frac{1}{\sigma_i^2}}{\sum_{j=1}^N \frac{1}{\sigma_j^2}} \quad i = 1, 2 \cdots N \quad . \quad (A9)$$

We may now evaluate the variance of $\hat{\mu}$ as follows. From Eq. (A5)

$$\sigma_{\hat{\mu}}^2 = \sum_{i=1}^N \omega_i^2 \sigma_i^2$$

and using Eq. (A9) we have

$$\sigma_{\hat{\mu}}^2 = \frac{\sum_{i=1}^N \left[\left(\frac{1}{\sigma_i^2} \right)^2 \sigma_i^2 \right]}{\left(\sum_{i=1}^N \frac{1}{\sigma_i^2} \right)^2} .$$

Thus,

$$\sigma_{\hat{\mu}}^2 = \frac{1}{N} \quad . \quad (A10)$$

Finally, if $\sigma_i^2 = \sigma^2$ for all i (all data of equal value), we have the standard unweighted average for minimum variance. That is,

$$w_i = \frac{1}{N} \quad i = 1, 2 \dots N$$

and

(A11)

$$\sigma_{\hat{\mu}}^2 = \frac{\sigma^2}{N} .$$

Appendix B

Summary of Sensor Measurements

In Tables B1–B12, the results from each of the individual sensor profiles are listed. The following list indicates which table corresponds to each sensor.

- B1 - Rawinsonde R0022 at 0825 GMT
- B2 - Rawinsonde R0023 at 1240 GMT
- B3 - Rawinsonde K0129 at 1233 GMT
- B4 - Rocketsonde 2022A at 1429 GMT
- B5 - Robin Sphere (XONICS) 2018 at 0855 GMT From XONICS Analysis
- B6 - Robin Sphere (XONICS) 2019A at 1041 GMT From XONICS Analysis
- B7 - Robin Sphere (XONICS) 2021 at 1243 GMT From XONICS Analysis
- B8 - Robin Sphere (ASL) 2018 at 0855 GMT From ASL Analysis
- B9 - Robin Sphere (ASL) 2019A at 1041 GMT From ASL Analysis
- B10 - Robin Sphere (ASL) 2021 at 1243 GMT From ASL Analysis
- B11 - AFGL Accelerometer Sphere at 1226 GMT
- B12 - Hypersonic Sphere at 1142 GMT From MIT Lincoln Laboratory Analysis

Table B1. Rawinsonde R0022 at 0825 GMT

ALTITUDE (KM)	TEMPERATURE (DEG.K)	DENSITY (KG/M**3)	DENSITY / MODEL	WIND SPEED (M/SEC)	WIND DIRECTION (DEG.)
.61	295.1	.111E+01	1.11	11.33	54.
.91	292.5	.109E+01	1.08	11.33	55.
1.22	290.4	.105E+01	1.04	9.78	66.
1.52	288.2	.102E+01	1.01	8.75	66.
1.83	287.5	.991E+00	1.01	7.72	68.
2.13	290.2	.943E+00	.99	7.72	69.
2.44	289.1	.918E+00	.99	6.18	73.
2.74	287.7	.890E+00	.99	5.15	76.
3.05	285.5	.865E+00	.99	4.63	73.
3.35	283.4	.841E+00	.99	4.12	66.
3.66	281.2	.817E+00	.99	4.12	55.
3.96	279.2	.793E+00	.99	3.60	47.
4.27	277.1	.770E+00	.99	4.63	46.
4.57	275.4	.746E+00	.99	6.18	52.
4.88	274.3	.721E+00	.99	7.72	54.
5.18	272.3	.700E+00	.99	9.78	55.
5.49	270.9	.677E+00	.99	11.84	59.
5.79	269.0	.656E+00	.99	12.36	64.
6.10	266.4	.637E+00	.99	14.41	66.
6.40	264.4	.618E+00	.99	16.99	66.
6.71	264.4	.594E+00	.98	18.02	65.
7.01	262.7	.575E+00	.98	17.50	64.
7.32	260.5	.557E+00	.98	16.99	64.
7.62	258.3	.540E+00	.99	15.44	55.
7.92	256.0	.523E+00	.99	13.90	57.
8.23	253.9	.507E+00	.99	12.87	70.
8.53	251.5	.491E+00	.99	11.84	74.
8.84	249.6	.475E+00	.99	11.33	76.
9.14	248.1	.458E+00	.99	10.81	74.
9.45	246.3	.442E+00	.99	10.81	77.
9.75	244.1	.428E+00	.99	10.81	96.
10.06	241.6	.414E+00	.99	10.30	93.
10.36	238.7	.402E+00	1.00	9.27	101.
10.67	235.8	.389E+00	1.00	9.27	106.
10.97	233.5	.376E+00	1.00	9.27	109.
11.28	231.0	.364E+00	1.01	7.72	104.
11.58	228.6	.351E+00	1.01	6.18	95.
11.89	226.1	.339E+00	1.01	4.12	93.
12.19	223.8	.328E+00	1.01	3.09	112.
12.50	221.4	.316E+00	1.01	3.60	125.
12.80	219.0	.305E+00	1.02	5.15	117.
13.11	216.5	.294E+00	1.02	6.69	109.
13.41	213.7	.284E+00	1.02	7.21	104.
13.72	210.8	.274E+00	1.03	6.69	105.
14.02	208.1	.264E+00	1.03	6.69	111.
14.33	205.5	.255E+00	1.03	6.18	122.
14.63	203.3	.245E+00	1.03	4.63	146.
14.94	201.0	.235E+00	1.03	4.12	132.
15.24	198.5	.226E+00	1.03	3.60	177.

Table B1. Rawinsonde R0022 at 0825 GMT (Cont.)

ALTITUDE (KM)	TEMPERATURE (DEG.K)	DENSITY (KG/M**3)	DENSITY / MOEL	WIND SPEED (M/SEC)	WIND DIRECTION (DEG.)
15.54	196.1	.217E+00	1.03	3.60	172.
15.85	193.3	.209E+00	1.04	3.09	132.
16.15	191.1	.200E+00	1.04	3.09	158.
16.46	189.9	.191E+00	1.04	5.15	133.
16.76	188.6	.182E+00	1.04	8.24	129.
17.07	186.1	.173E+00	1.04	9.72	124.
17.37	189.1	.163E+00	1.04	10.81	110.
17.68	192.4	.151E+00	1.03	11.84	36.
17.98	192.8	.143E+00	1.03	10.81	36.
18.29	193.0	.136E+00	1.04	7.21	99.
18.59	194.3	.128E+00	1.03	3.60	34.
18.90	197.5	.119E+00	1.02	7.06	128.
19.20	199.6	.112E+00	1.02	3.09	162.
19.51	203.0	.105E+00	1.00	3.09	142.
19.81	204.5	.988E-01	1.00	1.54	71.
20.12	204.3	.940E-01	1.01	4.12	30.
20.42	205.5	.888E-01	1.01	4.63	35.
20.73	207.3	.838E-01	1.00	2.57	32.
21.03	209.0	.791E-01	1.00	2.57	338.
21.34	210.8	.747E-01	1.00	5.15	322.
21.64	211.3	.707E-01	1.00	6.18	313.
21.95	212.3	.672E-01	1.00	6.69	301.
22.25	211.3	.642E-01	1.01	6.69	285.
22.56	213.8	.606E-01	1.00	7.21	271.
22.86	215.1	.574E-01	1.00	6.69	267.
23.16	214.6	.548E-01	1.00	7.21	264.
23.47	214.1	.524E-01	1.01	9.27	261.
23.77	214.3	.499E-01	1.01	8.24	262.
24.08	216.1	.471E-01	1.00	8.75	270.
24.38	217.1	.448E-01	1.00	9.78	280.
24.69	217.8	.425E-01	1.00	10.30	289.
24.99	219.6	.402E-01	.99	12.87	288.
25.30	220.9	.382E-01	.99	13.90	286.
25.60	221.2	.364E-01	.99	12.36	238.
25.91	221.1	.348E-01	1.00	11.84	295.
26.21	221.0	.332E-01	1.00	11.84	293.
26.52	221.0	.317E-01	1.00	9.27	295.
26.82	221.3	.302E-01	1.00	7.72	283.
27.13	222.5	.287E-01	1.00	7.21	274.
27.43	224.2	.272E-01	.99	5.66	230.
27.74	226.0	.258E-01	.99	3.09	319.
28.04	228.9	.243E-01	.98	4.12	11.
28.35	230.3	.231E-01	.97	4.63	27.
28.65	230.5	.221E-01	.98	3.60	35.
28.96	230.3	.211E-01	.98	1.54	18.
29.26	229.6	.203E-01	.99	3.09	277.
29.57	228.7	.194E-01	.99	5.66	278.
29.87	228.6	.186E-01	1.00	6.69	291.
30.18	230.1	.177E-01	.99	5.66	317.
30.48	231.1	.168E-01	.99	5.66	343.
30.78	231.9	.160E-01	.99	5.15	7.
31.09	233.1	.153E-01	.99	6.18	43.
31.39	234.0	.146E-01	.99		
31.70	234.5	.139E-01	.99		
32.00	234.5	.133E-01	.99		

Table B2. Rawinsonde R0023 at 1240 GMT

ALTITUDE (KM)	TEMPERATURE (DEG.K)	DENSITY (KG/M**3)	DENSITY / MODFL	WIND SPEED (M/SEC)	WIND DIRECTION (DEG.)
.61	294.3	.111E+01	1.12	10.81	61.
.91	291.7	.109E+01	1.08	10.81	61.
1.22	289.7	.105E+01	1.04	10.30	61.
1.52	287.9	.102E+01	1.01	10.30	62.
1.83	285.7	.995E+00	1.01	11.33	63.
2.13	285.2	.963E+00	1.01	6.69	78.
2.44	287.9	.921E+00	.99	5.15	97.
2.74	286.6	.893E+00	.99	6.18	89.
3.05	284.5	.867E+00	1.00	6.18	86.
3.35	282.8	.841E+00	.99	5.15	90.
3.66	280.6	.818E+00	.99	3.09	86.
3.96	278.6	.793E+00	.99	2.57	76.
4.27	276.7	.770E+00	.99	4.12	76.
4.57	275.0	.746E+00	.99	7.21	74.
4.88	273.7	.722E+00	.99	9.78	69.
5.18	272.1	.699E+00	.99	11.84	68.
5.49	269.6	.679E+00	.99	11.84	70.
5.79	267.5	.659E+00	.99	11.84	74.
6.10	265.4	.639E+00	.99	14.41	73.
6.40	264.2	.617E+00	.99	16.47	69.
6.71	263.7	.594E+00	.98	16.99	64.
7.01	262.1	.575E+00	.96	15.96	62.
7.32	260.0	.557E+00	.98	14.41	62.
7.62	258.0	.539E+00	.98	12.87	65.
7.92	255.6	.523E+00	.99	12.87	68.
8.23	253.4	.506E+00	.99	12.36	71.
8.53	251.0	.491E+00	.99	11.84	74.
8.84	248.8	.475E+00	.99	10.81	73.
9.14	247.6	.458E+00	.99	10.81	69.
9.45	245.8	.442E+00	.99	9.78	70.
9.75	243.3	.428E+00	.99	8.24	77.
10.06	240.5	.415E+00	.99	7.21	86.
10.36	237.7	.402E+00	1.00	7.72	94.
10.67	235.1	.389E+00	1.00	7.72	98.
10.97	232.6	.376E+00	1.00	7.21	107.
11.28	229.9	.364E+00	1.01	6.18	112.
11.58	227.3	.352E+00	1.01	5.66	102.
11.89	224.8	.340E+00	1.01	4.63	92.
12.19	222.1	.328E+00	1.01	3.09	88.
12.50	219.9	.317E+00	1.01	3.09	97.
12.80	217.4	.305E+00	1.02	4.12	108.
13.11	214.8	.295E+00	1.02	5.66	112.
13.41	212.1	.284E+00	1.02	5.66	114.
13.72	209.5	.274E+00	1.02	5.66	119.
14.02	207.1	.264E+00	1.03	4.63	131.
14.33	205.1	.253E+00	1.03	4.63	152.
14.63	202.9	.244E+00	1.03	4.63	172.
14.94	200.4	.234E+00	1.03	5.15	189.
15.24	198.0	.225E+00	1.03	6.69	203.

Table B2. Rawinsonde R0023 at 1240 GMT (Cont.)

ALTITUDE (KM)	TEMPERATURE (DEG.K)	DENSITY (KG/M**3)	DENSITY / MODEL	WIND SPEED (M/SEC)	WIND DIRECTION (DEG.)
15.54	195.7	.216E+00	1.03	7.21	204.
15.85	193.7	.207E+00	1.03	6.18	187.
16.15	191.7	.198E+00	1.03	6.18	155.
16.46	189.7	.190E+00	1.03	8.24	134.
16.76	188.3	.181E+00	1.04	9.27	122.
17.07	188.2	.171E+00	1.04	8.75	104.
17.37	189.5	.161E+00	1.03	8.75	82.
17.68	190.5	.152E+00	1.03	9.27	68.
17.98	190.3	.144E+00	1.04	9.78	65.
18.29	191.1	.136E+00	1.04	9.27	55.
18.59	194.0	.127E+00	1.03	7.21	63.
18.90	199.2	.117E+00	1.00	3.60	57.
19.20	202.7	.103E+00	.99	1.03	299.
19.51	203.1	.104E+00	1.00	2.57	271.
19.81	202.3	.990E-01	1.01	1.03	300.
20.12	203.1	.937E-01	1.01	1.03	41.
20.42	205.8	.890E-01	1.00	1.03	2.
20.73	208.3	.827E-01	.99	2.57	297.
21.03	211.1	.777E-01	.98	5.15	237.
21.34	210.5	.742E-01	.99	6.69	310.
21.64	209.8	.709E-01	1.00	7.21	298.
21.95	212.4	.667E-01	.99	8.24	290.
22.25	215.2	.627E-01	.98	9.27	243.
22.56	216.5	.594E-01	.98	9.78	277.
22.86	216.4	.567E-01	.99	8.75	271.
23.16	217.2	.533E-01	.98	7.72	263.
23.47	217.0	.514E-01	.99	7.72	259.
23.77	216.4	.491E-01	.99	8.75	258.
24.08	216.1	.469E-01	1.00	9.78	258.
24.38	216.4	.447E-01	1.00	9.78	258.
24.69	217.5	.424E-01	1.00	9.27	250.
24.99	219.4	.401E-01	.99	8.75	267.
25.30	220.6	.330E-01	.99	7.72	277.
25.60	220.8	.363E-01	.99	6.69	288.
25.91	221.3	.345E-01	.99		

Table B3. Rawinsonde K0129 at 1233 GMT

ALTITUDE (KM)	TEMPERATURE (DEG.K)	DENSITY (KG/M**3)	DENSITY / MODEL	WIND SPEED (M/SEC)	WIND DIRECTION (DEG.)
.61	295.1	.111E+01	1.11	10.37	65.
.91	292.3	.113E+01	1.06	10.81	70.
1.22	290.1	.105E+01	1.04	11.33	73.
1.52	288.6	.102E+01	1.01	10.81	75.
1.83	286.6	.991E+00	1.01	10.30	77.
2.13	291.0	.946E+00	.99	7.72	81.
2.44	289.3	.913E+00	.99	7.21	88.
2.74	287.7	.891E+00	.99	6.18	90.
3.05	285.5	.866E+00	.99	6.18	88.
3.35	283.3	.842E+00	.99	5.66	76.
3.66	281.4	.817E+00	.99	4.12	56.
3.96	279.3	.793E+00	.99	3.09	38.
4.27	277.1	.770E+00	.99	4.63	50.
4.57	276.2	.744E+00	.99	7.21	57.
4.88	274.7	.721E+00	.99	6.24	58.
5.18	273.0	.693E+00	.99	10.30	60.
5.49	270.7	.678E+00	.99	11.33	66.
5.79	268.4	.658E+00	.99	11.84	74.
6.10	265.6	.640E+00	.99	13.90	76.
6.40	264.2	.618E+00	.99	16.47	69.
6.71	264.1	.595E+00	.98	16.99	64.
7.01	262.6	.575E+00	.98	16.47	63.
7.32	260.8	.557E+00	.98	15.44	65.
7.62	258.7	.539E+00	.98	14.41	70.
7.92	256.5	.523E+00	.99	13.90	73.
8.23	254.1	.507E+00	.99	13.38	74.
8.53	252.2	.490E+00	.99	11.33	76.
8.84	250.5	.473E+00	.99	9.27	78.
9.14	248.5	.458E+00	.99	8.75	82.
9.45	246.7	.442E+00	.99	8.24	90.
9.75	244.4	.428E+00	.99	8.24	101.
10.06	241.7	.415E+00	.99	9.27	106.
10.36	239.0	.402E+00	1.00	9.27	109.
10.67	236.3	.393E+00	1.00	8.75	116.
10.97	233.9	.376E+00	1.00	8.24	114.
11.28	231.6	.363E+00	1.00	8.24	107.
11.58	229.0	.351E+00	1.01	7.21	101.
11.89	226.2	.340E+00	1.01	6.18	97.
12.19	223.5	.328E+00	1.01	6.18	101.
12.50	221.2	.317E+00	1.02	6.18	100.
12.80	218.5	.306E+00	1.02	6.69	98.
13.11	215.9	.295E+00	1.02	6.69	101.
13.41	213.3	.285E+00	1.02	6.18	106.
13.72	210.8	.274E+00	1.03	5.15	118.
14.02	208.9	.264E+00	1.03	4.63	137.
14.33	206.5	.254E+00	1.03	4.12	155.
14.63	204.3	.244E+00	1.03	3.60	133.
14.94	201.4	.235E+00	1.03	4.12	211.
15.24	198.8	.226E+00	1.03	4.63	221.

Table B3. Rawinsonde K0129 at 1233 GMT (Cont.)

ALTITUDE (KM)	TEMPERATURE (DEG.K)	DENSITY (KG/M**3)	DENSITY / MODEL	WIND SPEED (M/SEC)	WIND DIRECTION (DEG.)
15.54	196.5	.217E+00	1.03	4.63	218.
15.85	194.7	.203E+00	1.03	4.12	203.
16.15	192.0	.200E+00	1.04	4.12	179.
16.46	190.1	.191E+00	1.04	5.66	151.
16.76	188.6	.183E+00	1.04	7.72	132.
17.07	187.5	.174E+00	1.05	8.75	118.
17.37	186.9	.165E+00	1.06	9.27	102.
17.68	189.3	.154E+00	1.05	8.24	85.
17.98	191.7	.144E+00	1.04	7.72	66.
18.29	193.6	.135E+00	1.04	7.21	47.
18.59	194.9	.128E+00	1.03	6.18	34.
18.90	197.2	.120E+00	1.03	2.57	14.
19.20	201.7	.111E+00	1.01	1.54	297.
19.51	203.6	.105E+00	1.00	2.06	286.
19.81	203.4	.995E-01	1.01	1.54	340.
20.12	203.9	.944E-01	1.01	2.57	21.
20.42	206.2	.887E-01	1.01	1.54	20.
20.73	207.2	.879E-01	1.01	2.06	321.
21.03	209.8	.799E-01	1.00	4.12	306.
21.34	211.1	.747E-01	1.00	5.66	302.
21.64	211.3	.711E-01	1.00	7.21	297.
21.95	212.5	.677E-01	1.00	7.21	291.
22.25	214.3	.636E-01	1.00	7.72	284.
22.56	214.5	.605E-01	1.00	7.21	279.
22.86	215.3	.575E-01	1.00	7.72	272.
23.16	216.4	.545E-01	1.00	8.75	266.
23.47	217.3	.518E-01	1.00	10.81	261.
23.77	217.6	.493E-01	1.00	11.84	263.
24.08	217.9	.470E-01	1.00	11.84	265.
24.38	218.1	.448E-01	1.00	10.81	267.
24.69	218.3	.427E-01	1.00	10.30	272.
24.99	219.1	.406E-01	1.00	9.78	277.
25.30	220.7	.384E-01	1.00	9.78	278.
25.60	221.0	.366E-01	1.00	9.27	277.
25.91	220.8	.350E-01	1.00	9.27	275.
26.21	221.2	.337E-01	1.00	8.75	274.
26.52	223.1	.315E-01	1.00	6.75	277.
26.82	225.6	.298E-01	.99	7.72	285.
27.13	227.0	.287E-01	.98	6.18	297.
27.43	227.1	.270E-01	.99	4.12	239.
27.74	227.9	.257E-01	.99	2.06	269.
28.04	228.7	.246E-01	.99	2.57	235.
28.35	228.6	.235E-01	.99	3.03	241.
28.65	229.3	.224E-01	.99		
28.96	230.1	.213E-01	.99		
29.26	231.1	.203E-01	.99		

Table B4. Rocketsonde 2022A at 1429 GMT

ALTITUDE (KM)	TEMPERATURE (DEG.K)	DENSITY (KG/M**3)	DENSITY / MODEL	WIND SPEED (M/SEC)	WIND DIRECTION (DEG.)
20.99	208.6	.799E-01	.99	0.00	0.
21.00	208.5	.794E-01	.99	0.00	0.
21.25	209.0	.764E-01	.99	0.00	0.
21.50	209.4	.733E-01	1.00	0.00	0.
21.75	209.8	.702E-01	1.00	0.00	0.
22.00	210.2	.673E-01	1.00	6.00	288.
22.25	210.8	.645E-01	1.00	7.00	290.
22.50	214.9	.608E-01	.99	6.00	287.
22.75	215.4	.583E-01	.99	6.00	282.
23.00	215.8	.560E-01	.99	6.00	276.
23.25	216.3	.537E-01	.99	8.00	267.
23.50	216.7	.516E-01	1.00	8.00	268.
23.75	216.2	.497E-01	1.00	9.00	260.
24.00	215.6	.479E-01	1.01	8.00	265.
24.25	215.0	.462E-01	1.02	10.00	258.
24.50	215.7	.443E-01	1.02	9.00	272.
24.75	217.5	.422E-01	1.01	10.00	266.
25.00	219.1	.403E-01	1.01	10.00	277.
25.25	220.7	.385E-01	1.00	10.00	274.
25.50	221.3	.370E-01	1.00	10.00	293.
25.75	221.4	.356E-01	1.01	10.00	279.
26.00	221.5	.342E-01	1.01	10.00	286.
26.25	222.4	.328E-01	1.00	10.00	290.
26.50	223.6	.314E-01	1.00	9.00	294.
26.75	224.9	.301E-01	1.00	8.00	295.
27.00	226.0	.288E-01	.99	7.00	293.
27.25	226.4	.277E-01	.99	6.00	291.
27.50	226.1	.268E-01	.99	5.00	291.
27.75	225.7	.258E-01	1.00	5.00	280.
28.00	227.5	.247E-01	.99	4.00	287.
28.25	229.5	.236E-01	.98	4.00	283.
28.50	230.1	.227E-01	.98	4.00	302.
28.75	230.5	.218E-01	.98	4.00	279.
29.00	230.8	.210E-01	.98	4.00	307.
29.25	230.5	.203E-01	.98	3.00	286.
29.50	230.0	.196E-01	.99	3.00	321.
29.75	229.4	.189E-01	.99	2.00	331.
30.00	229.4	.182E-01	.99	3.00	343.
30.25	230.8	.175E-01	.99	4.00	25.
30.50	232.2	.167E-01	.98	5.00	34.
30.75	232.3	.161E-01	.98	7.00	58.
31.00	232.1	.156E-01	.99	9.00	72.
31.25	231.8	.150E-01	.99	11.00	82.
31.50	231.6	.145E-01	.99	12.00	89.
31.75	231.9	.140E-01	.99	14.00	89.
32.00	232.4	.135E-01	.99	15.00	90.
32.25	233.0	.129E-01	.99	16.00	88.
32.50	233.3	.125E-01	.99	18.00	94.
32.75	233.9	.120E-01	.99	20.00	95.
33.00	234.3	.116E-01	.99	20.00	99.
33.25	234.7	.111E-01	.99	21.00	99.

Table B4. Rocketsonde 2022A at 1429 GMT (Cont.)

ALTITUDE (KM)	TEMPERATURE (DEG.K)	DENSITY (KG/M**3)	DENSITY / MODEL	WIND SPEED (M/SEC)	WIND DIRECTION (DEG.)
33.50	235.2	.107E-01	.99	23.00	100.
33.75	235.6	.113E-01	.99	23.00	98.
34.00	236.8	.990E-02	.99	26.00	96.
34.25	239.7	.944E-02	.98	25.00	96.
34.50	239.3	.913E-02	.99	29.00	97.
34.75	238.8	.883E-02	.99	28.00	98.
35.00	238.6	.854E-02	.99	31.00	97.
35.25	240.3	.818E-02	.99	28.00	97.
35.50	242.0	.785E-02	.98	33.00	97.
35.75	243.7	.752E-02	.98	29.00	94.
36.00	243.2	.728E-02	.98	33.00	95.
36.25	243.8	.702E-02	.98	31.00	92.
36.50	244.7	.676E-02	.98	34.00	93.
36.75	245.8	.650E-02	.98	32.00	91.
37.00	246.8	.626E-02	.98	34.00	90.
37.25	247.8	.602E-02	.98	33.00	88.
37.50	248.9	.579E-02	.97	35.00	88.
37.75	249.5	.559E-02	.97	35.00	87.
38.00	250.0	.539E-02	.97	35.00	87.
38.25	250.6	.520E-02	.97	35.00	88.
38.50	251.0	.502E-02	.97	35.00	87.
38.75	251.4	.485E-02	.97	35.00	87.
39.00	251.9	.468E-02	.97	35.00	88.
39.25	252.4	.452E-02	.97	35.00	89.
39.50	252.7	.436E-02	.97	35.00	90.
39.75	253.9	.420E-02	.97	34.00	90.
40.00	255.8	.404E-02	.97	33.00	90.
40.25	257.3	.388E-02	.96	33.00	89.
40.50	257.3	.376E-02	.96	31.00	88.
40.75	257.1	.364E-02	.97	31.00	89.
41.00	256.9	.352E-02	.97	30.00	89.
41.25	258.5	.339E-02	.97	28.00	90.
41.50	261.7	.324E-02	.96	25.00	90.
41.75	265.0	.310E-02	.95	21.00	86.
42.00	268.3	.297E-02	.94	16.00	82.
42.25	271.3	.285E-02	.93	13.00	73.
42.50	274.3	.273E-02	.92	8.00	64.
42.75	277.6	.262E-02	.92	6.00	38.
43.00	280.7	.251E-02	.91	3.00	341.
43.25	280.4	.244E-02	.92	7.00	304.
43.50	279.4	.238E-02	.92	10.00	275.
43.75	278.5	.231E-02	.93	14.00	284.
44.00	277.8	.225E-02	.94	15.00	271.
44.25	276.8	.219E-02	.94	17.00	271.
44.50	276.0	.213E-02	.95	16.00	262.
44.75	275.3	.207E-02	.96	20.00	262.
45.00	274.4	.202E-02	.96	15.00	252.
45.25	273.7	.196E-02	.97	23.00	257.
45.50	272.9	.191E-02	.97	15.00	251.
45.75	271.9	.185E-02	.98	17.00	256.
46.00	271.2	.180E-02	.98	15.00	252.
46.25	271.0	.175E-02	.99	18.00	253.
46.50	271.4	.169E-02	.99	12.00	246.
46.75	271.7	.164E-02	.99	16.00	257.

Table B4. Rocketsonde 2022A at 1429 GMT (Cont.)

ALTITUDE (KM)	TEMPERATURE (DEG.K)	DENSITY (KG/M**3)	DENSITY / MODEL	WIND SPEED (M/SEC)	WIND DIRECTION (DEG.)
47.00	271.7	.159E-02	.99	12.00	240.
47.25	272.2	.154E-02	.99	13.00	247.
47.50	272.6	.149E-02	.99	13.00	241.
47.75	273.0	.144E-02	.99	11.00	237.
48.00	273.1	.140E-02	.99	14.00	238.
48.25	273.5	.135E-02	.99	12.00	244.
48.50	273.9	.131E-02	.99	12.00	247.
48.75	274.2	.127E-02	.99	7.00	254.
49.00	273.9	.123E-02	.99	9.00	266.
49.25	272.7	.120E-02	.99	6.00	296.
49.50	270.6	.117E-02	1.00	8.00	300.
49.75	270.5	.114E-02	1.00	8.00	329.
50.00	270.5	.110E-02	1.00	8.00	329.
50.25	271.0	.107E-02	1.00	11.00	330.
50.50	270.8	.104E-02	1.00	11.00	340.
50.75	271.0	.100E-02	1.00	12.00	351.
51.00	270.9	.974E-03	1.00	14.00	341.
51.25	271.1	.944E-03	1.00	13.00	337.
51.50	271.3	.914E-03	1.00	15.00	326.
51.75	270.5	.889E-03	1.00	12.00	331.
52.00	269.6	.865E-03	1.00	16.00	318.
52.25	268.7	.841E-03	1.00	14.00	324.
52.50	268.5	.816E-03	1.00	19.00	316.
52.75	267.5	.794E-03	1.01	17.00	326.
53.00	266.7	.772E-03	1.01	21.00	316.
53.25	266.0	.750E-03	1.01	22.00	319.
53.50	265.3	.728E-03	1.01	22.00	321.
53.75	264.4	.708E-03	1.01	25.00	326.
54.00	263.8	.687E-03	1.01	24.00	324.
54.25	263.4	.667E-03	1.01	26.00	326.
54.50	262.5	.648E-03	1.01	25.00	324.
54.75	261.7	.630E-03	1.01	26.00	323.
55.00	261.0	.611E-03	1.01	23.00	319.
55.25	260.3	.594E-03	1.01	24.00	318.
55.50	259.4	.577E-03	1.01	22.00	317.
55.75	258.9	.560E-03	1.01	22.00	310.
56.00	259.3	.541E-03	1.01	21.00	308.
56.25	260.0	.522E-03	1.01	23.00	303.
56.50	260.7	.505E-03	1.00	22.00	303.
56.75	261.3	.487E-03	1.00	24.00	301.
57.00	262.4	.470E-03	.99	24.00	304.
57.25	262.7	.455E-03	.99	26.00	307.
57.50	261.9	.442E-03	.99	26.00	312.
57.75	261.0	.430E-03	.99	28.00	315.
58.00	260.1	.417E-03	.99	29.00	319.
58.25	259.2	.406E-03	1.00	29.00	324.
58.50	258.2	.394E-03	1.00	29.00	328.
58.75	257.1	.383E-03	1.00	29.00	331.
59.00	256.1	.372E-03	1.00	29.00	333.
59.25	255.2	.362E-03	1.00	29.00	334.
59.50	254.3	.351E-03	1.00	29.00	333.
59.75	253.4	.341E-03	1.01	29.00	331.
60.00	252.4	.331E-03	1.01	29.00	329.
60.25	251.5	.322E-03	1.01	29.00	325.

Table B4. Rocketsonde 2022A at 1429 GMT (Cont.)

ALTITUDE (KM)	TEMPERATURE (DEG.K)	DENSITY (KG/M**3)	DENSITY / MODEL	WIND SPEED (M/SEC)	WIND DIRECTION (DEG.)
60.50	250.7	.312E-03	1.01	29.00	322.
60.75	249.9	.303E-03	1.01	29.00	319.
61.00	249.1	.294E-03	1.01	30.00	315.
61.25	248.2	.285E-03	1.01	30.00	312.
61.50	247.3	.277E-03	1.01	30.00	310.
61.75	246.4	.268E-03	1.01	30.00	309.
62.00	245.4	.261E-03	1.01	30.00	309.
62.25	245.1	.252E-03	1.01	29.00	309.
62.50	244.5	.244E-03	1.01	27.00	309.
62.75	243.3	.237E-03	1.01	27.00	308.
63.00	241.9	.231E-03	1.01	28.00	306.
63.25	240.4	.224E-03	1.01	28.00	304.
63.50	239.0	.218E-03	1.02	28.00	302.
63.75	237.7	.211E-03	1.02	29.00	299.
64.00	236.4	.205E-03	1.02	29.00	296.
64.25	234.9	.199E-03	1.02	29.00	293.
64.50	233.4	.193E-03	1.02	30.00	290.
64.75	231.9	.188E-03	1.02	31.00	287.
65.00	230.6	.182E-03	1.02	32.00	284.
65.25	229.4	.177E-03	1.02	32.00	281.
65.50	227.2	.172E-03	1.03	31.00	279.
65.75	225.4	.167E-03	1.03	29.00	277.
66.00	224.4	.162E-03	1.03	28.00	275.
66.25	223.6	.156E-03	1.03	26.00	274.
66.50	222.9	.151E-03	1.03	25.00	273.
66.75	222.2	.146E-03	1.03	23.00	273.
67.00	231.9	.140E-03	1.01	21.00	273.
67.25	0.0	0.	0.00	20.00	270.
67.50	0.0	0.	0.00	19.00	266.
67.75	0.0	0.	0.00	19.00	258.
68.00	0.0	0.	0.00	19.00	250.
68.25	0.0	0.	0.00	21.00	246.
68.50	0.0	0.	0.00	22.00	245.
68.75	0.0	0.	0.00	24.00	245.
69.00	0.0	0.	0.00	26.00	245.
69.25	0.0	0.	0.00	28.00	245.
69.50	0.0	0.	0.00	29.00	245.
69.75	0.0	0.	0.00	29.00	247.
70.00	0.0	0.	0.00	28.00	250.
70.25	0.0	0.	0.00	26.00	256.
70.50	0.0	0.	0.00	23.00	263.
70.75	0.0	0.	0.00	21.00	272.
71.00	0.0	0.	0.00	18.00	281.
71.25	0.0	0.	0.00	16.00	291.
71.50	0.0	0.	0.00	14.00	302.
71.75	0.0	0.	0.00	13.00	316.
72.00	0.0	0.	0.00	12.00	329.
72.25	0.0	0.	0.00	12.00	343.
72.50	0.0	0.	0.00	12.00	356.
72.75	0.0	0.	0.00	13.00	8.
73.00	0.0	0.	0.00	16.00	17.
73.25	0.0	0.	0.00	19.00	24.
73.50	0.0	0.	0.00	24.00	27.
73.75	0.0	0.	0.00	27.00	31.

Table B5. Robin Sphere (XONICS) 2018 at 0855 GMT From XONICS Analysis

ALTITUDE (KM)	TEMPERATURE (DEG.K)	DENSITY (KG/M**3)	DENSITY / MODEL	WIND SPEED (M/SEC)	WIND DIRECTION (DEG.)
109.50	246.2	.111E-06	1.16	265.00	281.
109.25	215.8	.132E-06	1.33	211.00	274.
109.00	214.1	.134E-06	1.34	158.00	274.
108.75	218.7	.140E-06	1.30	108.00	276.
108.50	200.8	.159E-06	1.42	83.00	255.
108.25	175.7	.190E-06	1.63	93.00	226.
108.00	156.9	.223E-06	1.84	124.00	206.
107.75	153.8	.240E-06	1.90	150.00	196.
107.50	159.3	.245E-06	1.86	160.00	189.
107.25	172.3	.238E-06	1.73	163.00	185.
107.00	187.1	.229E-06	1.60	166.00	185.
106.75	191.1	.234E-06	1.56	166.00	190.
106.50	190.1	.246E-06	1.57	159.00	199.
106.25	190.0	.257E-06	1.57	146.00	208.
106.00	195.6	.260E-06	1.52	139.00	217.
105.75	204.8	.259E-06	1.45	117.00	229.
105.50	216.7	.255E-06	1.37	111.00	242.
105.25	228.4	.251E-06	1.29	108.00	253.
105.00	246.7	.240E-06	1.17	106.00	269.
104.75	261.8	.234E-06	1.09	116.00	283.
104.50	250.5	.252E-06	1.13	133.00	283.
104.25	241.2	.271E-06	1.16	154.00	283.
104.00	255.1	.265E-06	1.08	176.00	283.
103.75	273.0	.256E-06	.99	174.00	281.
103.50	288.0	.250E-06	.93	167.00	281.
103.25	293.1	.252E-06	.89	159.00	281.
103.00	283.9	.268E-06	.91	152.00	279.
102.75	269.1	.291E-06	.94	148.00	276.
102.50	262.0	.308E-06	.95	147.00	273.
102.25	258.4	.323E-06	.95	141.00	270.
102.00	249.5	.345E-06	.97	121.00	262.
101.75	233.0	.383E-06	1.02	99.00	243.
101.50	211.0	.439E-06	1.12	92.00	217.
101.25	193.8	.497E-06	1.21	100.00	195.
101.00	180.0	.560E-06	1.30	114.00	181.
100.75	173.9	.607E-06	1.35	126.00	172.
100.50	172.6	.642E-06	1.36	134.00	167.
100.25	172.6	.673E-06	1.37	135.00	165.
100.00	174.2	.699E-06	1.36	128.00	164.
99.75	177.0	.722E-06	1.34	120.00	163.
99.50	179.2	.747E-06	1.33	110.00	160.
99.25	181.6	.771E-06	1.31	94.00	158.
99.00	182.8	.802E-06	1.30	84.00	157.
98.75	182.5	.840E-06	1.30	82.00	153.
98.50	183.0	.877E-06	1.30	85.00	147.
98.25	187.2	.896E-06	1.27	92.00	138.
98.00	192.9	.908E-06	1.23	101.00	131.
97.75	195.4	.936E-06	1.21	110.00	126.
97.50	192.5	.991E-06	1.23	112.00	126.
97.25	187.9	.106E-05	1.25	108.00	127.
97.00	186.4	.112E-05	1.26	100.00	128.

Table B5. Robin Sphere (XONICS) 2018 at 0855 GMT from XONICS Analysis (Cont.)¹

ALTITUDE (KM)	TEMPERATURE (CEG. K)	DENSITY (KG/M**3)	DENSITY / MODEL	WIND SPEED (M/SEC)	WIND DIRECTION (DEG.)
96.75	188.6	.115E-05	1.24	90.00	128.
96.50	193.6	.117E-05	1.20	79.00	124.
96.25	199.7	.119E-05	1.17	71.00	118.
96.00	205.1	.120E-05	1.12	68.00	111.
95.75	207.7	.124E-05	1.11	70.00	106.
95.50	206.9	.129E-05	1.10	74.00	106.
95.25	205.4	.136E-05	1.10	80.00	106.
95.00	204.2	.142E-05	1.10	90.00	106.
94.75	203.0	.149E-05	1.10	99.00	106.
94.50	202.1	.156E-05	1.10	107.00	107.
94.25	202.7	.162E-05	1.09	115.00	103.
94.00	205.1	.166E-05	1.06	119.00	98.
93.75	205.4	.173E-05	1.05	117.00	94.
93.50	202.4	.183E-05	1.06	109.00	91.
93.25	199.5	.193E-05	1.07	99.00	87.
93.00	198.7	.202E-05	1.06	91.00	82.
92.75	199.2	.210E-05	1.05	87.00	77.
92.50	199.5	.219E-05	1.05	85.00	72.
92.25	199.6	.228E-05	1.04	83.00	66.
92.00	199.5	.238E-05	1.03	84.00	60.
91.75	200.0	.247E-05	1.02	91.00	53.
91.50	200.3	.257E-05	1.01	101.00	47.
91.25	200.0	.269E-05	1.01	111.00	42.
91.00	198.9	.282E-05	1.01	117.00	38.
90.75	197.8	.295E-05	1.01	119.00	36.
90.50	198.8	.306E-05	1.00	121.00	33.
90.25	201.7	.314E-05	.98	128.00	28.
90.00	204.0	.324E-05	.96	137.00	23.
89.75	204.7	.336E-05	.95	142.00	19.
89.50	203.6	.352E-05	.95	135.00	19.
89.25	203.7	.366E-05	.94	124.00	20.
89.00	205.3	.379E-05	.93	112.00	21.
88.75	207.4	.390E-05	.92	96.00	21.
88.50	209.1	.403E-05	.90	80.00	18.
88.25	210.3	.417E-05	.89	66.00	15.
88.00	211.3	.431E-05	.88	55.00	13.
87.75	213.4	.444E-05	.86	49.00	15.
87.50	215.1	.458E-05	.85	44.00	22.
87.25	215.8	.474E-05	.84	39.00	32.
87.00	216.0	.492E-05	.83	34.00	46.
86.75	217.1	.509E-05	.82	29.00	63.
86.50	219.1	.524E-05	.81	27.00	80.
86.25	220.8	.540E-05	.79	25.00	92.
86.00	221.2	.559E-05	.78	23.00	98.
85.75	221.2	.581E-05	.78	20.00	88.
85.50	220.8	.604E-05	.77	22.00	64.
85.25	218.6	.634E-05	.77	31.00	50.
85.00	214.6	.671E-05	.78	38.00	45.
84.75	210.3	.711E-05	.79	43.00	46.
84.50	207.1	.752E-05	.80	45.00	49.
84.25	204.0	.794E-05	.80	44.00	56.
84.00	201.9	.837E-05	.81	39.00	68.
83.75	200.9	.876E-05	.81	35.00	84.
83.50	200.9	.913E-05	.80	35.00	100.

Table B5. Robin Sphere (XONICS) 2018 at 0855 GMT from XONICS Analysis (Cont.)

ALTITUDE (KM)	TEMPERATURE (DEG.K)	DENSITY (KG/M**3)	DENSITY / MODEL	WIND SPEED (M/SEC)	WIND DIRECTION (DEG.)
83.25	201.0	.951E-05	.80	39.00	112.
83.00	200.8	.992E-05	.80	45.00	122.
82.75	200.7	.103E-04	.79	53.00	125.
82.50	200.8	.108E-04	.79	62.00	127.
82.25	200.9	.112E-04	.79	71.00	129.
82.00	201.0	.117E-04	.79	79.00	131.
81.75	201.4	.122E-04	.79	86.00	133.
81.50	201.9	.126E-04	.78	92.00	134.
81.25	201.6	.132E-04	.78	94.00	134.
81.00	199.7	.139E-04	.79	91.00	130.
80.75	196.9	.147E-04	.80	86.00	121.
80.50	192.7	.157E-04	.82	84.00	108.
80.25	187.7	.168E-04	.84	84.00	95.
80.00	184.5	.179E-04	.86	84.00	84.
79.75	181.9	.190E-04	.87	89.00	74.
79.50	181.7	.199E-04	.88	89.00	65.
79.25	182.7	.207E-04	.88	89.00	58.
79.00	184.3	.214E-04	.87	87.00	52.
78.75	186.2	.222E-04	.87	82.00	49.
78.50	187.6	.230E-04	.87	75.00	48.
78.25	188.2	.240E-04	.87	63.00	51.
78.00	188.4	.251E-04	.87	47.00	59.
77.75	188.2	.262E-04	.88	32.00	76.
77.50	186.8	.276E-04	.89	23.00	106.
77.25	184.2	.293E-04	.91	22.00	138.
77.00	180.4	.313E-04	.93	22.00	157.
76.75	175.9	.336E-04	.97	20.00	167.
76.50	172.3	.360E-04	1.00	15.00	183.
76.25	170.5	.382E-04	1.02	12.00	222.
76.00	170.0	.402E-04	1.03	16.00	260.
75.75	170.7	.421E-04	1.04	23.00	277.
75.50	172.4	.437E-04	1.04	30.00	283.
75.25	173.5	.456E-04	1.05	33.00	283.
75.00	174.1	.477E-04	1.05	34.00	276.
74.75	174.9	.498E-04	1.06	34.00	264.
74.50	175.6	.520E-04	1.07	34.00	252.
74.25	176.4	.542E-04	1.07	36.00	242.
74.00	177.5	.565E-04	1.08	37.00	232.
73.75	178.9	.588E-04	1.08	38.00	224.
73.50	180.1	.611E-04	1.09	39.00	219.
73.25	181.6	.635E-04	1.09	39.00	215.
73.00	182.8	.660E-04	1.09	38.00	213.
72.75	184.3	.685E-04	1.09	38.00	211.
72.50	186.2	.709E-04	1.09	38.00	210.
72.25	187.8	.735E-04	1.09	37.00	209.
72.00	189.5	.762E-04	1.09	35.00	210.
71.75	191.3	.788E-04	1.09	34.00	213.
71.50	193.3	.815E-04	1.09	34.00	217.
71.25	196.2	.838E-04	1.08	34.00	222.
71.00	198.2	.865E-04	1.08	33.00	224.
70.75	199.8	.895E-04	1.08	32.00	224.
70.50	202.3	.921E-04	1.07	30.00	224.
70.25	204.1	.951E-04	1.07	29.00	223.
70.00	205.2	.985E-04	1.07	28.00	221.

Table B5. Robin Sphere (XONICS) 2018 at 0855 GMT from XONICS Analysis (Cont.)

ALTITUDE (KM)	TEMPERATURE (DEG.K)	DENSITY (KG/M**3)	DENSITY / MODEL	WIND SPEED (M/SEC)	WIND DIRECTION (DEG.)
69.75	205.8	.102E-03	1.07	26.00	217.
69.50	206.9	.106E-03	1.07	26.00	218.
69.25	205.6	.111E-03	1.09	25.00	218.
69.00	204.5	.116E-03	1.10	20.00	213.
68.75	204.6	.121E-03	1.11	15.00	205.
68.50	208.4	.124E-03	1.10	12.00	200.
68.25	212.1	.127E-03	1.09	10.00	212.
68.00	215.1	.130E-03	1.08	10.00	230.
67.75	218.3	.133E-03	1.06	12.00	244.
67.50	221.0	.136E-03	1.05	13.00	255.
67.25	223.3	.140E-03	1.05	13.00	264.
67.00	225.1	.144E-03	1.04	14.00	273.
66.75	227.1	.148E-03	1.04	15.00	283.
66.50	229.0	.153E-03	1.04	16.00	292.
66.25	230.1	.157E-03	1.03	16.00	300.
66.00	231.6	.162E-03	1.03	17.00	306.
65.75	234.1	.166E-03	1.03	18.00	311.
65.50	235.8	.171E-03	1.02	18.00	314.
65.25	236.3	.177E-03	1.03	20.00	312.
65.00	235.4	.184E-03	1.03	22.00	306.
64.75	234.6	.191E-03	1.04	25.00	301.
64.50	234.8	.198E-03	1.05	27.00	299.
64.25	235.8	.204E-03	1.04	29.00	299.
64.00	236.8	.211E-03	1.05	29.00	300.
63.75	238.5	.217E-03	1.04	30.00	301.
63.50	240.1	.223E-03	1.04	31.00	302.
63.25	242.1	.229E-03	1.04	32.00	302.
63.00	244.3	.235E-03	1.03	33.00	303.
62.75	245.5	.242E-03	1.03	33.00	304.
62.50	246.8	.249E-03	1.03	34.00	306.
62.25	247.7	.256E-03	1.03	35.00	308.
62.00	249.0	.264E-03	1.03	36.00	310.
61.75	250.2	.271E-03	1.02	38.00	312.
61.50	251.4	.279E-03	1.02	41.00	314.
61.25	252.8	.287E-03	1.02	43.00	315.
61.00	254.4	.295E-03	1.01	44.00	317.
60.75	255.8	.303E-03	1.01	45.00	319.
60.50	257.6	.311E-03	1.01	46.00	321.
60.25	259.7	.318E-03	1.00	46.00	321.
60.00	262.0	.326E-03	.99	46.00	320.
59.75	264.2	.333E-03	.98	44.00	319.
59.50	265.5	.343E-03	.98	44.00	317.
59.25	268.2	.350E-03	.97	42.00	314.
59.00	268.7	.360E-03	.97	40.00	310.
58.75	268.5	.372E-03	.97	36.00	307.
58.50	266.9	.386E-03	.98	31.00	305.
58.25	264.4	.402E-03	.99	29.00	303.
58.00	263.9	.416E-03	.99	28.00	301.
57.75	266.2	.425E-03	.98	27.00	301.
57.50	264.4	.442E-03	.99	26.00	302.
57.25	262.2	.460E-03	1.00	27.00	304.
57.00	259.9	.479E-03	1.01	27.00	303.
56.75	260.8	.493E-03	1.01	26.00	302.
56.50	266.8	.498E-03	.99	25.00	299.

Table B5. Robin Sphere (XONICS) 2081 at 0855 GMT from XONICS Analysis (Cont.)

ALTITUDE (KM)	TEMPERATURE (DEG. K)	DENSITY (KG/M**3)	DENSITY / MODEL	WIND SPEED (M/SEC)	WIND DIRECTION (DEG.)
56.25	268.9	.509E-03	.98	23.00	292.
56.00	265.4	.533E-03	1.00	22.00	292.
55.75	262.2	.557E-03	1.01	22.00	297.
55.50	261.3	.577E-03	1.01	24.00	301.
55.25	260.6	.597E-03	1.02	27.00	312.
55.00	264.4	.608E-03	1.01	29.00	305.
54.75	269.2	.616E-03	.99	30.00	308.
54.50	272.4	.628E-03	.98	31.00	309.
54.25	274.4	.642E-03	.97	31.00	310.
54.00	275.6	.659E-03	.97	31.00	309.
53.75	277.0	.676E-03	.97	30.00	309.
53.50	277.2	.697E-03	.97	27.00	308.
53.25	278.6	.714E-03	.96	24.00	309.
53.00	280.0	.732E-03	.96	20.00	311.
52.75	279.3	.757E-03	.96	16.00	312.
52.50	281.0	.775E-03	.95	13.00	325.
52.25	280.9	.798E-03	.95	12.00	342.
52.00	278.8	.829E-03	.96	13.00	355.
51.75	279.7	.851E-03	.96	15.00	10.
51.50	277.1	.885E-03	.97	16.00	12.
51.25	274.6	.921E-03	.97	15.00	10.
51.00	273.3	.954E-03	.98	14.00	4.
50.75	274.0	.982E-03	.98	12.00	356.
50.50	272.0	.102E-02	.99	9.00	344.
50.25	268.5	.107E-02	1.00	7.00	321.
50.00	268.4	.110E-02	1.00	4.00	280.
49.75	270.0	.113E-02	1.00	4.00	244.
49.50	270.7	.116E-02	.99	6.00	224.
49.25	272.4	.119E-02	.99	6.00	223.
49.00	273.5	.122E-02	.98	5.00	233.
48.75	271.9	.127E-02	.99	6.00	249.
48.50	268.8	.132E-02	.99	8.00	254.
48.25	266.2	.138E-02	1.01	10.00	253.
48.00	267.0	.142E-02	1.00	9.00	251.
47.75	273.3	.143E-02	.98	6.00	251.
47.50	275.6	.146E-02	.97	6.00	265.
47.25	270.6	.153E-02	.98	9.00	274.
47.00	265.0	.162E-02	1.01	13.00	276.
46.75	266.6	.166E-02	1.00	16.00	276.
46.50	264.6	.172E-02	1.00	19.00	271.
46.25	268.4	.175E-02	.99	19.00	268.
46.00	270.1	.180E-02	.98	19.00	267.
45.75	267.7	.187E-02	.99	20.00	267.
45.50	267.1	.194E-02	.99	20.00	270.
45.25	272.9	.196E-02	.97	19.00	276.
45.00	271.6	.203E-02	.97	20.00	279.
44.75	269.2	.211E-02	.97	20.00	284.
44.50	269.5	.217E-02	.97	20.00	289.
44.25	267.9	.225E-02	.97	20.00	292.
44.00	266.7	.234E-02	.97	19.00	294.
43.75	268.0	.240E-02	.97	15.00	296.
43.50	270.0	.246E-02	.96	10.00	297.
43.25	268.5	.255E-02	.96	3.00	303.
43.00	266.0	.266E-02	.97	5.00	102.

Table B5. Robin Sphere (XONICS) 2018 at 0855 GMT from XONICS Analysis (Cont.)

ALTITUDE (KM)	TEMPERATURE (DEG.K)	DENSITY (KG/M**3)	DENSITY % MODEL	WIND SPEED (M/SEC)	WIND DIRECTION (DEG.)
42.75	267.3	.273E-02	.96	14.00	98.
42.50	278.3	.270E-02	.92	25.00	93.
42.25	278.1	.279E-02	.91	29.00	91.
42.00	269.1	.297E-02	.94	29.00	90.
41.75	262.4	.314E-02	.96	27.00	90.
41.50	260.8	.327E-02	.96	28.00	90.
41.25	271.1	.324E-02	.92	31.00	89.
41.00	265.1	.342E-02	.94	31.00	92.
40.75	269.5	.348E-02	.92	35.00	94.
40.50	268.4	.360E-02	.92	36.00	97.
40.25	258.8	.385E-02	.95	37.00	100.
40.00	260.6	.395E-02	.94	40.00	101.
39.75	256.6	.415E-02	.96	43.00	102.
39.50	257.7	.427E-02	.95	44.00	102.
39.25	256.0	.444E-02	.96	43.00	101.
39.00	257.0	.457E-02	.95	41.00	99.
38.75	268.8	.451E-02	.91	40.00	100.

Table B6. Robin Sphere (XONICS) 2019A at 1041 GMT from XONICS Analysis

ALTITUDE (KM)	TEMPERATURE (DEG. K)	DENSITY (KG/M**3)	DENSITY / MODEL	WIND SPEED (M/SEC)	WIND DIRECTION (DEG.)
104.50	200.7	.315E-06	1.41	97.00	240.
104.25	193.4	.341E-06	1.45	99.00	244.
104.00	208.1	.330E-06	1.34	77.00	252.
103.75	228.1	.313E-06	1.22	55.00	264.
103.50	236.7	.312E-06	1.16	44.00	268.
103.25	232.8	.329E-06	1.16	42.00	254.
103.00	214.9	.369E-06	1.25	56.00	233.
102.75	194.7	.425E-06	1.37	76.00	220.
102.50	185.5	.465E-06	1.43	91.00	213.
102.25	187.1	.482E-06	1.42	97.00	209.
102.00	194.0	.486E-06	1.36	96.00	207.
101.75	201.3	.488E-06	1.31	90.00	205.
101.50	204.4	.501E-06	1.28	83.00	204.
101.25	206.1	.517E-06	1.26	73.00	202.
101.00	209.2	.530E-06	1.23	61.00	198.
100.75	208.4	.553E-06	1.23	54.00	193.
100.50	200.3	.599E-06	1.27	55.00	190.
100.25	191.1	.655E-06	1.33	61.00	188.
100.00	191.6	.682E-06	1.32	76.00	183.
99.75	198.3	.688E-06	1.28	98.00	177.
99.50	206.8	.687E-06	1.22	110.00	171.
99.25	213.4	.693E-06	1.18	115.00	164.
99.00	209.6	.733E-06	1.19	120.00	161.
98.75	199.0	.804E-06	1.25	123.00	161.
98.50	190.7	.875E-06	1.30	124.00	161.
98.25	188.0	.928E-06	1.32	123.00	160.
98.00	189.8	.960E-06	1.30	122.00	155.
97.75	191.6	.993E-06	1.29	121.00	150.
97.50	189.4	.105E-05	1.30	120.00	147.
97.25	187.3	.111E-05	1.31	120.00	145.
97.00	187.8	.116E-05	1.31	120.00	143.
96.75	189.6	.120E-05	1.29	121.00	141.
96.50	190.8	.124E-05	1.27	123.00	139.
96.25	192.1	.129E-05	1.26	124.00	138.
96.00	194.0	.133E-05	1.24	126.00	136.
95.75	195.1	.138E-05	1.23	127.00	135.
95.50	196.4	.143E-05	1.22	127.00	133.
95.25	200.0	.146E-05	1.19	127.00	129.
95.00	206.2	.148E-05	1.15	130.00	124.
94.75	209.9	.151E-05	1.12	133.00	123.
94.50	208.9	.158E-05	1.11	129.00	121.
94.25	207.2	.166E-05	1.11	121.00	117.
94.00	208.2	.172E-05	1.10	115.00	109.
93.75	210.2	.177E-05	1.08	112.00	99.
93.50	208.2	.186E-05	1.08	107.00	92.
93.25	204.6	.197E-05	1.09	102.00	84.
93.00	202.8	.207E-05	1.09	100.00	77.
92.75	203.1	.215E-05	1.08	102.00	70.
92.50	203.6	.223E-05	1.07	105.00	64.
92.25	202.9	.234E-05	1.07	106.00	60.
92.00	201.4	.245E-05	1.06	105.00	56.

Table B6. Robin Sphere (XONICS) 2019A at 1041 GMT from XONICS Analysis (Cont.)

ALTITUDE (KM)	TEMPERATURE (DEG.K)	DENSITY (KG/M**3)	DENSITY / MODEL	WIND SPEED (M/SEC)	WIND DIRECTION (DEG.)
91.75	200.1	.257E-05	1.06	104.00	54.
91.50	198.9	.270E-05	1.06	103.00	51.
91.25	199.6	.280E-05	1.05	103.00	49.
91.00	201.1	.290E-05	1.04	105.00	48.
90.75	201.9	.301E-05	1.03	105.00	47.
90.50	201.4	.314E-05	1.02	102.00	46.
90.25	200.9	.328E-05	1.02	99.00	45.
90.00	202.1	.340E-05	1.01	98.00	44.
89.75	202.9	.353E-05	1.00	96.00	43.
89.50	202.9	.367E-05	.99	92.00	42.
89.25	202.8	.383E-05	.99	88.00	41.
89.00	203.7	.397E-05	.98	86.00	40.
88.75	204.4	.412E-05	.97	83.00	41.
88.50	203.8	.430E-05	.96	78.00	42.
88.25	202.6	.451E-05	.96	72.00	44.
88.00	201.8	.472E-05	.96	67.00	45.
87.75	203.0	.489E-05	.95	64.00	46.
87.50	205.1	.504E-05	.94	63.00	47.
87.25	206.8	.520E-05	.92	61.00	48.
87.00	207.9	.538E-05	.91	59.00	49.
86.75	208.9	.557E-05	.90	57.00	49.
86.50	211.0	.574E-05	.88	57.00	50.
86.25	213.4	.590E-05	.87	57.00	51.
86.00	214.7	.610E-05	.86	56.00	52.
85.75	215.6	.631E-05	.84	55.00	53.
85.50	215.8	.655E-05	.84	53.00	56.
85.25	215.3	.683E-05	.83	51.00	59.
85.00	214.0	.714E-05	.83	47.00	63.
84.75	212.5	.747E-05	.83	44.00	69.
84.50	211.0	.783E-05	.83	42.00	75.
84.25	208.9	.822E-05	.83	40.00	84.
84.00	206.7	.865E-05	.83	39.00	92.
83.75	204.7	.909E-05	.84	40.00	100.
83.50	203.4	.953E-05	.84	42.00	105.
83.25	202.2	.999E-05	.84	45.00	109.
83.00	201.4	.105E-04	.84	48.00	111.
82.75	201.0	.109E-04	.84	53.00	111.
82.50	201.0	.114E-04	.84	53.00	109.
82.25	201.1	.118E-04	.83	56.00	106.
82.00	201.0	.124E-04	.83	59.00	103.
81.75	200.7	.129E-04	.83	61.00	100.
81.50	200.0	.135E-04	.83	63.00	96.
81.25	198.7	.141E-04	.83	65.00	93.
81.00	197.0	.149E-04	.84	66.00	90.
80.75	195.0	.157E-04	.85	66.00	88.
80.50	192.5	.166E-04	.86	66.00	86.
80.25	189.4	.176E-04	.88	65.00	85.
80.00	186.3	.187E-04	.90	63.00	84.
79.75	183.8	.198E-04	.91	60.00	83.
79.50	182.2	.209E-04	.92	59.00	82.
79.25	181.0	.221E-04	.94	57.00	81.
79.00	180.6	.232E-04	.95	55.00	81.
78.75	180.4	.243E-04	.95	52.00	81.
78.50	180.7	.254E-04	.96	50.00	81.

Table B6. Robin Sphere (XONICS) 2019A at 1041 GMT from XONICS Analysis (Cont.)

ALTITUDE (KM)	TEMPERATURE (DEG.K)	DENSITY (KG/M**3)	DENSITY / MODEL	WIND SPEED (M/SEC)	WIND DIRECTION (DEG.)
78.25	181.5	.264E-04	.96	48.00	80.
78.00	183.0	.275E-04	.96	46.00	79.
77.75	184.6	.285E-04	.95	44.00	76.
77.50	186.5	.295E-04	.95	42.00	73.
77.25	188.0	.306E-04	.95	39.00	69.
77.00	189.0	.318E-04	.95	35.00	65.
76.75	189.1	.332E-04	.95	31.00	59.
76.50	188.3	.348E-04	.96	26.00	53.
76.25	187.9	.365E-04	.97	21.00	45.
76.00	187.4	.382E-04	.98	17.00	34.
75.75	187.4	.400E-04	.99	15.00	22.
75.50	188.0	.417E-04	.99	13.00	10.
75.25	189.5	.432E-04	.99	13.00	3.
75.00	191.6	.446E-04	.99	13.00	358.
74.75	192.5	.464E-04	.99	13.00	349.
74.50	193.9	.481E-04	.99	13.00	334.
74.25	195.4	.498E-04	.99	13.00	319.
74.00	196.6	.516E-04	.99	15.00	307.
73.75	196.6	.539E-04	.99	16.00	295.
73.50	195.9	.564E-04	1.00	19.00	285.
73.25	195.4	.590E-04	1.01	22.00	278.
73.00	195.4	.616E-04	1.02	24.00	273.
72.75	195.7	.642E-04	1.03	26.00	270.
72.50	196.2	.668E-04	1.03	27.00	268.
72.25	196.6	.695E-04	1.03	27.00	268.
72.00	197.7	.721E-04	1.04	28.00	268.
71.75	198.0	.751E-04	1.04	28.00	268.
71.50	198.4	.782E-04	1.05	27.00	269.
71.25	199.2	.812E-04	1.05	27.00	271.
71.00	199.8	.844E-04	1.05	26.00	272.
70.75	200.3	.878E-04	1.06	25.00	273.
70.50	201.9	.938E-04	1.06	24.00	273.
70.25	202.7	.942E-04	1.06	24.00	271.
70.00	203.0	.980E-04	1.06	24.00	267.
69.75	203.0	.102E-03	1.07	26.00	263.
69.50	202.4	.107E-03	1.08	29.00	259.
69.25	200.6	.112E-03	1.10	29.00	257.
69.00	199.8	.117E-03	1.11	25.00	258.
68.75	200.4	.122E-03	1.12	20.00	260.
68.50	205.2	.124E-03	1.10	17.00	264.
68.25	207.8	.128E-03	1.10	17.00	265.
68.00	210.4	.131E-03	1.08	18.00	267.
67.75	213.5	.135E-03	1.08	19.00	269.
67.50	215.4	.139E-03	1.08	19.00	272.
67.25	217.5	.143E-03	1.07	18.00	275.
67.00	219.7	.147E-03	1.07	18.00	279.
66.75	221.6	.151E-03	1.06	18.00	283.
66.50	223.6	.156E-03	1.06	18.00	289.
66.25	225.3	.160E-03	1.05	19.00	294.
66.00	227.2	.165E-03	1.05	20.00	297.
65.75	229.4	.169E-03	1.04	21.00	298.
65.50	230.3	.175E-03	1.05	23.00	297.
65.25	229.7	.182E-03	1.06	26.00	293.
65.00	229.1	.189E-03	1.06	28.00	291.

Table B6. Robin Sphere (XONICS) 2019A at 1041 GMT from XONICS Analysis (Cont.)

ALTITUDE (KM)	TEMPERATURE (DEG.K)	DENSITY (KG/M**3)	DENSITY / MODEL	WIND SPEED (M/SEC)	WIND DIRECTION (DEG.)
64.75	230.3	.195E-03	1.06	30.00	293.
64.50	231.9	.201E-03	1.06	31.00	295.
64.25	233.9	.206E-03	1.05	31.00	298.
64.00	235.1	.213E-03	1.06	31.00	299.
63.75	236.1	.220E-03	1.06	32.00	300.
63.50	237.9	.226E-03	1.06	32.00	301.
63.25	241.1	.231E-03	1.05	32.00	303.
63.00	243.5	.236E-03	1.04	32.00	306.
62.75	245.3	.243E-03	1.04	32.00	307.
62.50	246.0	.250E-03	1.03	32.00	309.
62.25	246.3	.259E-03	1.04	33.00	310.
62.00	246.8	.267E-03	1.04	34.00	313.
61.75	247.8	.275E-03	1.04	35.00	316.
61.50	249.3	.283E-03	1.03	37.00	319.
61.25	250.2	.292E-03	1.04	38.00	322.
61.00	251.3	.300E-03	1.03	40.00	325.
60.75	253.1	.308E-03	1.03	41.00	328.
60.50	255.0	.316E-03	1.02	42.00	330.
60.25	256.7	.324E-03	1.02	42.00	330.
60.00	257.1	.334E-03	1.02	41.00	329.
59.75	257.3	.345E-03	1.02	39.00	326.
59.50	259.3	.354E-03	1.01	37.00	322.
59.25	260.2	.364E-03	1.01	34.00	314.
59.00	260.2	.376E-03	1.01	32.00	307.
58.75	262.1	.385E-03	1.00	30.00	304.
58.50	264.4	.394E-03	1.00	29.00	303.
58.25	263.7	.408E-03	1.00	29.00	303.
58.00	263.1	.422E-03	1.00	28.00	303.
57.75	262.9	.436E-03	1.01	26.00	303.
57.50	262.0	.452E-03	1.01	25.00	301.
57.25	261.3	.468E-03	1.02	24.00	295.
57.00	260.0	.486E-03	1.02	23.00	289.
56.75	260.1	.501E-03	1.02	22.00	284.
56.50	261.1	.516E-03	1.02	21.00	280.
56.25	262.4	.530E-03	1.02	20.00	277.
56.00	263.3	.545E-03	1.02	20.00	276.
55.75	265.1	.559E-03	1.01	21.00	282.
55.50	264.7	.578E-03	1.02	22.00	291.
55.25	265.3	.595E-03	1.02	24.00	300.
55.00	265.2	.614E-03	1.02	25.00	303.
54.75	264.7	.635E-03	1.02	27.00	300.
54.50	267.1	.649E-03	1.01	28.00	302.
54.25	272.8	.656E-03	.99	28.00	304.
54.00	274.8	.671E-03	.99	27.00	302.
53.75	275.0	.692E-03	.99	27.00	300.
53.50	277.1	.708E-03	.98	26.00	301.
53.25	277.3	.729E-03	.98	24.00	300.
53.00	276.0	.755E-03	.99	23.00	300.
52.75	276.1	.778E-03	.99	22.00	305.
52.50	277.9	.796E-03	.98	19.00	312.
52.25	276.7	.824E-03	.98	17.00	318.
52.00	275.1	.855E-03	.99	16.00	325.
51.75	278.4	.870E-03	.98	15.00	340.
51.50	280.4	.891E-03	.97	15.00	353.

Table B6. Robin Sphere (XONICS) 2019A at 1041 GMT from XONICS Analysis (Cont.)

ALTITUDE (KM)	TEMPERATURE (DEG.K)	DENSITY (KG/M**3)	DENSITY / MODEL	WIND SPEED (M/SEC)	WIND DIRECTION (DEG.)
51.25	279.5	.921E-03	.97	17.00	360.
51.00	280.5	.945E-03	.97	19.00	5.
50.75	277.7	.984E-03	.98	19.00	360.
50.50	277.1	.102E-02	.99	18.00	354.
50.25	279.3	.104E-02	.97	16.00	354.
50.00	281.6	.106E-02	.96	11.00	353.
49.75	276.8	.111E-02	.98	6.00	334.
49.50	270.1	.118E-02	1.01	4.00	278.
49.25	268.4	.122E-02	1.01	5.00	230.
49.00	269.9	.125E-02	1.00	5.00	213.
48.75	270.7	.129E-02	1.00	6.00	211.
48.50	270.6	.133E-02	1.00	7.00	221.
48.25	267.5	.139E-02	1.02	9.00	226.
48.00	263.5	.145E-02	1.03	10.00	227.
47.75	267.6	.148E-02	1.01	7.00	218.
47.50	266.2	.153E-02	1.02	6.00	224.
47.25	262.5	.160E-02	1.03	7.00	247.
47.00	261.4	.166E-02	1.03	10.00	263.
46.75	263.4	.171E-02	1.03	12.00	269.
46.50	263.5	.176E-02	1.03	15.00	265.
46.25	262.4	.182E-02	1.03	18.00	262.
46.00	265.9	.186E-02	1.01	18.00	262.
45.75	270.9	.188E-02	.99	16.00	262.
45.50	269.3	.195E-02	.99	16.00	263.
45.25	270.5	.201E-02	.99	15.00	271.
45.00	277.7	.201E-02	.96	14.00	286.
44.75	275.6	.209E-02	.96	15.00	297.
44.50	270.8	.220E-02	.98	17.00	306.
44.25	270.9	.226E-02	.97	18.00	315.
44.00	270.1	.234E-02	.97	18.00	317.
43.75	266.4	.245E-02	.99	16.00	315.
43.50	265.5	.254E-02	.99	12.00	312.
43.25	266.7	.261E-02	.98	5.00	324.
43.00	266.4	.269E-02	.98	5.00	82.
42.75	269.8	.275E-02	.96	15.00	92.
42.50	272.6	.280E-02	.95	23.00	90.
42.25	261.9	.301E-02	.99	24.00	89.
42.00	256.7	.317E-02	1.00	23.00	87.
41.75	258.2	.326E-02	1.00	22.00	85.
41.50	264.6	.328E-02	.97	25.00	82.
41.25	261.3	.343E-02	.98	27.00	82.
41.00	264.4	.350E-02	.96	29.00	81.
40.75	256.3	.373E-02	.99	29.00	84.
40.50	258.9	.382E-02	.98	30.00	87.
40.25	256.3	.398E-02	.99	33.00	93.
40.00	255.4	.413E-02	.99	37.00	96.
39.75	257.2	.424E-02	.98	40.00	96.
39.50	259.9	.433E-02	.97	41.00	93.
39.25	254.2	.458E-02	.99	40.00	91.
39.00	252.0	.478E-02	.99	39.00	89.
38.75	255.3	.487E-02	.98	40.00	89.
38.50	251.7	.511E-02	.99	38.00	89.
38.25	248.4	.536E-02	1.00	36.00	88.
38.00	249.0	.552E-02	1.00	35.00	89.

Table B7. Robin Sphere (XONICS) 2021 at 1243 GMT from XONICS Analysis

ALTITUDE (KM)	TEMPERATURE (DEG.K)	DENSITY (KG/M**3)	DENSITY / MODEL	WIND SPEED (M/SEC)	WIND DIRECTION (DEG.)
109.00	219.5	.137E-06	1.33	282.00	309.
108.75	186.1	.168E-06	1.57	162.00	287.
108.50	206.3	.158E-06	1.41	96.00	248.
108.25	202.7	.167E-06	1.44	54.00	221.
108.00	205.3	.172E-06	1.42	27.00	153.
107.75	197.1	.186E-06	1.47	69.00	113.
107.50	193.2	.198E-06	1.50	83.00	117.
107.25	177.3	.226E-06	1.65	94.00	138.
107.00	166.3	.253E-06	1.77	117.00	151.
106.75	170.4	.259E-06	1.73	138.00	153.
106.50	177.1	.261E-06	1.67	151.00	154.
106.25	183.2	.265E-06	1.62	155.00	154.
106.00	192.2	.263E-06	1.54	147.00	154.
105.75	197.5	.267E-06	1.50	128.00	154.
105.50	198.2	.278E-06	1.49	102.00	158.
105.25	197.1	.291E-06	1.49	73.00	164.
105.00	209.6	.285E-06	1.39	42.00	170.
104.75	229.7	.270E-06	1.26	14.00	198.
104.50	233.7	.275E-06	1.23	25.00	294.
104.25	199.2	.336E-06	1.43	38.00	290.
104.00	189.3	.369E-06	1.50	35.00	278.
103.75	198.4	.367E-06	1.43	39.00	319.
103.50	219.8	.345E-06	1.28	62.00	349.
103.25	231.4	.340E-06	1.20	77.00	1.
103.00	224.0	.364E-06	1.23	71.00	9.
102.75	205.2	.413E-06	1.33	52.00	19.
102.50	181.7	.487E-06	1.50	28.00	36.
102.25	164.7	.563E-06	1.65	14.00	92.
102.00	160.8	.607E-06	1.70	19.00	122.
101.75	167.4	.613E-06	1.64	20.00	97.
101.50	178.0	.605E-06	1.55	25.00	62.
101.25	185.7	.607E-06	1.48	27.00	47.
101.00	185.8	.634E-06	1.48	15.00	49.
100.75	181.6	.678E-06	1.51	12.00	176.
100.50	178.5	.722E-06	1.53	43.00	190.
100.25	175.6	.769E-06	1.56	80.00	188.
100.00	174.3	.813E-06	1.58	124.00	180.
99.75	177.4	.837E-06	1.55	173.00	174.
99.50	185.0	.840E-06	1.49	199.00	171.
99.25	191.6	.848E-06	1.44	220.00	170.
99.00	197.1	.860E-06	1.40	231.00	169.
98.75	200.6	.880E-06	1.37	231.00	169.
98.50	198.2	.929E-06	1.38	224.00	171.
98.25	191.1	.100E-05	1.42	211.00	175.
98.00	187.7	.107E-05	1.45	194.00	179.
97.75	192.0	.109E-05	1.41	172.00	183.
97.50	199.6	.110E-05	1.36	148.00	185.
97.25	204.5	.111E-05	1.31	129.00	187.
97.00	203.0	.117E-05	1.32	117.00	188.
96.75	199.4	.124E-05	1.33	112.00	186.
96.50	195.5	.132E-05	1.36	112.00	182.

Table B7. Robin Sphere (XONICS) 2021 at 1243 GMT from XONICS Analysis (Cont.)

ALTITUDE (KM)	TEMPERATURE (DEG. K)	DENSITY (KG/M**3)	DENSITY / MODEL	WIND SPEED (M/SEC)	WIND DIRECTION (DEG.)
96.25	192.9	.139E-05	1.36	116.00	177.
96.00	192.8	.146E-05	1.37	120.00	170.
95.75	194.4	.151E-05	1.35	125.00	162.
95.50	195.1	.157E-05	1.34	129.00	156.
95.25	194.0	.164E-05	1.33	130.00	152.
95.00	192.9	.172E-05	1.33	127.00	148.
94.75	193.3	.180E-05	1.33	121.00	142.
94.50	194.3	.187E-05	1.32	114.00	137.
94.25	194.6	.194E-05	1.30	105.00	133.
94.00	195.7	.202E-05	1.29	96.00	127.
93.75	198.0	.208E-05	1.27	91.00	119.
93.50	200.0	.214E-05	1.24	86.00	111.
93.25	201.4	.222E-05	1.23	85.00	105.
93.00	202.5	.230E-05	1.21	84.00	99.
92.75	203.6	.238E-05	1.19	83.00	95.
92.50	204.5	.247E-05	1.18	84.00	93.
92.25	204.5	.257E-05	1.17	86.00	93.
92.00	204.6	.268E-05	1.16	86.00	94.
91.75	206.1	.277E-05	1.15	92.00	95.
91.50	208.8	.284E-05	1.12	96.00	92.
91.25	210.8	.293E-05	1.10	97.00	92.
91.00	210.6	.305E-05	1.09	94.00	93.
90.75	209.8	.318E-05	1.09	89.00	93.
90.50	210.2	.331E-05	1.08	85.00	92.
90.25	212.0	.341E-05	1.06	82.00	89.
90.00	214.5	.350E-05	1.04	81.00	85.
89.75	214.5	.364E-05	1.03	82.00	88.
89.50	212.8	.381E-05	1.03	86.00	97.
89.25	211.0	.400E-05	1.03	89.00	106.
89.00	211.9	.414E-05	1.02	77.00	104.
88.75	213.8	.427E-05	1.00	65.00	98.
88.50	214.2	.443E-05	.99	53.00	88.
88.25	213.6	.462E-05	.99	43.00	72.
88.00	213.4	.480E-05	.98	39.00	51.
87.75	214.4	.497E-05	.97	42.00	33.
87.50	214.8	.516E-05	.96	47.00	23.
87.25	213.6	.539E-05	.96	50.00	17.
87.00	212.4	.563E-05	.95	50.00	15.
86.75	213.0	.584E-05	.94	49.00	17.
86.50	213.7	.605E-05	.93	47.00	22.
86.25	213.4	.630E-05	.93	45.00	31.
86.00	212.0	.660E-05	.93	44.00	44.
85.75	211.2	.688E-05	.92	45.00	56.
85.50	211.6	.715E-05	.91	48.00	65.
85.25	211.7	.743E-05	.90	52.00	71.
85.00	211.2	.775E-05	.90	55.00	75.
84.75	211.0	.806E-05	.89	57.00	78.
84.50	210.7	.840E-05	.89	59.00	85.
84.25	211.1	.872E-05	.88	55.00	83.
84.00	211.3	.906E-05	.87	50.00	73.
83.75	211.4	.942E-05	.87	48.00	64.
83.50	212.0	.977E-05	.86	46.00	56.
83.25	212.3	.101E-04	.85	43.00	54.
83.00	212.2	.106E-04	.85	41.00	59.

Table B7. Robin Sphere (XONICS) 2021 at 1243 GMT from XONICS Analysis (Cont.)

ALTITUDE (KM)	TEMPERATURE (DEG. K)	DENSITY (KG/M**3)	DENSITY / MODEL	WIND SPEED (M/SEC)	WIND DIRECTION (DEG.)
82.75	211.6	.110E-04	.85	42.00	70.
82.50	210.5	.115E-04	.85	49.00	84.
82.25	209.2	.120E-04	.84	59.00	96.
82.00	208.1	.126E-04	.85	72.00	103.
81.75	207.1	.132E-04	.85	87.00	107.
81.50	206.7	.137E-04	.84	98.00	109.
81.25	206.9	.143E-04	.84	105.00	109.
81.00	207.4	.148E-04	.84	108.00	108.
80.75	207.9	.154E-04	.84	106.00	105.
80.50	208.4	.160E-04	.83	100.00	100.
80.25	208.6	.166E-04	.83	93.00	92.
80.00	207.6	.174E-04	.83	88.00	83.
79.75	207.1	.182E-04	.84	80.00	71.
79.50	206.1	.190E-04	.84	74.00	60.
79.25	205.1	.199E-04	.84	70.00	51.
79.00	203.7	.208E-04	.85	66.00	46.
78.75	202.3	.219E-04	.86	65.00	46.
78.50	200.7	.230E-04	.87	64.00	50.
78.25	198.8	.242E-04	.88	65.00	57.
78.00	196.7	.255E-04	.89	69.00	65.
77.75	194.5	.269E-04	.90	74.00	72.
77.50	192.9	.283E-04	.91	78.00	75.
77.25	191.6	.297E-04	.92	78.00	76.
77.00	191.2	.311E-04	.93	77.00	73.
76.75	191.7	.324E-04	.93	74.00	67.
76.50	193.1	.336E-04	.93	71.00	60.
76.25	194.6	.348E-04	.93	68.00	52.
76.00	196.1	.360E-04	.92	65.00	45.
75.75	197.1	.374E-04	.92	61.00	40.
75.50	197.6	.389E-04	.93	57.00	39.
75.25	197.8	.405E-04	.93	50.00	40.
75.00	197.9	.423E-04	.94	44.00	47.
74.75	198.3	.440E-04	.94	38.00	49.
74.50	198.0	.460E-04	.95	32.00	50.
74.25	197.3	.481E-04	.95	27.00	49.
74.00	197.4	.501E-04	.96	22.00	45.
73.75	198.7	.520E-04	.96	18.00	33.
73.50	199.1	.541E-04	.96	15.00	10.
73.25	198.7	.565E-04	.97	15.00	342.
73.00	198.2	.591E-04	.98	17.00	318.
72.75	198.1	.616E-04	.98	18.00	300.
72.50	197.4	.645E-04	.99	17.00	284.
72.25	196.6	.676E-04	1.01	15.00	261.
72.00	195.1	.710E-04	1.02	14.00	235.
71.75	194.4	.744E-04	1.03	15.00	213.
71.50	194.8	.775E-04	1.04	16.00	207.
71.25	195.2	.807E-04	1.04	16.00	214.
71.00	196.2	.838E-04	1.05	16.00	232.
70.75	197.2	.870E-04	1.05	18.00	253.
70.50	197.6	.906E-04	1.05	22.00	266.
70.25	198.6	.940E-04	1.06	27.00	267.
70.00	199.3	.977E-04	1.06	29.00	260.
69.75	198.9	.102E-03	1.07	29.00	256.
69.50	199.6	.106E-03	1.07	31.00	257.

Table B7. Robin Sphere (XONICS) 2031 at 1243 GMT from XONICS Analysis (Cont.)

ALTITUDE (KM)	TEMPERATURE (DEG.K)	DENSITY (KG/M**3)	DENSITY / MODEL	WIND SPEED (M/SEC)	WIND DIRECTION (DEG.)
69.25	201.0	.110E-03	1.08	31.00	256.
69.00	200.7	.115E-03	1.09	29.00	253.
68.75	199.4	.120E-03	1.10	23.00	253.
68.50	199.5	.125E-03	1.11	16.00	260.
68.25	203.8	.128E-03	1.10	15.00	279.
68.00	207.9	.130E-03	1.08	17.00	292.
67.75	211.7	.133E-03	1.06	20.00	296.
67.50	214.7	.137E-03	1.06	21.00	293.
67.25	215.8	.141E-03	1.06	20.00	285.
67.00	216.6	.146E-03	1.06	20.00	279.
66.75	218.9	.151E-03	1.06	20.00	251.
66.50	222.2	.154E-03	1.05	22.00	241.
66.25	226.0	.157E-03	1.03	24.00	312.
66.00	228.5	.161E-03	1.03	26.00	308.
65.75	229.0	.167E-03	1.03	25.00	355.
65.50	227.7	.174E-03	1.04	25.00	249.
65.25	226.6	.181E-03	1.05	26.00	297.
65.00	227.6	.167E-03	1.05	29.00	302.
64.75	230.4	.192E-03	1.05	30.00	307.
64.50	232.5	.197E-03	1.04	32.00	311.
64.25	234.5	.203E-03	1.04	33.00	314.
64.00	236.1	.209E-03	1.04	33.00	318.
63.75	237.6	.215E-03	1.04	33.00	316.
63.50	239.1	.221E-03	1.03	33.00	316.
63.25	241.4	.227E-03	1.03	35.00	316.
63.00	243.5	.233E-03	1.02	36.00	315.
62.75	244.5	.240E-03	1.02	37.00	314.
62.50	245.0	.248E-03	1.02	38.00	312.
62.25	244.6	.256E-03	1.03	38.00	310.
62.00	244.6	.265E-03	1.03	38.00	311.
61.75	245.9	.273E-03	1.03	38.00	314.
61.50	248.6	.280E-03	1.02	39.00	318.
61.25	251.4	.286E-03	1.01	40.00	324.
61.00	253.3	.293E-03	1.01	41.00	327.
60.75	254.3	.302E-03	1.01	42.00	331.
60.50	254.4	.312E-03	1.01	41.00	334.
60.25	254.3	.322E-03	1.01	41.00	336.
60.00	254.8	.332E-03	1.01	41.00	336.
59.75	255.6	.342E-03	1.01	41.00	335.
59.50	255.2	.354E-03	1.01	40.00	335.
59.25	255.8	.365E-03	1.01	41.00	332.
59.00	257.7	.375E-03	1.01	39.00	328.
58.75	262.6	.380E-03	.99	39.00	322.
58.50	268.3	.383E-03	.97	38.00	317.
58.25	266.3	.399E-03	.98	34.00	316.
58.00	259.8	.422E-03	1.00	29.00	314.
57.75	258.9	.437E-03	1.01	27.00	312.
57.50	260.9	.448E-03	1.00	28.00	309.
57.25	261.0	.462E-03	1.00	26.00	304.
57.00	261.1	.477E-03	1.01	20.00	287.
56.75	260.7	.493E-03	1.01	16.00	272.
56.50	257.5	.516E-03	1.02	13.00	282.
56.25	254.1	.540E-03	1.04	14.00	293.
56.00	253.8	.559E-03	1.04	16.00	300.

Table B7. Robin Sphere (XONICS) 2021 at 1243 GMT from XONICS Analysis (Cont.)

ALTITUDE (KM)	TEMPERATURE (DEG. K)	DENSITY (KG/M**3)	DENSITY / MODEL	WIND SPEED (M/SEC)	WIND DIRECTION (DEG.)
55.75	254.3	.577E-03	1.05	19.00	303.
55.50	258.6	.586E-03	1.03	24.00	299.
55.25	261.7	.598E-03	1.02	23.00	295.
55.00	260.8	.620E-03	1.03	22.00	301.
54.75	262.6	.635E-03	1.02	23.00	304.
54.50	265.6	.648E-03	1.01	27.00	308.
54.25	265.3	.670E-03	1.02	23.00	304.
54.00	266.0	.690E-03	1.01	21.00	298.
53.75	268.7	.704E-03	1.01	23.00	303.
53.50	269.2	.725E-03	1.01	21.00	307.
53.25	268.8	.749E-03	1.01	17.00	306.
53.00	269.2	.772E-03	1.01	17.00	309.
52.75	269.0	.797E-03	1.01	13.00	315.
52.50	269.5	.821E-03	1.01	11.00	322.
52.25	272.0	.838E-03	1.00	15.00	330.
52.00	268.4	.877E-03	1.02	17.00	330.
51.75	264.7	.917E-03	1.03	18.00	326.
51.50	264.3	.948E-03	1.03	22.00	323.
51.25	264.8	.977E-03	1.03	19.00	326.
51.00	267.4	.998E-03	1.02	18.00	330.
50.75	267.6	.103E-02	1.03	17.00	332.
50.50	271.3	.105E-02	1.01	13.00	346.
50.25	279.2	.105E-02	.98	13.00	353.
50.00	283.4	.107E-02	.97	12.00	350.
49.75	284.9	.109E-02	.96	13.00	336.
49.50	285.0	.112E-02	.96	13.00	321.
49.25	287.2	.115E-02	.95	14.00	317.
49.00	285.9	.119E-02	.95	12.00	306.
48.75	279.8	.125E-02	.97	11.00	284.
48.50	276.9	.130E-02	.98	9.00	258.
48.25	277.7	.134E-02	.98	9.00	230.
48.00	281.5	.136E-02	.96	9.00	214.
47.75	280.1	.141E-02	.97	11.00	211.
47.50	269.9	.151E-02	1.00	14.00	214.
47.25	266.3	.158E-02	1.01	15.00	211.
47.00	273.6	.158E-02	.98	13.00	203.
46.75	278.6	.160E-02	.96	10.00	200.
46.50	275.9	.167E-02	.97	9.00	214.
46.25	271.6	.175E-02	.99	9.00	235.
46.00	273.0	.179E-02	.98	10.00	251.
45.75	271.3	.186E-02	.98	13.00	253.
45.50	274.5	.190E-02	.97	14.00	252.
45.25	273.1	.196E-02	.97	17.00	250.
45.00	273.8	.202E-02	.96	17.00	251.
44.75	278.7	.205E-02	.95	15.00	260.
44.50	284.2	.207E-02	.92	13.00	274.
44.25	283.2	.214E-02	.92	12.00	288.
44.00	276.1	.226E-02	.94	12.00	297.
43.75	276.2	.233E-02	.94	10.00	315.
43.50	273.5	.242E-02	.94	8.00	333.
43.25	262.6	.260E-02	.98	5.00	7.
43.00	263.6	.268E-02	.97	11.00	62.
42.75	268.1	.272E-02	.95	20.00	73.
42.50	268.2	.280E-02	.95	25.00	76.

Table B7. Robin Sphere (XONICS) 2021 at 1243 GMT from XONICS Analysis (Cont.)

ALTITUDE (KM)	TEMPERATURE (DEG.K)	DENSITY (KG/M**3)	DENSITY / MODEL	WIND SPEED (M/SEC)	WIND DIRECTION (DEG.)
42.25	257.6	.301E-02	.99	25.00	76.
42.00	252.4	.318E-02	1.01	24.00	75.
41.75	255.2	.325E-02	.99	25.00	73.
41.50	256.5	.334E-02	.99	26.00	74.
41.25	252.5	.351E-02	1.00	27.00	77.
41.00	257.8	.355E-02	.98	29.00	79.
40.75	254.3	.372E-02	.99	28.00	83.
40.50	255.2	.383E-02	.98	29.00	85.
40.25	255.2	.396E-02	.98	30.00	87.
40.00	253.0	.413E-02	.99	32.00	88.
39.75	252.2	.428E-02	.99	33.00	89.
39.50	253.1	.441E-02	.98	34.00	89.
39.25	255.4	.452E-02	.97	35.00	88.
39.00	252.0	.473E-02	.98	36.00	90.
38.75	249.9	.494E-02	.99	36.00	90.
38.50	248.8	.513E-02	.99	36.00	89.
38.25	249.0	.530E-02	.99	34.00	88.
38.00	253.8	.538E-02	.97	35.00	87.
37.75	259.7	.544E-02	.95	37.00	85.

Table B8. Robin Sphere (ASL) 2018 at 0855 GMT from ASL Analysis

ALTITUDE (KM)	TEMPERATURE (DEG.K)	DENSITY (KG/M**3)	DENSITY / MODEL	WIND SPEED (M/SEC)	WIND DIRECTION (DEG.)
95.25	196.0	.143E-05	1.16	71.00	72.
94.25	199.0	.166E-05	1.11	72.00	52.
93.25	202.0	.194E-05	1.07	74.00	39.
92.25	205.0	.223E-05	1.02	72.00	31.
91.25	207.0	.259E-05	.97	67.00	27.
90.24	207.0	.304E-05	.94	60.00	29.
89.24	207.0	.357E-05	.92	53.00	37.
88.24	209.0	.415E-05	.89	51.00	49.
87.24	210.0	.484E-05	.86	50.00	63.
86.24	209.0	.571E-05	.84	53.00	73.
85.24	208.0	.673E-05	.82	56.00	80.
84.23	205.0	.799E-05	.81	56.00	83.
83.23	199.0	.976E-05	.82	55.00	86.
82.23	194.0	.119E-04	.83	51.00	87.
81.23	189.0	.145E-04	.85	45.00	89.
80.23	184.0	.177E-04	.88	38.00	90.
79.23	181.0	.216E-04	.91	29.00	92.
78.22	179.0	.262E-04	.94	21.00	96.
77.22	177.0	.318E-04	.98	11.00	111.
76.22	177.0	.385E-04	1.02	7.00	171.
75.22	176.0	.465E-04	1.06	13.00	218.
74.22	179.0	.553E-04	1.09	22.00	227.
73.21	183.0	.652E-04	1.11	29.00	227.
72.21	187.0	.760E-04	1.12	33.00	223.
71.21	198.0	.867E-04	1.11	34.00	218.
70.21	201.0	.998E-04	1.12	30.00	214.
69.21	207.0	.114E-03	1.12	23.00	215.
68.20	215.0	.129E-03	1.10	16.00	228.
67.20	227.0	.142E-03	1.06	12.00	264.
66.20	232.0	.161E-03	1.06	16.00	297.
65.20	235.0	.184E-03	1.06	24.00	305.
64.20	237.0	.210E-03	1.07	30.00	304.
63.19	244.0	.235E-03	1.06	34.00	304.
62.19	250.0	.261E-03	1.04	38.00	310.
61.19	253.0	.296E-03	1.04	42.00	318.
60.19	259.0	.326E-03	1.02	44.00	319.

Table B9. Robin Sphere (ASL) 2019A at 1041 GMT from ASL Analysis

ALTITUDE (KM)	TEMPERATURE (DEG.K)	DENSITY (KG/M**3)	DENSITY / MODEL	WIND SPEED (M/SEC)	WIND DIRECTION (DEG.)
95.25	193.0	.156E-05	1.27	129.00	81.
94.25	202.0	.176E-05	1.18	124.00	76.
93.25	214.0	.195E-05	1.08	104.00	69.
92.25	234.0	.215E-05	.93	83.00	61.
91.25	232.0	.238E-05	.89	64.00	51.
90.24	215.0	.298E-05	.92	49.00	41.
89.24	194.0	.333E-05	1.10	42.00	31.
88.24	192.0	.468E-05	1.00	36.00	29.
87.24	196.0	.545E-05	.96	32.00	39.
86.24	203.0	.620E-05	.91	33.00	59.
85.24	207.0	.715E-05	.87	37.00	73.
84.23	209.0	.829E-05	.84	43.00	92.
83.23	207.0	.988E-05	.83	49.00	87.
82.23	200.0	.120E-04	.84	53.00	39.
81.23	192.0	.149E-04	.88	55.00	89.
80.23	183.0	.186E-04	.92	55.00	88.
79.23	181.0	.225E-04	.95	52.00	86.
78.22	182.0	.268E-04	.97	45.00	82.
77.22	186.0	.314E-04	.97	37.00	75.
76.22	186.0	.377E-04	1.00	25.00	60.
75.22	187.0	.447E-04	1.02	15.00	32.
74.22	189.0	.529E-04	1.04	13.00	336.
73.21	192.0	.620E-04	1.06	20.00	298.
72.21	196.0	.721E-04	1.07	27.00	291.
71.21	206.0	.811E-04	.90	31.00	270.
70.21	198.0	.986E-04	1.10	30.00	265.
69.21	199.0	.116E-03	1.13	25.00	260.
68.20	208.0	.132E-03	1.13	19.00	259.
67.20	223.0	.144E-03	1.07	20.00	270.
66.20	225.0	.166E-03	1.08	24.00	285.
65.20	233.0	.184E-03	1.06	27.00	295.
64.20	232.0	.214E-03	1.09	31.00	301.
63.19	236.0	.243E-03	1.09	33.00	306.
62.19	268.0	.245E-03	.97	34.00	315.
61.19	245.0	.306E-03	1.08	37.00	324.
60.19	254.0	.337E-03	1.05	40.00	327.

Table B10. Robin Sphere (ASL) 2021 at 1243 GMT from ASL Analysis

ALTITUDE (KM)	TEMPERATURE (DEG.K)	DENSITY (KG/M**3)	DENSITY / MODEL	WIND SPEED (M/SEC)	WIND DIRECTION (DEG.)
95.25	198.0	.173E-05	1.41	96.00	144.
94.25	209.0	.192E-05	1.29	89.00	134.
93.25	220.0	.212E-05	1.17	66.00	122.
92.25	225.0	.241E-05	1.10	57.00	109.
91.25	222.0	.282E-05	1.06	52.00	96.
90.24	216.0	.337E-05	1.05	53.00	88.
89.24	209.0	.407E-05	1.05	48.00	82.
88.24	217.0	.482E-05	1.03	48.00	80.
87.24	206.0	.570E-05	1.01	51.00	80.
86.24	207.0	.666E-05	.98	57.00	80.
85.24	211.0	.766E-05	.93	61.00	81.
84.23	214.0	.880E-05	.89	65.00	80.
83.23	214.0	.103E-04	.87	70.00	80.
82.23	212.0	.122E-04	.86	72.00	78.
81.23	208.0	.146E-04	.86	73.00	77.
80.23	202.0	.176E-04	.88	71.00	75.
79.23	197.0	.214E-04	.90	68.00	72.
78.22	194.0	.257E-04	.93	65.00	69.
77.22	193.0	.307E-04	.95	58.00	65.
76.22	192.0	.365E-04	.97	48.00	59.
75.22	195.0	.428E-04	.98	38.00	52.
74.22	197.0	.502E-04	.99	26.00	41.
73.21	200.0	.586E-04	1.00	13.00	19.
72.21	198.0	.696E-04	1.03	9.00	302.
71.21	197.0	.829E-04	1.07	17.00	260.
70.21	196.0	.986E-04	1.10	24.00	248.
69.21	201.0	.114E-03	1.11	24.00	248.
68.20	209.0	.129E-03	1.10	23.00	260.
67.20	218.0	.145E-03	1.08	22.00	230.
66.20	225.0	.163E-03	1.07	26.00	239.
65.20	230.0	.185E-03	1.06	29.00	309.
64.20	235.0	.209E-03	1.06	32.00	312.
63.19	244.0	.231E-03	1.04	34.00	313.
62.19	248.0	.260E-03	1.04	38.00	316.
61.19	251.0	.294E-03	1.03	41.00	324.
60.19	253.0	.332E-03	1.03	42.00	332.

Table B11. AFGL Accelerometer Sphere at 1226 GMT

ALTITUDE (KM)	TEMPERATURE (CEG.K)	DENSITY (KG/M**3)	DENSITY / MODEL
75.88	194.8	.332E-04	.84
75.06	183.6	.409E-04	.91
74.92	182.0	.420E-04	.92
74.78	180.4	.430E-04	.92
74.64	179.0	.440E-04	.92
74.51	177.8	.453E-04	.93
74.37	176.7	.470E-04	.95
74.23	175.7	.489E-04	.97
74.09	175.0	.510E-04	.99
73.95	174.5	.532E-04	1.01
73.82	174.2	.554E-04	1.03
73.68	174.0	.571E-04	1.04
73.54	174.0	.587E-04	1.05
73.40	174.1	.601E-04	1.05
73.26	174.2	.614E-04	1.05
73.12	174.2	.624E-04	1.05
72.98	174.2	.640E-04	1.06
72.84	174.1	.657E-04	1.06
72.71	173.9	.675E-04	1.07
72.57	173.7	.693E-04	1.08
72.43	173.5	.708E-04	1.08
72.29	173.4	.726E-04	1.09
72.15	173.3	.748E-04	1.10
72.01	173.4	.777E-04	1.12
71.87	173.6	.801E-04	1.13
71.73	174.0	.820E-04	1.13
71.59	174.5	.837E-04	1.13
71.45	175.1	.858E-04	1.14
71.31	175.8	.878E-04	1.14
71.17	176.5	.898E-04	1.15
71.03	177.3	.917E-04	1.15
70.89	178.1	.931E-04	1.14
70.75	178.9	.947E-04	1.14
70.61	179.7	.964E-04	1.14
70.47	180.6	.983E-04	1.14
70.33	181.6	.100E-03	1.14
70.18	182.7	.103E-03	1.15
70.04	183.9	.106E-03	1.15
69.90	185.2	.108E-03	1.16
69.76	186.6	.110E-03	1.16
69.62	188.1	.112E-03	1.16
69.48	189.8	.114E-03	1.15
69.34	191.5	.115E-03	1.14
69.20	193.4	.117E-03	1.14
69.06	195.2	.118E-03	1.13
68.91	197.2	.120E-03	1.12
68.77	199.1	.121E-03	1.11
68.63	201.1	.123E-03	1.10
68.49	203.1	.124E-03	1.10
68.35	205.1	.126E-03	1.09
68.20	207.1	.128E-03	1.09

Table B11. AFGL Accelerometer Sphere at 1226 GMT (Cont.)

ALTITUDE (KM)	TEMPERATURE (CEG.K)	DENSITY (KG/M**3)	DENSITY / MODEL
68.06	209.1	.129E-03	1.08
67.92	211.1	.130E-03	1.07
67.78	213.0	.131E-03	1.06
67.64	214.9	.133E-03	1.05
67.49	216.7	.134E-03	1.04
67.35	218.4	.137E-03	1.04
67.21	219.9	.139E-03	1.04
67.06	221.3	.142E-03	1.04
66.92	222.5	.144E-03	1.04
66.78	223.5	.147E-03	1.04
66.64	224.3	.150E-03	1.04
66.49	225.0	.152E-03	1.03
66.35	225.5	.155E-03	1.03
66.21	225.9	.158E-03	1.04
66.06	226.2	.161E-03	1.04
65.92	226.4	.165E-03	1.04
65.78	226.5	.168E-03	1.04
65.63	226.5	.172E-03	1.04
65.49	226.7	.175E-03	1.05
65.34	226.8	.179E-03	1.05
65.20	227.2	.182E-03	1.05
65.06	227.7	.186E-03	1.05
64.91	228.4	.189E-03	1.05
64.77	229.4	.192E-03	1.05
64.62	230.5	.196E-03	1.05
64.48	231.7	.199E-03	1.05
64.34	233.0	.202E-03	1.04
64.19	234.2	.205E-03	1.04
64.05	235.4	.208E-03	1.04
63.90	236.4	.211E-03	1.03
63.76	237.3	.214E-03	1.03
63.61	238.0	.218E-03	1.03
63.47	238.7	.221E-03	1.03
63.32	239.4	.226E-03	1.03
63.18	240.0	.230E-03	1.03
63.03	240.7	.234E-03	1.03
62.89	241.5	.238E-03	1.03
62.74	242.4	.242E-03	1.03
62.60	243.3	.246E-03	1.03
62.45	244.2	.250E-03	1.03
62.31	245.1	.254E-03	1.02
62.16	246.0	.258E-03	1.02
62.01	246.8	.262E-03	1.02
61.87	247.6	.267E-03	1.02
61.72	248.2	.272E-03	1.02
61.58	248.9	.276E-03	1.02
61.43	249.5	.281E-03	1.02
61.28	250.1	.286E-03	1.02
61.14	250.8	.291E-03	1.02
60.99	251.5	.295E-03	1.01
60.85	252.3	.300E-03	1.01
60.70	253.1	.305E-03	1.01
60.55	254.0	.310E-03	1.01
60.40	254.9	.314E-03	1.01

Table B11. AFGL Accelerometer Sphere at 1226 GMT (Cont.)

ALTITUDE (KM)	TEMPERATURE (DEG.K)	DENSITY (KG/M**3)	DENSITY / MODEL
60.26	255.8	.320E-03	1.00
60.11	256.6	.325F-03	1.00
59.96	257.5	.330E-03	1.00
59.82	258.3	.335E-03	1.00
59.67	259.0	.341E-03	1.00
59.52	259.7	.346F-03	.99
59.38	260.4	.352E-03	.99
59.23	261.0	.358E-03	.99
59.08	261.5	.364E-03	.99
58.94	262.0	.370E-03	.99
58.79	262.5	.376E-03	.99
58.64	262.9	.382E-03	.98
58.49	263.3	.389E-03	.98
58.35	263.6	.396E-03	.98
58.20	263.9	.403E-03	.98
58.05	264.1	.411E-03	.98
57.90	264.3	.419F-03	.98
57.75	264.4	.427E-03	.99
57.60	264.5	.435E-03	.99
57.46	264.5	.443E-03	.99
57.31	264.5	.452E-03	.99
57.16	264.4	.460E-03	.99
57.01	264.4	.469E-03	.99
56.86	264.3	.478E-03	.99
56.71	264.3	.486E-03	.99
56.57	264.3	.496E-03	.99
56.42	264.3	.505E-03	.99
56.27	264.3	.515E-03	.99
56.12	264.4	.524E-03	.99
55.97	264.6	.534E-03	.99
55.82	264.9	.544E-03	.99
55.67	265.2	.554E-03	.99
55.52	265.6	.564E-03	.99
55.38	266.0	.573F-03	.99
55.23	266.4	.583E-03	.99
55.08	266.9	.593E-03	.99
54.93	267.3	.603E-03	.99
54.78	267.7	.613E-03	.99
54.63	268.2	.624E-03	.99
54.48	268.6	.635E-03	.99
54.33	269.0	.646E-03	.99
54.18	269.4	.657E-03	.99
54.03	269.8	.669E-03	.99
53.88	270.2	.680E-03	.99
53.73	270.6	.692E-03	.99
53.58	271.0	.704E-03	.99
53.43	271.4	.716E-03	.98
53.28	271.7	.728E-03	.98
53.13	272.1	.741E-03	.98
52.98	272.4	.754E-03	.98
52.83	272.7	.767E-03	.98
52.68	272.9	.781E-03	.98
52.53	273.1	.795E-03	.98
52.38	273.3	.809E-03	.98

Table B11. AFGL Accelerometer Sphere at 1226 GMT (Cont.)

ALTITUDE (KM)	TEMPERATURE (DEG.K)	DENSITY (KG/M**3)	DENSITY / MODEL
52.23	273.5	.824E-03	.98
52.38	273.6	.839E-03	.98
51.93	273.7	.854E-03	.98
51.78	273.7	.870E-03	.98
51.63	273.7	.886E-03	.98
51.48	273.7	.903E-03	.98
51.33	273.6	.920E-03	.98
51.18	273.4	.938E-03	.98
51.03	273.2	.956E-03	.98
50.88	273.0	.975E-03	.99
50.73	272.7	.994E-03	.99
50.58	272.4	.101E-02	.99
50.42	272.1	.103E-02	.99
50.27	271.7	.106E-02	.99
50.12	271.4	.108E-02	.99
49.97	271.0	.110E-02	.99
49.82	270.7	.112E-02	.99
49.67	270.4	.114E-02	1.00
49.52	270.2	.116E-02	1.00
49.37	269.9	.119E-02	1.00
49.22	269.8	.121E-02	1.00
49.07	269.6	.123E-02	1.00
48.92	269.5	.126E-02	1.00
48.76	269.4	.128E-02	1.00
48.61	269.3	.131E-02	1.00
48.46	269.3	.133E-02	1.00
48.31	269.3	.136E-02	1.00
48.16	269.2	.138E-02	1.00
48.01	269.2	.141E-02	1.00
47.86	269.2	.144E-02	1.00
47.71	269.1	.147E-02	1.00
47.56	269.0	.149E-02	1.00
47.41	268.9	.152E-02	1.00
47.25	268.9	.155E-02	1.00
47.10	268.8	.158E-02	1.00
46.95	268.7	.161E-02	1.00
46.80	268.7	.165E-02	1.00
46.65	268.6	.168E-02	1.00
46.50	268.6	.171E-02	1.00
46.35	268.5	.174E-02	.99
46.20	268.5	.178E-02	.99
46.04	268.3	.181E-02	.99
45.89	268.2	.185E-02	.99
45.74	268.0	.188E-02	.99
45.59	267.8	.192E-02	.99
45.44	267.6	.196E-02	.99
45.29	267.3	.200E-02	.99
45.14	267.0	.204E-02	.99
44.99	266.7	.208E-02	.99
44.83	266.4	.212E-02	.99
44.68	266.0	.217E-02	.99
44.53	265.6	.221E-02	.99
44.38	265.2	.226E-02	.99
44.23	264.7	.231E-02	.99

Table B12. Hypersonic Sphere at 1142 GMT from MIT
Lincoln Laboratory Analysis

ALTITUDE (KM)	TEMPERATURE (DEG.K)	DENSITY (KG/M**3)	DENSITY / MODEL
130.20	426.5	.114E-07	1.59
129.91	440.3	.113E-07	1.54
129.62	444.8	.114E-07	1.51
129.32	436.2	.119E-07	1.54
129.03	433.1	.122E-07	1.54
128.73	421.7	.128E-07	1.57
128.44	417.8	.132E-07	1.58
128.15	411.0	.137E-07	1.60
127.85	429.0	.135E-07	1.53
127.56	439.7	.134E-07	1.48
127.26	450.8	.134E-07	1.44
126.97	439.4	.140E-07	1.46
126.68	424.3	.148E-07	1.51
126.38	410.2	.156E-07	1.55
126.09	403.1	.163E-07	1.57
125.79	394.9	.170E-07	1.60
125.50	399.7	.172E-07	1.58
125.20	419.5	.167E-07	1.50
124.91	442.3	.162E-07	1.41
124.61	462.6	.158E-07	1.34
124.32	470.9	.159E-07	1.31
124.02	479.3	.159E-07	1.28
123.73	483.8	.161E-07	1.26
123.43	477.7	.166E-07	1.26
123.14	460.9	.175E-07	1.30
122.84	456.0	.181E-07	1.30
122.55	443.1	.190E-07	1.33
122.25	430.1	.200E-07	1.35
121.96	412.8	.213E-07	1.39
121.66	405.1	.222E-07	1.41
121.37	400.3	.230E-07	1.41
121.07	400.2	.235E-07	1.39
120.78	397.1	.243E-07	1.38
120.48	396.8	.249E-07	1.36
120.19	400.0	.252E-07	1.33
119.89	399.0	.259E-07	1.31
119.60	399.9	.264E-07	1.29
119.30	400.1	.271E-07	1.26
119.01	400.8	.276E-07	1.24
118.71	399.8	.284E-07	1.22
118.41	397.0	.292E-07	1.20
118.12	386.7	.308E-07	1.21
117.82	377.9	.322E-07	1.21
117.53	366.5	.341E-07	1.23
117.23	352.5	.364E-07	1.25
116.94	338.2	.389E-07	1.28
116.64	328.6	.412E-07	1.30
116.34	320.9	.435E-07	1.31
116.05	318.7	.450E-07	1.30
115.75	316.5	.467E-07	1.29
115.46	316.3	.481E-07	1.27

Table B12. Hypersonic Sphere at 1142 GMT from MIT
Lincoln Laboratory Analysis (Cont.)

ALTITUDE (KM)	TEMPERATURE (DEG .K)	DENSITY (KG/M**3)	DENSITY / MODEL
115.16	316.7	.495E-07	1.25
114.86	315.4	.512E-07	1.23
114.57	313.9	.530E-07	1.22
114.27	313.8	.547E-07	1.20
113.97	313.5	.564E-07	1.19
113.33	312.8	.603E-07	1.15
113.03	310.5	.627E-07	1.14
112.73	305.9	.656E-07	1.14
112.44	300.1	.690E-07	1.14
112.14	294.7	.725E-07	1.15
111.84	288.2	.766E-07	1.16
111.55	283.7	.804E-07	1.16
111.25	279.6	.844E-07	1.16
110.95	274.9	.888E-07	1.17
110.66	270.8	.934E-07	1.17
110.36	266.1	.984E-07	1.18
110.06	262.8	.103E-06	1.18
109.76	259.9	.108E-06	1.18
109.47	264.3	.110E-06	1.15
109.17	260.4	.116E-06	1.16
108.87	258.8	.121E-06	1.15
108.58	253.9	.128E-06	1.16
108.28	251.1	.135E-06	1.17
107.98	245.5	.143E-06	1.18
107.68	242.3	.151E-06	1.18
107.39	239.4	.159E-06	1.19
107.09	236.7	.168E-06	1.19
106.79	235.3	.176E-06	1.18
106.49	230.4	.187E-06	1.19
106.20	226.0	.199E-06	1.21
105.90	225.0	.208E-06	1.20
105.60	226.4	.216E-06	1.18
105.30	226.8	.225E-06	1.16
105.01	224.8	.237E-06	1.16
104.71	222.1	.250E-06	1.16
104.41	219.3	.265E-06	1.16
104.11	216.7	.280E-06	1.16
103.81	214.0	.297E-06	1.17
103.52	208.2	.320E-06	1.19
103.22	201.5	.346E-06	1.22
102.92	194.5	.377E-06	1.25
102.62	190.6	.404E-06	1.27
102.32	187.3	.433E-06	1.29
102.02	185.0	.462E-06	1.30
101.73	183.4	.492E-06	1.31
101.43	183.4	.519E-06	1.31
101.13	185.5	.541E-06	1.29
100.83	187.0	.565E-06	1.28
100.53	188.7	.590E-06	1.26
100.23	189.0	.620E-06	1.26
99.93	190.7	.648E-06	1.24
99.64	192.0	.677E-06	1.23
99.34	194.0	.705E-06	1.22
99.04	194.3	.741E-06	1.21

Table B12. Hypersonic Sphere at 1142 GMT from MIT
Lincoln Laboratory Analysis (Cont.)

ALTITUDE (KM)	TEMPERATURE (DEG.K)	DENSITY / (KG/M**3)	DENSITY / MODEL
98.74	194.5	.779E-06	1.21
98.44	194.2	.821E-06	1.20
98.14	193.3	.868E-06	1.21
97.84	192.2	.919E-06	1.21
97.54	191.2	.973E-06	1.21
97.25	191.0	.103E-05	1.21
96.95	190.8	.108E-05	1.21
96.65	191.8	.113E-05	1.20
96.35	192.8	.119E-05	1.19
96.05	194.6	.124E-05	1.17
95.75	196.0	.130E-05	1.16
95.45	197.5	.135E-05	1.14
95.15	198.3	.142E-05	1.13
94.85	199.5	.148E-05	1.12
94.55	200.5	.155E-05	1.10
94.25	201.2	.162E-05	1.09
93.95	201.0	.171E-05	1.08
93.65	200.1	.180E-05	1.08
93.36	199.1	.190E-05	1.07
93.05	198.9	.200E-05	1.07
92.76	199.5	.210E-05	1.05
92.46	200.2	.220E-05	1.04
92.16	201.6	.229E-05	1.03
91.86	203.5	.239E-05	1.01
91.56	205.4	.248E-05	.99
91.26	207.9	.257E-05	.97
90.96	209.3	.268E-05	.95
90.66	210.0	.280E-05	.94
90.36	210.0	.294E-05	.93
90.06	209.3	.309E-05	.93
89.76	209.7	.324E-05	.92
89.46	207.6	.343E-05	.92
89.16	204.8	.365E-05	.92
88.86	200.8	.391E-05	.94
88.56	196.6	.420E-05	.95
88.26	194.0	.447E-05	.96
87.96	192.7	.474E-05	.96
87.66	194.2	.495E-05	.95
87.36	197.2	.513E-05	.93
87.06	199.7	.533E-05	.91
86.76	201.7	.554E-05	.90
86.46	202.5	.580E-05	.89
86.16	203.3	.606E-05	.88
85.86	203.7	.636E-05	.87
85.56	204.6	.664E-05	.86
85.26	204.8	.697E-05	.85
84.96	203.5	.736E-05	.85
84.66	202.0	.779E-05	.85
84.36	201.1	.822E-05	.85
84.06	200.2	.867E-05	.85
83.76	200.7	.909E-05	.84
83.46	200.5	.956E-05	.84
83.16	200.5	.100E-04	.83
82.86	201.6	.105E-04	.82

Table B12. Hypersonic Sphere at 1142 GMT from MIT
Lincoln Laboratory Analysis (Cont.)

ALTITUDE (KM)	TEMPERATURE (DEG. K)	DENSITY (KG/M**3)	DENSITY / MODEL
82.56	202.5	.110E-04	.82
82.26	203.8	.115E-04	.81
81.96	204.9	.120E-04	.80
81.66	206.3	.125E-04	.79
81.36	207.8	.130E-04	.78
81.06	208.4	.136E-04	.78
80.76	206.7	.144E-04	.78
80.46	203.7	.153E-04	.79
80.16	199.7	.164E-04	.81
79.86	196.6	.175E-04	.82
79.57	195.3	.185E-04	.83
79.27	194.7	.196E-04	.83
78.97	194.8	.206E-04	.83
78.67	194.4	.217E-04	.84
78.37	194.4	.228E-04	.84
78.07	194.1	.240E-04	.85
77.77	193.9	.253E-04	.85
77.47	193.4	.267E-04	.86
77.17	193.3	.282E-04	.86
76.87	194.0	.295E-04	.86
76.57	195.5	.308E-04	.86
76.28	197.0	.322E-04	.86
75.98	196.9	.338E-04	.86
75.68	195.9	.358E-04	.87
75.38	195.3	.377E-04	.88
75.08	195.8	.396E-04	.89
74.79	197.4	.413E-04	.88
74.49	198.3	.432E-04	.89
74.25	198.0	.450E-04	.89
73.95	197.5	.475E-04	.90
73.65	196.7	.501E-04	.91
73.35	196.6	.527E-04	.92
73.06	196.9	.553E-04	.92
72.76	197.9	.578E-04	.92
72.47	199.0	.604E-04	.93
72.17	199.0	.635E-04	.93
71.87	198.4	.669E-04	.94
71.58	197.6	.705E-04	.95
71.28	197.1	.743E-04	.96
70.70	196.1	.824E-04	.99
70.40	194.5	.874E-04	1.00
70.11	193.4	.924E-04	1.02
69.82	192.4	.977E-04	1.03
69.52	193.5	.102E-03	1.04
69.23	194.9	.107E-03	1.04
68.94	196.3	.111E-03	1.04
68.65	198.1	.116E-03	1.04
68.36	200.6	.120E-03	1.04
68.07	203.4	.124E-03	1.04
67.78	205.8	.128E-03	1.03
67.49	208.0	.133E-03	1.03
67.20	210.0	.138E-03	1.03
66.91	212.1	.143E-03	1.03
66.62	213.9	.148E-03	1.02

Table B12. Hypersonic Sphere at 1142 GMT from MIT
Lincoln Laboratory Analysis (Cont.)

ALTITUDE (KM)	TEMPERATURE (DEG.K)	DENSITY (KG/M**3)	DENSITY / MODEL
66.33	215.7	.154E-03	1.02
66.05	217.5	.159E-03	1.02
65.76	219.2	.165E-03	1.02
65.48	220.8	.171E-03	1.02
65.19	222.0	.177E-03	1.02
64.91	222.7	.185E-03	1.02
64.63	223.2	.192E-03	1.03
64.34	224.4	.199E-03	1.03
64.06	226.1	.206E-03	1.03
63.78	227.0	.214E-03	1.03
63.50	229.8	.220E-03	1.03
63.22	232.0	.227E-03	1.02
62.94	232.4	.235E-03	1.03
62.67	233.9	.243E-03	1.03
62.39	236.1	.251E-03	1.02
62.11	238.2	.258E-03	1.02
61.84	239.4	.267E-03	1.02
61.56	240.7	.276E-03	1.02
61.29	241.4	.285E-03	1.02
61.02	241.8	.296E-03	1.02
60.75	242.4	.306E-03	1.02
60.48	243.0	.317E-03	1.02
60.21	244.1	.327E-03	1.02
59.94	244.7	.338E-03	1.02
59.68	245.2	.350E-03	1.02
59.41	246.2	.361E-03	1.02
59.15	247.4	.372E-03	1.02
58.89	248.8	.384E-03	1.02
58.62	249.8	.396E-03	1.02
58.10	251.2	.421E-03	1.02
57.85	251.7	.435E-03	1.02
57.59	252.6	.448E-03	1.02
57.34	252.8	.463E-03	1.02
57.08	252.0	.480E-03	1.02
56.83	251.7	.497E-03	1.03
56.58	251.5	.514E-03	1.03
56.33	250.5	.533E-03	1.04
56.08	250.2	.552E-03	1.04
55.84	250.9	.569E-03	1.04
55.59	252.3	.584E-03	1.04
55.35	254.1	.598E-03	1.03
55.11	255.5	.614E-03	1.03
54.87	256.8	.630E-03	1.03
54.63	258.5	.645E-03	1.02
54.39	260.6	.660E-03	1.02
54.16	262.5	.675E-03	1.01
53.93	263.7	.692E-03	1.01
53.70	264.5	.710E-03	1.01
53.47	265.4	.728E-03	1.01
53.24	265.9	.748E-03	1.00
53.01	265.3	.771E-03	1.01
52.79	265.4	.792E-03	1.01
52.57	266.1	.812E-03	1.01
52.35	266.4	.834E-03	1.01

Table B12. Hypersonic Sphere at 1142 GMT from MIT
Lincoln Laboratory Analysis (Cont.)

ALTITUDE (KM)	TEMPERATURE (DEG.K)	DENSITY (KG/M**3)	DENSITY / MODEL
52.13	267.2	.854E-03	1.01
51.91	268.5	.873E-03	1.00
51.70	269.6	.893E-03	1.00
51.49	271.0	.912E-03	.99
51.27	272.6	.930E-03	.99
51.07	272.9	.953E-03	.99
50.86	271.3	.983E-03	.99
50.65	268.6	.102E-02	1.00
50.45	267.0	.105E-02	1.01
50.25	266.9	.108E-02	1.01
50.05	267.6	.110E-02	1.01
49.85	268.5	.112E-02	1.00
49.66	269.3	.115E-02	1.00
49.46	270.2	.117E-02	1.00
49.27	271.2	.120E-02	.99
49.08	271.7	.122E-02	.99
48.90	271.0	.125E-02	.99
48.71	269.9	.129E-02	1.00
48.53	268.7	.132E-02	1.00
48.35	267.7	.136E-02	1.00
48.17	266.6	.139E-02	1.01
47.99	265.3	.143E-02	1.01
47.81	265.2	.146E-02	1.01
47.64	266.2	.149E-02	1.01
47.47	266.8	.152E-02	1.00
47.30	265.9	.156E-02	1.01
47.13	265.0	.159E-02	1.01
46.97	265.1	.163E-02	1.01
46.81	265.3	.166E-02	1.01
46.65	265.7	.169E-02	1.00
46.49	266.5	.172E-02	1.00
46.33	267.3	.175E-02	.99
46.17	268.1	.177E-02	.99
46.02	269.2	.180E-02	.98

Appendix C

Robin Sphere Analysis

The robin sphere is used to determine density, temperature and wind velocity from the radar tracking data. The tracking data must be smoothed by a filter to remove random fluctuations which would severely effect the time derivatives in determining velocity and acceleration. The measurements of range, azimuth, elevation and range rate (doppler velocity) must be used to determine position, velocity and acceleration vectors. To determine the wind velocity, the assumption is made that the wind vector lies in the horizontal plane and any vertical wind component is neglected. The vertical component of acceleration due to gravity must be vectorially removed from the total acceleration to obtain the drag acceleration used to calculate density. The filter used to smooth the data can remove some of the atmospheric structure, as was discussed in the text of this report. In Figures C1-C4, the results of the measurements for robin sphere 2018 are presented. This set of figures provides an example of the effect of the smoothing filter applied to two different radars tracking simultaneously the same sphere. The smoothing intervals for the ALCOR radar data processed by XONICS and the TPQ18 radar data processed by ASL are given in Tables 4 and 5. The point to notice is that the smaller smoothing interval of the ALCOR data provides much better detail in the atmospheric structure of the density, temperature and wind profiles in Figures C1-C4.

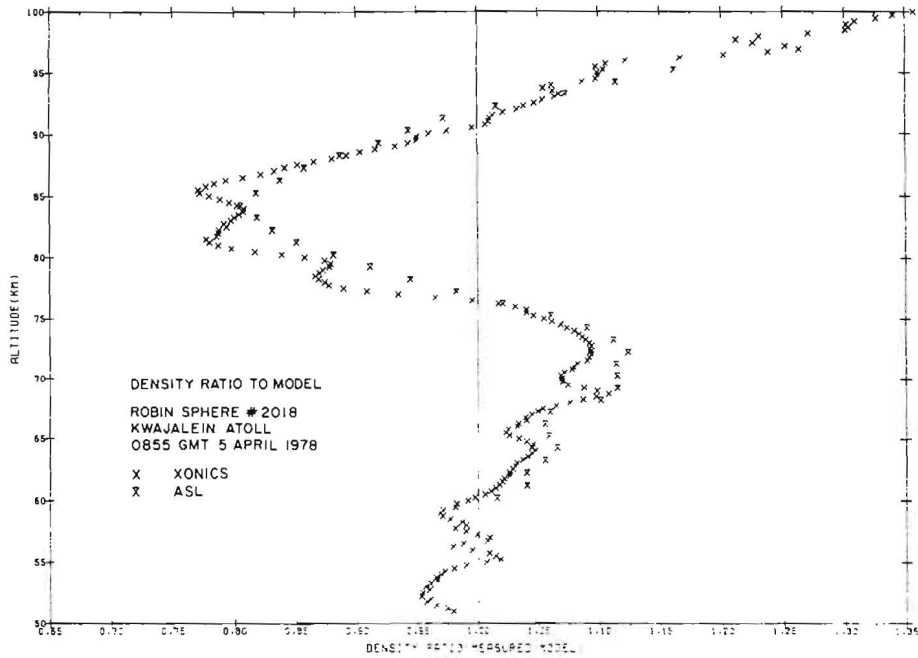


Figure C1. Comparison of the 2108 Robin Density Measurements to the Model for the ALCOR (XONICS) and TPQ-18 (ASL) Data Analysis. The effect of the longer smoothing interval used in the ASL analysis removes some of the structure seen in the XONICS profile

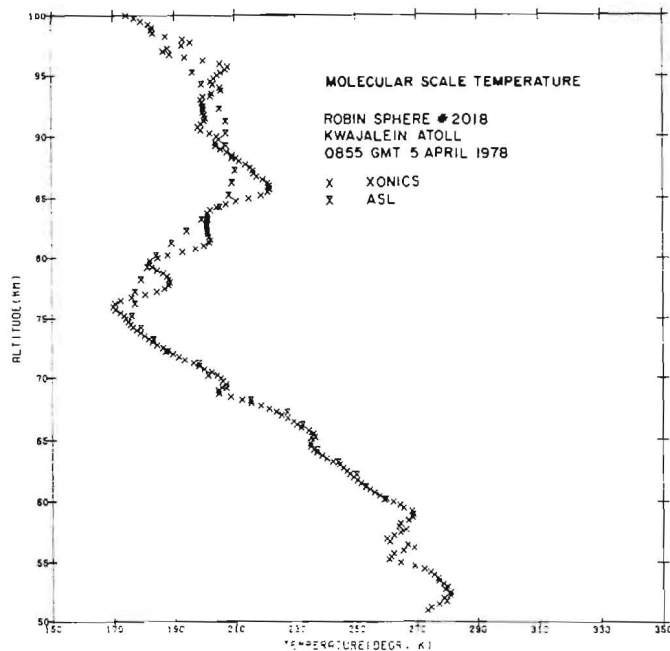


Figure C2. Comparison of the Temperature Measurements for the 2018 Robin From the XONICS and ASL Analysis

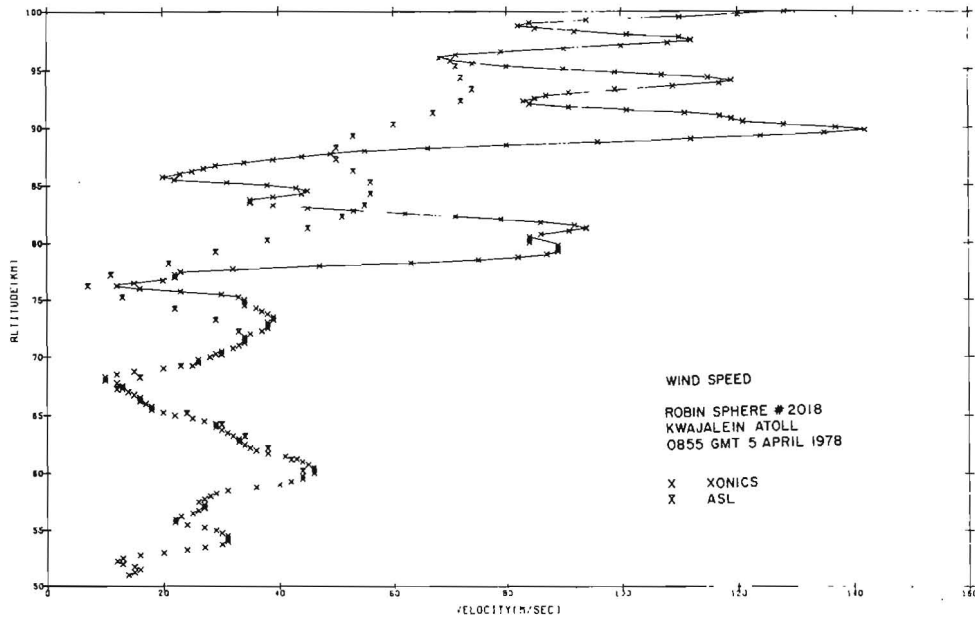


Figure C3. Comparison of the Wind Speed Measurements for the 2018 Robin From the XONICS and ASL Analysis

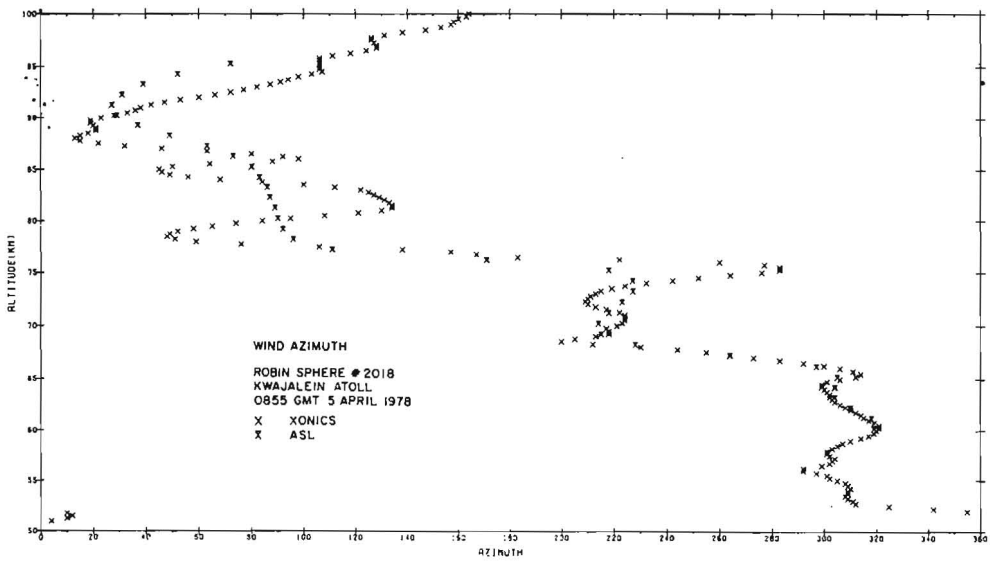


Figure C4. Comparison of the Wind Azimuth Measurements for the 2018 Robin From the XONICS and ASL Analysis

Appendix D

Hypersonic Sphere Analysis

The high velocity of the hypersonic sphere allows higher altitude measurements of atmospheric density than other passive sphere techniques because of the larger drag acceleration. Below 100 km the errors due to acceleration measurements become quite small, less than 1 percent (see Tables 6 and 7). The small smoothing interval required for the radar data results in profiles with good spatial resolution, showing the atmospheric small scale structure (see Figure 8). The hypersonic sphere data must, however, be assigned a relatively large error due to uncertainty in drag coefficient. The drag coefficient is poorly known in the free molecular and transitional (low Reynolds number) flow regions. Also, errors in drag coefficient are expected at lower altitudes because of higher sphere surface temperatures caused by aerodynamic heating. In the two summaries of drag coefficient measurements considered here, significant scatter of the measurements is apparent. In the study of Lin,¹ the reported data were parameterized as a ratio of C_D/C_{DFM} (where C_{DFM} is the free molecular drag coefficient) versus the rarification parameter $M_\infty / \sqrt{Re_\infty}$ (ratio of free stream Mach number to the square root of the free stream Reynolds number). This procedure allows a calculation of C_D with a continuously updated C_{DFM} (calculated from Schaaf and Chambre²). Also an estimate of the effect of surface heating can be included because the C_{DFM}

1. Lin, T.C. (1975) Private communication of unpublished AVCO report, Sphere-
Drag in Rarefied Flow Regime.
2. Schaaf, S.A. and Chambre, P.L. (1958) Fundamentals of Gas Dynamics, 687.

calculation includes T_w/T_∞ (ratio of wall to free stream temperatures). The value of the temperature ratio chosen for the profile used in the analysis of this report was $T_w/T_\infty = 3$. A more recent analysis of Bailey³ has been completed using all available measurements at the higher Mach numbers. The results of the Bailey study are shown in Figure 6b and listed in Table D1. The drag coefficient profiles for the conditions of the present experiment are shown in Figure 6a. Note that the Lin curve for $T_w/T_\infty = 3$ (the one chosen for the present analyses) generally lies between the $T_w/T_\infty = 1$ and the curve from the Bailey study (which corresponds to $T_w/T_\infty \simeq 1.5$ based on the weight of the various sets of data studied). Figures D1 and D2 show the comparison of the three density and temperature profiles that correspond to the drag coefficients shown in Figure 6a. The choice of Lin's profile and the case $T_w/T_\infty = 3$ is somewhat arbitrary but the assigned errors encompass the other cases. The results of the analyses are listed in Tables D2, D3 and D4 for those parameters necessary to calculate atmospheric density. This data could be refined when better drag coefficient values become available. The other parameters needed besides the data in the tables are the mass (186.4 gm) and diameter (10.16 cm) of the sphere.

Table D1. Drag Coefficient for Hypersonic Flow as a Function of Mach and Reynolds Numbers From Study of Bailey³

Re	Mach								
	10	12	14	16	18	20	22	24	26
20	1.5	1.65	1.84	1.965	2.05	2.125	2.185	2.235	2.28
50	1.345	1.515	1.715	1.845	1.935	1.995	2.055	2.10	2.15
100	1.23	1.39	1.585	1.710	1.795	1.855	1.913	1.962	2.01
200	1.12	1.25	1.425	1.530	1.60	1.665	1.725	1.775	1.83
500	1.03	1.105	1.182	1.25	1.305	1.37	1.425	1.475	1.54
1000	.98	1.005	1.035	1.07	1.11	1.16	1.212	1.272	1.345
2000	.947	.955	.97	.985	1.015	1.04	1.083	1.13	1.185
5000	.92	.92	.92	.925	.945	.945	.980	1.00	1.036
10,000	.91	.905	.905	.912	.920	.920	.938	.943	.965

3. Bailey, A.B. (1978) Private communication of results of recent study of drag coefficients at high Mach numbers.

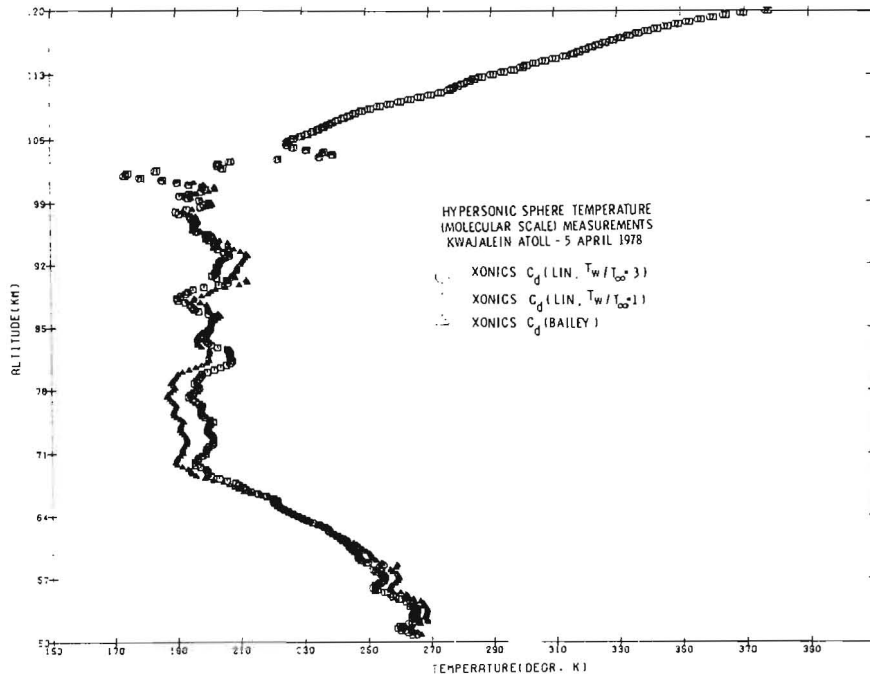


Figure D1. Comparison of the Hypersonic Sphere Determined Density to Model Atmosphere for the Three Cases of Drag Coefficient Presented in Figure 6a.

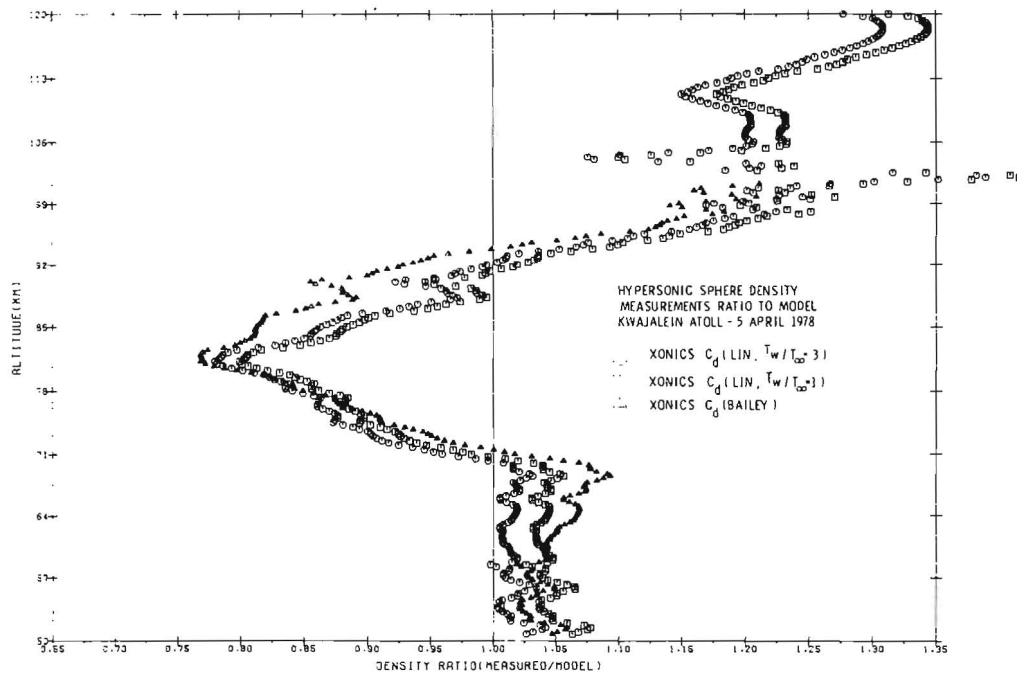


Figure D2. Temperature Profiles From Analysis of the Hypersonic Sphere Data Corresponding to the Density Profiles of Figure D1

Table D2. Calculated Parameters From Analysis of the Hypersonic Sphere by Lincoln Laboratory Using the Drag Coefficient of Lin^1 for $T_w/T_\infty = 3$

ALTITUDE (KM)	DENSITY (KG/M**3)	D RAG COEFFICIENT	TEMPERATURE (DEG. K)	D RAG ACC. (M/SEC**2)	VELOCITY (M/SEC)
130.204	.11426E -7	2.16833	426.50	-.024961	6806.473
129.910	.11301E -7	2.17115	440.32	-.024724	6806.879
129.616	.11421E -7	2.17200	444.76	-.024998	6807.281
129.322	.11889E -7	2.17014	436.16	-.026003	6807.664
129.028	.12226E -7	2.16943	433.10	-.026735	6808.074
128.734	.12827E -7	2.16696	421.69	-.028021	6808.469
128.440	.13232E -7	2.16605	417.76	-.028996	6808.891
128.146	.13747E -7	2.16455	411.03	-.030004	6809.297
127.852	.13461E -7	2.16828	428.96	-.029435	6809.691
127.558	.13411E -7	2.17045	439.73	-.029357	6810.094
127.264	.13352E -7	2.17267	450.83	-.029262	6810.504
126.969	.13986E -7	2.17023	439.35	-.030520	6810.914
126.675	.14792E -7	2.16702	424.31	-.032340	6811.293
126.381	.15641E -7	2.16395	410.17	-.034153	6811.703
126.086	.16276E -7	2.16238	403.14	-.035517	6812.102
125.792	.17000E -7	2.16054	394.93	-.037070	6812.520
125.497	.17190E -7	2.16149	399.66	-.037506	6812.914
125.203	.16747E -7	2.16566	419.53	-.036614	6813.320
124.908	.16229E -7	2.17034	442.31	-.035559	6813.707
124.613	.15930E -7	2.17443	462.77	-.034757	6814.129
124.319	.15867E -7	2.17600	470.91	-.034868	6814.523
124.024	.15998E -7	2.17758	479.25	-.034965	6814.930
123.729	.16056E -7	2.17840	483.76	-.035330	6815.328
123.434	.16576E -7	2.17712	477.70	-.036458	6815.734
123.139	.17522E -7	2.17369	460.94	-.038432	6816.137
122.844	.18072E -7	2.17262	456.04	-.039676	6816.547
122.549	.18987E -7	2.16931	443.12	-.041637	6816.941
122.254	.19982E -7	2.16716	430.10	-.043768	6817.359
121.959	.21281E -7	2.16347	412.83	-.046540	6817.758
121.664	.22187E -7	2.16175	405.06	-.048488	6818.145
121.369	.22977E -7	2.16065	400.25	-.050195	6818.566
121.074	.23521E -7	2.16056	400.17	-.051387	6818.957
120.778	.24260E -7	2.15984	397.11	-.052991	6819.367
120.483	.24852E -7	2.15971	396.84	-.054287	6819.758
120.188	.25241E -7	2.16031	399.96	-.055158	6820.156
119.892	.25900E -7	2.16003	398.95	-.056599	6820.562
119.597	.26448E -7	2.16017	399.90	-.057806	6820.977
119.301	.27058E -7	2.16014	400.08	-.059146	6821.363
119.006	.27647E -7	2.16023	400.78	-.060442	6821.766
118.710	.28369E -7	2.15995	399.78	-.062020	6822.180
118.414	.29248E -7	2.15928	396.95	-.063930	6822.586
118.119	.30750E -7	2.15700	386.66	-.067151	6822.980
117.823	.32241E -7	2.15504	377.89	-.070351	6823.383
117.527	.34092E -7	2.15246	366.46	-.074308	6823.781
117.231	.36379E -7	2.14928	352.46	-.079185	6824.172
116.935	.38949E -7	2.14599	338.22	-.084660	6824.590
116.639	.41229E -7	2.14371	328.59	-.089530	6824.960
116.343	.43455E -7	2.14185	320.85	-.094293	6825.383
116.047	.45048E -7	2.14128	318.66	-.097737	6825.777
115.751	.46711E -7	2.14071	316.49	-.101330	6826.160

Table D2. Calculated Parameters From Analysis of the Hypersonic Sphere by Lincoln Laboratory Using the Drag Coefficient of Lin^1 for $T_w/T_\infty = 3$ (Cont.)

ALTITUDE (KM)	DENSITY (KG/M**3)	DRAG COEFFICIENT	TEMPERATURE (DEG.K)	DRAG ACC. (M/SEC**2)	VELOCITY (M/SEC)
115.455	.48140E -7	2.14061	316.31	-.104437	6826.574
115.159	.49531E -7	2.14064	316.65	-.107468	6826.968
114.862	.51218E -7	2.14029	315.44	-.111122	6827.359
114.566	.53027E -7	2.13987	313.93	-.115033	6827.770
114.270	.54664E -7	2.13978	313.79	-.118593	6828.168
113.973	.56389E -7	2.13964	313.47	-.122348	6828.555
113.326	.60344E -7	2.13935	312.82	-.130944	6829.430
113.030	.62674E -7	2.13872	310.46	-.135977	6829.828
112.733	.65581E -7	2.13759	305.94	-.142224	6830.219
112.437	.68973E -7	2.13613	300.11	-.149437	6830.621
112.140	.72512E -7	2.13477	294.69	-.157085	6831.012
111.843	.76584E -7	2.13314	288.23	-.165797	6831.410
111.546	.80435E -7	2.13196	283.66	-.174053	6831.785
111.249	.84405E -7	2.13039	279.57	-.182580	6832.195
110.953	.88821E -7	2.12968	274.91	-.192044	6832.574
110.656	.93357E -7	2.12860	270.80	-.201773	6832.984
110.359	.98416E -7	2.12736	266.12	-.212607	6833.348
110.062	.10329E -6	2.12647	262.83	-.223065	6833.746
109.764	.10032E -6	2.12567	259.91	-.233876	6834.121
109.467	.11049E -6	2.12671	264.27	-.238687	6834.508
109.170	.11630E -6	2.12565	260.36	-.251160	6834.910
108.873	.12138E -6	2.12520	258.82	-.262083	6835.285
108.576	.12842E -6	2.12389	253.93	-.277151	6835.664
108.278	.13489E -6	2.12309	251.08	-.291040	6836.051
107.981	.14336E -6	2.12159	245.52	-.309144	6836.422
107.684	.15110E -6	2.12068	242.27	-.325727	6836.797
107.386	.15909E -6	2.11988	239.44	-.342865	6837.187
107.089	.16757E -6	2.11909	236.68	-.361023	6837.551
106.791	.17555E -6	2.11866	235.29	-.378195	6837.930
106.493	.18685E -6	2.11729	230.37	-.402325	6838.293
106.196	.19868E -6	2.11606	225.98	-.427573	6838.656
105.898	.20826E -6	2.11573	224.90	-.443176	6839.031
105.600	.21594E -6	2.11606	225.42	-.464840	6839.387
105.302	.22498E -6	2.11609	226.77	-.484361	6839.750
105.005	.23690E -6	2.11550	224.76	-.509317	6840.105
104.707	.25040E -6	2.11470	222.06	-.538832	6840.461
104.409	.26496E -6	2.11388	219.28	-.569997	6840.824
104.111	.28027E -6	2.11312	216.73	-.602787	6841.164
103.813	.29696E -6	2.11211	213.97	-.638441	6841.516
103.515	.31963E -6	2.10874	208.16	-.686146	6841.852
103.217	.34617E -6	2.10506	201.54	-.741898	6842.191
102.918	.37671E -6	2.10120	194.52	-.805353	6842.527
102.620	.40447E -6	2.09851	190.55	-.864316	6842.852
102.322	.43322E -6	2.09611	187.31	-.924775	6843.176
102.024	.46219E -6	2.09227	185.00	-.984304	6843.461
101.725	.49157E -6	2.08875	183.40	-1.045842	6843.770
101.427	.51855E -6	2.08612	183.36	-1.101941	6844.066
101.128	.54057E -6	2.08467	185.46	-1.143033	6844.371
100.830	.56499E -6	2.08299	187.01	-1.199030	6844.648
100.531	.58996E -6	2.08142	188.68	-1.251193	6844.930

Table D2. Calculated Parameters From Analysis of the Hypersonic Sphere by Lincoln Laboratory Using the Drag Coefficient of Lin^1 for $T_w/T_\infty = 3$ (Cont.)

ALTITUDE (KM)	DENSITY (KG/M**3)	DRAW COEFFICIENT	TEMPERATURE (DEG.K)	DRAW ACC. (M/SEC**2)	VELOCITY (M/SEC)
100.233	.62027E -6	2.07926	189.02	-1.314201	6845.203
99.934	.64753E -6	2.07779	190.67	-1.371102	6845.473
99.636	.67712E -6	2.07619	191.98	-1.432759	6845.742
99.337	.70539E -6	2.07335	193.56	-1.490651	6845.980
99.038	.74076E -6	2.06907	194.34	-1.562283	6846.254
98.739	.77681E -6	2.06473	194.50	-1.639202	6846.473
98.441	.82071E -6	2.06021	194.22	-1.723736	6846.723
98.142	.86816E -6	2.05534	193.25	-1.819190	6846.941
97.843	.91909E -6	2.04735	192.19	-1.918537	6847.164
97.544	.97316E -6	2.03509	191.17	-2.019359	6847.348
97.245	.10263E -5	2.02409	190.97	-2.118220	6847.559
96.946	.10824E -5	2.01335	190.76	-2.222349	6847.723
96.647	.11343E -5	2.00431	191.76	-2.318490	6847.867
96.348	.11885E -5	1.99550	192.79	-2.413806	6848.059
96.049	.12402E -5	1.98622	194.55	-2.512271	6848.203
95.749	.12959E -5	1.97050	195.99	-2.604390	6848.336
95.450	.13534E -5	1.95524	197.46	-2.699113	6848.469
95.151	.14182E -5	1.93917	198.25	-2.805221	6848.578
94.852	.14816E -5	1.92435	199.53	-2.908293	6848.684
94.552	.15491E -5	1.90950	200.54	-3.017353	6848.797
94.253	.16225E -5	1.89439	201.17	-3.135364	6848.867
93.954	.17061E -5	1.87836	200.99	-3.269225	6848.941
93.654	.18013E -5	1.86133	200.05	-3.420320	6848.992
93.355	.19025E -5	1.84423	199.08	-3.579245	6849.047
93.055	.20022E -5	1.82665	198.86	-3.735103	6849.059
92.756	.20985E -5	1.81471	199.45	-3.884976	6849.070
92.456	.21975E -5	1.80134	200.20	-4.038218	6849.043
92.157	.22932E -5	1.78926	201.59	-4.185354	6849.004
91.857	.23863E -5	1.77828	203.51	-4.328826	6848.969
91.557	.24764E -5	1.76824	205.88	-4.456999	6848.910
91.258	.25732E -5	1.75806	207.93	-4.614749	6848.840
90.958	.26813E -5	1.74732	209.32	-4.779122	6848.746
90.658	.28028E -5	1.73565	210.02	-4.962040	6848.637
90.359	.29397E -5	1.72271	210.00	-5.165439	6848.520
90.059	.30929E -5	1.70924	209.34	-5.391930	6848.363
89.759	.32385E -5	1.69729	209.65	-5.605935	6848.184
89.459	.34305E -5	1.68263	207.56	-5.886651	6847.992
89.160	.36483E -5	1.66737	204.79	-6.203297	6847.754
88.860	.39080E -5	1.65031	200.77	-6.573225	6847.477
88.560	.41963E -5	1.63418	196.56	-6.991910	6847.172
88.260	.44747E -5	1.61971	193.95	-7.388862	6846.809
87.960	.47418E -5	1.60708	192.67	-7.767897	6846.387
87.660	.49523E -5	1.59800	194.19	-8.065839	6845.953
87.360	.51310E -5	1.58953	197.18	-8.311511	6845.480
87.060	.53263E -5	1.58066	199.70	-8.578390	6844.984
86.760	.55419E -5	1.57138	201.66	-8.872027	6844.461
86.460	.57959E -5	1.56109	202.54	-9.216416	6843.906
86.160	.60632E -5	1.55097	203.32	-9.577255	6843.305
85.860	.63550E -5	1.54065	203.69	-9.969373	6842.660
85.560	.66431E -5	1.53114	204.57	-10.355066	6841.968

Table D2. Calculated Parameters From Analysis of the Hypersonic Sphere by Lincoln Laboratory Using the Drag Coefficient of Lin¹ for $T_w/T_\infty = 3$ (Cont.)

ALTITUDE (KM)	DENSITY (KG/M**3)	DRAG COEFFICIENT	TEMPERATURE (DEG. K)	DRAG ACC. (M/SEC**2)	VELOCITY (M/SEC)
85.260	.69658E -5	1.52117	204.79	-10.785038	6841.258
84.961	.73607E -5	1.50729	203.46	-11.289898	6840.492
84.661	.77869E -5	1.49234	201.99	-11.822355	6839.664
84.361	.82153E -5	1.47849	201.12	-12.353779	6838.766
84.061	.86711E -5	1.46490	200.22	-12.915710	6837.812
83.761	.90909E -5	1.45330	200.67	-13.429862	6836.820
83.461	.95585E -5	1.44128	200.54	-13.999470	6835.734
83.161	.10045E -4	1.42968	200.51	-14.589171	6834.625
82.861	.10495E -4	1.41968	201.63	-15.130804	6833.426
82.561	.10977E -4	1.40967	202.49	-15.703303	6832.177
82.261	.11452E -4	1.39966	203.32	-16.264933	6830.867
81.962	.11959E -4	1.38942	204.88	-16.854706	6829.496
81.662	.12463E -4	1.37988	206.33	-17.436966	6828.055
81.362	.12984E -4	1.37062	207.78	-18.035823	6826.551
81.062	.13575E -4	1.36078	208.44	-18.712326	6824.996
80.763	.14363E -4	1.34856	206.66	-19.611587	6823.359
80.463	.15293E -4	1.33536	203.71	-20.666656	6821.617
80.164	.16388E -4	1.32122	199.68	-21.899841	6819.723
79.864	.17503E -4	1.30827	196.56	-23.146606	6817.727
79.565	.18527E -4	1.29784	195.34	-24.289703	6815.551
79.265	.19552E -4	1.28824	194.74	-25.427872	6813.277
78.966	.20567E -4	1.27948	194.80	-26.546661	6810.902
78.667	.21683E -4	1.27054	194.42	-27.771454	6808.391
78.367	.22824E -4	1.26165	194.35	-29.005951	6805.727
78.068	.24049E -4	1.25023	194.11	-30.260620	6802.934
77.769	.25335E -4	1.23914	193.90	-31.569443	6800.031
77.470	.26733E -4	1.22796	193.36	-32.987152	6796.961
77.172	.28155E -4	1.21754	193.26	-34.408020	6793.730
76.873	.29517E -4	1.20825	194.00	-35.761612	6790.336
76.574	.30823E -4	1.20003	195.46	-37.051498	6786.828
76.276	.32163E -4	1.19341	196.99	-38.407730	6783.160
75.978	.33825E -4	1.18569	196.94	-40.085403	6779.367
75.680	.35763E -4	1.17732	195.37	-42.033157	6775.363
75.382	.37729E -4	1.16951	195.27	-43.994644	6771.129
75.084	.39578E -4	1.16275	195.78	-45.823563	6766.641
74.786	.41261E -4	1.15707	197.44	-47.474258	6762.035
74.489	.43189E -4	1.15092	198.26	-49.357956	6757.234
74.245	.45037E -4	1.14511	198.01	-51.148209	6753.160
73.948	.47466E -4	1.13773	197.46	-53.476975	6747.914
73.651	.50085E -4	1.13037	196.70	-55.973480	6742.410
73.354	.52690E -4	1.12364	196.56	-58.431564	6736.664
73.058	.55281E -4	1.11745	196.93	-60.857483	6730.602
72.762	.57813E -4	1.11183	197.90	-63.206650	6724.305
72.466	.60417E -4	1.10645	198.97	-65.602661	6717.765
72.170	.63459E -4	1.10051	198.98	-68.400620	6710.988
71.874	.66861E -4	1.09433	198.39	-71.510605	6703.871
71.579	.70508E -4	1.08707	197.64	-74.743164	6696.348
71.284	.74279E -4	1.07949	197.12	-78.008820	6688.500
70.695	.82445E -4	1.06489	196.11	-84.987303	6671.812
70.401	.87336E -4	1.05700	194.45	-89.185547	6662.875

Table D2. Calculated Parameters From Analysis of the Hypersonic Sphere by Lincoln Laboratory Using the Drag Coefficient of Lin^1 for $T_w/T_\infty = 3$ (Cont.)

ALTITUDE (KM)	DENSITY (KG/M**3)	DRAW COEFFICIENT	TEMPERATURE (DEG.K)	DRAW ACC. (M/SEC**2)	VELOCITY (M/SEC)
70.108	.92389E -4	1.04972	193.40	-93.365372	6653.422
69.815	.97677E -4	1.04262	192.37	-97.748154	6643.461
69.522	.10210E -3	1.03719	193.51	-101.329681	6633.109
69.230	.10654E -3	1.03211	194.92	-104.878876	6622.375
68.938	.11113E -3	1.02719	196.34	-108.503708	6611.254
68.647	.11565E -3	1.02266	198.12	-112.030670	6599.734
68.356	.11985E -3	1.01884	200.64	-115.245972	6587.852
68.065	.12400E -3	1.01577	203.38	-118.438934	6575.637
67.775	.12844E -3	1.01263	205.77	-121.837509	6563.062
67.486	.13312E -3	1.00949	207.95	-125.387177	6550.109
67.197	.13799E -3	1.00639	210.01	-129.043243	6536.770
66.909	.14298E -3	1.00339	212.06	-132.750351	6523.027
66.621	.14820E -3	1.00041	213.94	-136.594553	6508.883
66.334	.15363E -3	.99746	215.71	-140.556137	6494.309
66.048	.15923E -3	.99460	217.45	-144.586121	6479.309
65.762	.16495E -3	.99184	219.21	-148.651932	6463.863
65.477	.17094E -3	.98855	220.80	-152.786865	6447.980
65.192	.17739E -3	.98510	222.02	-157.199397	6431.641
64.908	.18450E -3	.98148	222.67	-162.052567	6414.865
64.625	.19200E -3	.97789	223.17	-167.110260	6397.414
64.343	.19912E -3	.97470	224.36	-171.778793	6379.484
64.061	.20599E -3	.97183	226.05	-176.161331	6361.082
63.780	.21369E -3	.96875	227.03	-181.084625	6342.203
63.500	.21986E -3	.96651	229.80	-184.744629	6322.734
63.221	.22664E -3	.96413	232.03	-188.788940	6303.066
62.943	.23545E -3	.96105	232.39	-194.244293	6282.723
62.665	.24334E -3	.95853	233.90	-198.893387	6261.871
62.389	.25065E -3	.95660	236.10	-203.068085	6240.523
62.113	.25824E -3	.95503	238.15	-207.422104	6218.770
61.838	.26691E -3	.95324	239.36	-212.453537	6196.480
61.564	.27566E -3	.95155	240.69	-217.412033	6173.637
61.292	.28535E -3	.94971	241.38	-222.928116	6150.273
61.020	.29573E -3	.94782	241.76	-228.777573	6126.238
60.749	.30614E -3	.94606	242.35	-234.490937	6101.609
60.479	.31674E -3	.94438	243.02	-240.176498	6076.336
60.211	.32712E -3	.94286	244.06	-245.545441	6050.477
59.943	.33836E -3	.94126	244.66	-251.343033	6024.039
59.677	.34998E -3	.93970	245.20	-257.212891	5996.926
59.412	.36126E -3	.93831	246.19	-262.667969	5969.219
59.148	.37240E -3	.93705	247.43	-267.846436	5940.930
58.885	.38364E -3	.93586	248.76	-272.912354	5912.102
58.623	.39550E -3	.93465	249.83	-278.194092	5882.711
58.104	.42129E -3	.93215	251.20	-289.492920	5822.191
57.846	.43488E -3	.93094	251.74	-295.252930	5790.969
57.590	.44833E -3	.92984	252.55	-300.688965	5759.145
57.335	.46309E -3	.92863	252.80	-306.707764	5726.742
57.082	.48029E -3	.92719	251.39	-313.939941	5693.613
56.830	.49700E -3	.92594	251.72	-320.567627	5659.645
56.579	.51420E -3	.92473	251.47	-327.190674	5625.082
56.330	.53347E -3	.92337	250.48	-334.703369	5589.687

Table D2. Calculated Parameters From Analysis of the Hypersonic Sphere by Lincoln Laboratory Using the Drag Coefficient of Lin¹ for $T_w/T_\infty = 3$ (Cont.)

ALTITUDE (KM)	DENSITY (KG/M**3)	DRAG COEFFICIENT	TEMPERATURE (DEG.K)	DRAG ACC. (M/SEC**2)	VELOCITY (M/SEC)
56.082	.55190E -3	.92224	250.17	-341.376953	5553.496
55.836	.56853E -3	.92141	250.38	-346.703613	5516.652
55.592	.58382E -3	.92090	252.30	-350.990234	5479.309
55.349	.59849E -3	.92032	254.05	-354.685053	5441.539
55.108	.61408E -3	.91981	255.48	-358.637695	5403.398
54.868	.63028E -3	.91929	256.75	-362.650391	5364.777
54.630	.64542E -3	.91894	258.50	-365.844233	5325.766
54.394	.65982E -3	.91871	260.60	-368.411377	5286.449
54.160	.67482E -3	.91847	262.48	-371.069092	5246.887
53.927	.68966E -3	.91811	263.70	-374.421631	5206.968
53.696	.70996E -3	.91766	264.46	-378.224854	5166.699
53.467	.72791E -3	.91734	265.43	-381.558350	5125.908
53.239	.74764E -3	.91691	265.86	-385.476313	5084.977
53.013	.77057E -3	.91628	265.31	-390.565318	5043.414
52.790	.79210E -3	.91556	265.41	-394.467793	5001.297
52.567	.81219E -3	.91487	266.11	-397.363037	4958.887
52.347	.83387E -3	.91412	266.39	-400.638672	4916.152
52.129	.85433E -3	.91354	267.15	-403.844922	4873.035
51.912	.87304E -3	.91318	268.52	-404.432373	4829.781
51.697	.89278E -3	.91279	269.61	-405.999323	4786.359
51.485	.91164E -3	.91263	271.01	-406.986323	4742.766
51.274	.92986E -3	.91276	272.61	-407.576660	4699.133
51.065	.95286E -3	.91261	272.87	-409.855713	4655.410
50.857	.98303E -3	.91205	271.25	-414.602783	4611.285
50.652	.10179E -2	.91129	268.62	-420.687744	4566.539
50.449	.10504E -2	.91080	266.96	-425.256592	4521.098
50.248	.10773E -2	.91072	266.85	-427.362549	4475.359
50.048	.11013E -2	.91088	267.57	-428.040039	4429.461
49.851	.11246E -2	.91113	268.51	-428.175049	4383.574
49.656	.11487E -2	.91138	269.26	-428.371826	4337.648
49.462	.11722E -2	.91171	270.20	-428.073369	4291.723
49.271	.11953E -2	.91211	271.24	-427.437256	4245.867
49.082	.12214E -2	.91240	271.66	-427.509033	4200.074
48.895	.12525E -2	.91248	271.02	-428.924995	4154.195
48.709	.12867E -2	.91246	269.87	-430.905129	4108.107
48.526	.13217E -2	.91273	268.70	-432.839344	4061.797
48.345	.13569E -2	.91311	267.66	-434.409668	4015.285
48.166	.13931E -2	.91350	266.55	-435.900879	3968.639
47.989	.14310E -2	.91389	265.28	-437.427493	3921.805
47.814	.14632E -2	.91459	265.17	-436.958008	3874.833
47.641	.14992E -2	.91560	266.23	-434.529953	3828.101
47.470	.15181E -2	.91652	266.77	-432.716797	3781.652
47.301	.15551E -2	.91716	265.94	-432.778320	3735.312
47.134	.15938E -2	.91737	264.95	-432.901611	3688.049
46.969	.16263E -2	.91925	265.07	-431.343019	3642.483
46.806	.16581E -2	.92070	265.32	-429.394531	3596.359
46.645	.16890E -2	.92222	265.74	-427.003662	3550.415
46.486	.17177E -2	.92385	266.54	-423.903320	3504.808
46.329	.17462E -2	.92552	267.34	-420.637207	3459.540
46.174	.17748E -2	.92721	268.12	-417.280029	3414.641

Table D3. The Hypersonic Sphere Results From XONICS Analysis Using the Bailey Drag Coefficient

ALTITUDE (KM)	DENSITY (KG/M**3)	DRAG COEFFICIENT	TEMPERATURE (DEG.K)	DRAG ACC. (M/SEC**2)	VELOCITY (M/SEC)
101.250	.49967E -6	2.19966	195.84	1.119514	6844.211
101.000	.51328E -6	2.19360	198.83	1.146683	6844.457
100.750	.52540E -6	2.18744	202.37	1.170671	6844.695
100.500	.54658E -6	2.18131	202.62	1.214610	6844.934
100.250	.57507E -6	2.17532	211.63	1.274425	6845.172
100.000	.61269E -6	2.16946	196.31	1.354139	6845.395
99.750	.65038E -6	2.16372	192.78	1.435264	6845.617
99.500	.67176E -6	2.15733	194.94	1.476567	6845.828
99.250	.68887E -6	2.15093	198.25	1.509789	6846.047
99.000	.70747E -6	2.14469	201.19	1.546199	6846.250
98.750	.73558E -6	2.13870	201.60	1.603643	6846.457
98.500	.77031E -6	2.13324	199.08	1.688475	6846.652
98.250	.82575E -6	2.12801	195.16	1.791767	6846.840
98.000	.87496E -6	2.12271	192.20	1.893145	6847.020
97.750	.90966E -6	2.11657	193.18	1.969321	6847.195
97.500	.93331E -6	2.10937	196.24	2.007251	6847.359
97.250	.97189E -6	2.10169	190.54	2.082211	6847.521
97.000	1.01113E -5	2.09337	196.98	2.158024	6847.672
96.750	1.0551E -5	2.08425	195.90	2.242152	6847.820
96.500	1.1034E -5	2.07529	190.77	2.334885	6847.961
96.250	1.1525E -5	2.06649	196.09	2.423552	6848.094
96.000	1.2014E -5	2.05794	195.19	2.521317	6848.215
95.750	1.2424E -5	2.05014	197.37	2.596998	6848.332
95.500	1.2750E -5	2.04306	211.97	2.656176	6848.438
95.250	1.3218E -5	2.03524	201.97	2.743314	6848.530
95.000	1.3743E -5	2.02725	202.37	2.840397	6848.617
94.750	1.4208E -5	2.01976	203.87	2.926240	6848.723
94.500	1.4609E -5	2.01277	206.43	2.993523	6848.801
94.250	1.5208E -5	2.00488	206.41	3.109679	6848.871
94.000	1.5602E -5	1.99719	206.77	3.210649	6848.934
93.750	1.6322E -5	1.98937	203.31	3.312672	6848.984
93.500	1.6814E -5	1.98300	210.37	3.410597	6849.027
93.250	1.7339E -5	1.97603	212.16	3.494357	6849.067
93.000	1.7974E -5	1.96375	212.78	3.509498	6849.090
92.750	1.8771E -5	1.96104	211.64	3.754522	6849.105
92.500	1.9533E -5	1.95319	211.16	3.901043	6849.105
92.250	2.0422E -5	1.94337	210.59	4.047633	6849.094
92.000	2.1257E -5	1.93159	210.43	4.187351	6849.067
91.750	2.2236E -5	1.91870	209.27	4.351333	6849.031
91.500	2.3134E -5	1.90741	209.26	4.500730	6848.977
91.250	2.4072E -5	1.89616	209.22	4.655532	6848.910
91.000	2.5173E -5	1.88397	208.17	4.837516	6848.820
90.750	2.6308E -5	1.87205	207.29	5.023135	6848.727
90.500	2.7179E -5	1.86266	208.00	5.162451	6848.617
90.250	2.7623E -5	1.85523	212.14	5.263755	6848.492
90.000	2.8871E -5	1.84513	212.58	5.432359	6848.359
89.750	3.0406E -5	1.83224	209.92	5.680578	6848.207
89.500	3.2322E -5	1.81801	205.51	5.991693	6848.027
89.250	3.4187E -5	1.80510	202.36	6.292490	6847.816
89.000	3.5069E -5	1.79376	200.96	6.559980	6847.566

Table D3. The Hypersonic Sphere Results From XONICS Analysis Using the Bailey Drag Coefficient (Cont.)

ALTITUDE (KM)	DENSITY (KG/M**3)	DRAG COEFFICIENT	TEMPERATURE (DEG.K)	DRAG ACC. (M/SEC**2)	VELOCITY (M/SEC)
88.750	.37547E -5	1.78280	200.07	6.824835	6847.332
88.500	.39557E -5	1.76528	197.99	7.119544	6847.051
88.250	.41741E -5	1.74497	195.69	7.426087	6846.742
88.000	.43598E -5	1.72882	195.46	7.663584	6846.406
87.750	.44988E -5	1.71703	197.58	7.872791	6846.055
87.500	.46441E -5	1.70520	199.56	8.070324	6845.680
87.250	.48337E -5	1.69081	199.86	8.327347	6845.289
87.000	.50389E -5	1.67616	199.84	8.604931	6844.875
86.750	.52332E -5	1.66285	200.55	8.864783	6844.430
86.500	.53838E -5	1.65263	203.12	9.062239	6843.960
86.250	.55844E -5	1.64006	203.96	9.329164	6843.488
86.000	.58381E -5	1.62531	203.21	9.663853	6842.977
85.750	.61151E -5	1.61031	202.11	10.027170	6842.441
85.500	.63992E -5	1.59600	201.24	10.397103	6841.863
85.250	.66901E -5	1.58224	200.60	10.773581	6841.262
85.000	.69916E -5	1.56885	200.07	11.161112	6840.621
84.750	.73218E -5	1.55531	199.15	11.584353	6839.940
84.500	.76780E -5	1.54182	198.01	12.039269	6839.227
84.250	.80362E -5	1.52897	197.30	12.493619	6838.469
84.000	.84164E -5	1.51627	196.49	12.973573	6837.668
83.750	.87864E -5	1.50425	196.34	13.433134	6836.824
83.500	.91590E -5	1.49261	196.48	13.890879	6835.938
83.250	.95547E -5	1.47962	196.47	14.364161	6835.016
83.000	.99628E -5	1.46615	196.55	14.835616	6834.039
82.750	.10325E -4	1.45370	197.81	15.238509	6833.035
82.500	.10637E -4	1.44270	200.19	15.575262	6831.996
82.250	.11074E -4	1.42958	200.43	16.062546	6830.918
82.000	.11545E -4	1.41640	200.38	16.585251	6829.797
81.750	.12060E -4	1.40312	199.95	17.157410	6828.617
81.500	.12578E -4	1.39037	199.84	17.725891	6827.395
81.250	.13086E -4	1.37821	200.22	18.273712	6826.117
81.000	.13697E -4	1.36543	199.42	18.942896	6824.785
80.750	.14398E -4	1.35239	197.82	19.713389	6823.391
80.500	.15162E -4	1.33955	195.94	20.554683	6821.922
80.250	.15994E -4	1.32697	193.93	21.469284	6820.375
80.000	.16882E -4	1.31476	191.72	22.439514	6818.746
79.750	.17774E -4	1.30306	190.19	23.4401367	6817.023
79.500	.18622E -4	1.29194	189.65	24.293489	6815.227
79.250	.19497E -4	1.28134	189.26	25.213226	6813.340
79.000	.20447E -4	1.27087	188.58	26.211700	6811.363
78.750	.21447E -4	1.26051	187.91	27.254669	6809.297
78.500	.22306E -4	1.25041	188.32	28.099977	6807.141
78.250	.23245E -4	1.24048	189.34	29.032579	6804.906
78.000	.24358E -4	1.23063	188.81	30.162764	6802.578
77.750	.25584E -4	1.22085	187.87	31.406113	6800.145
77.500	.26876E -4	1.21117	186.95	32.704880	6797.599
77.250	.28166E -4	1.20162	186.51	33.973663	6794.934
77.000	.29276E -4	1.19235	187.60	35.010422	6792.164
76.750	.30479E -4	1.18324	188.34	36.138947	6789.297
76.500	.31715E -4	1.17433	189.16	37.269371	6786.316

Table D3. The Hypersonic Sphere Results From XONICS Analysis Using the Bailey Drag Coefficient (Cont.)

ALTITUDE (KM)	DENSITY (KG/M**3)	DRAW COEFFICIENT	TEMPERATURE (DEG.K)	DRAW ACC. (M/SEC**2)	VELOCITY (M/SEC)
76.250	.33038E -4	1.16556	189.73	38.522369	6783.230
76.000	.34592E -4	1.15682	189.74	39.597909	6780.020
75.750	.36230E -4	1.14825	189.91	41.539333	6776.868
75.500	.37883E -4	1.14029	188.80	43.089691	6773.150
75.250	.39536E -4	1.13276	189.05	44.624054	6769.547
75.000	.41150E -4	1.12532	189.79	46.086330	6765.777
74.750	.42712E -4	1.11799	191.02	47.468333	6761.887
74.500	.44384E -4	1.11083	191.99	48.954697	6757.850
74.250	.46520E -4	1.10383	191.30	50.920749	6753.620
74.000	.48697E -4	1.09688	190.89	52.897217	6749.317
73.750	.50847E -4	1.08999	190.96	54.814270	6744.750
73.500	.53156E -4	1.08313	190.81	56.851440	6738.227
73.250	.55349E -4	1.07644	191.41	58.746094	6733.547
73.000	.57561E -4	1.07007	192.22	60.714913	6736.441
72.750	.59924E -4	1.06384	192.80	62.826943	6740.285
72.500	.62474E -4	1.05760	193.08	65.072123	6741.098
72.250	.65202E -4	1.05135	193.16	67.434341	6739.070
72.000	.68193E -4	1.04506	192.83	69.994974	6734.164
71.750	.71539E -4	1.03874	191.94	72.83892	6727.350
71.500	.74870E -4	1.03250	191.55	75.621460	6720.781
71.250	.78203E -4	1.02639	191.53	78.378479	6715.617
71.000	.81631E -4	1.02038	191.64	81.190334	6710.645
70.750	.85620E -4	1.01434	190.84	84.517543	6706.207
70.500	.89901E -4	1.00834	189.90	88.081375	6703.449
70.250	.94013E -4	1.00302	189.74	91.502699	6702.535
70.000	.98424E -4	.99860	189.33	95.207793	6698.789
69.750	.10259E -3	.99432	189.35	93.593323	6692.895
69.500	.10625E -3	.99022	191.51	101.441940	6685.965
69.250	.10992E -3	.98660	193.31	104.271393	6676.465
69.000	.11422E -3	.98310	194.21	107.586710	6662.117
68.750	.11904E -3	.97949	194.51	111.216156	6642.801
68.500	.12339E -3	.97627	195.86	114.357452	6622.055
68.250	.12694E -3	.97363	195.59	116.845521	6604.887
68.000	.13062E -3	.97111	201.22	119.496230	6592.527
67.750	.13403E -3	.96884	204.74	121.741437	6582.480
67.500	.13821E -3	.96640	206.77	125.050958	6573.887
67.250	.14276E -3	.96335	203.30	128.448334	6565.211
67.000	.14775E -3	.96146	209.17	132.146317	6554.559
66.750	.15250E -3	.95918	210.36	135.550399	6541.715
66.500	.15682E -3	.95716	213.29	138.503220	6526.664
66.250	.16095E -3	.95522	216.05	141.235489	6510.543
66.000	.16544E -3	.95290	213.42	144.178695	6495.617
65.750	.17088E -3	.95015	219.67	147.929672	6483.317
65.500	.17722E -3	.94760	220.01	152.412582	6472.164
65.250	.18379E -3	.94506	220.34	156.977005	6459.441
65.000	.19021E -3	.94252	221.11	161.258026	6443.828
64.750	.19644E -3	.93996	222.31	165.234207	6425.891
64.500	.20260E -3	.93748	223.78	169.050171	6407.227
64.250	.20895E -3	.93505	225.20	172.963053	6388.879
64.000	.21537E -3	.93267	226.70	176.873734	6371.121

Table D3. The Hypersonic Sphere Results From XONICS Analysis Using the Bailey Drag Coefficient (Cont.)

ALTITUDE (KM)	DENSITY (KG/M**3)	DRAW COEFFICIENT	TEMPERATURE (DEG.K)	DRAW ACC. (M/SEC**2)	VELOCITY (M/SEC)
63.750	.22195E -3	.93035	228.21	180.643155	6353.734
63.500	.22371E -3	.92812	229.69	184.905762	6336.859
63.250	.23529E -3	.92613	231.51	188.785202	6320.270
63.000	.24169E -3	.92433	233.62	192.552216	6303.719
62.750	.24836E -3	.92362	235.59	196.506744	6287.055
62.500	.25562E -3	.92261	237.13	200.382928	6270.355
62.250	.26364E -3	.92180	238.14	205.772156	6252.316
62.000	.27152E -3	.92083	239.47	210.294006	6231.090
61.750	.27935E -3	.92051	240.99	214.756699	6206.922
61.500	.28726E -3	.92050	242.59	219.149048	6180.594
61.250	.29593E -3	.92050	243.72	223.981689	6153.301
61.000	.30423E -3	.92046	245.31	228.423126	6126.406
60.750	.31338E -3	.92043	246.38	233.370209	6099.164
60.500	.32324E -3	.92039	247.10	238.711700	6071.934
60.250	.33286E -3	.92031	248.20	243.789642	6046.195
60.000	.34273E -3	.92022	249.29	248.973892	6021.867
59.750	.35282E -3	.92011	250.40	254.189270	5997.914
59.500	.36418E -3	.92001	250.82	260.114990	5972.598
59.250	.37591E -3	.91990	251.22	266.264648	5950.090
59.000	.38693E -3	.91974	252.31	271.784663	5928.574
58.750	.39702E -3	.91953	254.16	276.469238	5906.767
58.500	.40250E -3	.91919	259.00	277.741455	5883.324
58.250	.41638E -3	.91901	258.59	284.473633	5854.723
58.000	.43299E -3	.91887	256.87	292.750732	5824.688
57.750	.44593E -3	.91853	257.67	298.273438	5795.352
57.500	.45620E -3	.91793	259.02	303.109375	5766.574
57.250	.47250E -3	.91741	259.42	309.100330	5737.789
57.000	.48769E -3	.91690	259.57	315.360107	5707.594
56.750	.50426E -3	.91641	259.27	321.963867	5672.273
56.500	.52291E -3	.91598	258.25	329.376465	5633.277
56.250	.54233E -3	.91554	257.21	336.951660	5594.738
56.000	.56164E -3	.91506	256.60	344.151123	5557.586
55.750	.57887E -3	.91443	257.21	349.748535	5521.445
55.500	.59146E -3	.91355	260.02	352.333008	5487.496
55.250	.60665E -3	.91277	261.77	355.937988	5448.414
55.000	.62469E -3	.91209	262.46	360.790283	5406.883
54.750	.64089E -3	.91131	264.10	364.154053	5364.516
54.500	.65592E -3	.91046	266.32	366.599609	5322.738
54.250	.67440E -3	.90976	267.29	370.767334	5281.523
54.000	.69580E -3	.90920	267.31	376.196289	5239.734
53.750	.71510E -3	.90862	268.36	379.827881	5194.313
53.500	.73729E -3	.90810	269.53	384.479492	5146.824
53.250	.76141E -3	.90761	268.27	389.644287	5098.719
53.000	.79630E -3	.90711	268.02	394.632080	5049.441
52.750	.81221E -3	.90660	267.72	399.467529	4998.188
52.500	.83581E -3	.90603	268.42	402.618896	4946.391
52.250	.86186E -3	.90550	268.56	406.535545	4895.297
52.000	.89690E -3	.90512	266.29	414.203857	4844.594
51.750	.93553E -3	.90477	263.50	422.764648	4794.180
51.500	.96581E -3	.90428	262.68	427.983643	4742.109

Table D4. The Hypersonic Sphere Results From XONICS Analysis Using The Lin
 $[T_W/T_\infty = 3]$ Drag Coefficient

ALTITUDE (KM)	DENSITY (KG/M**3)	DRAG COEFFICIENT	TEMPERATURE (DEG.K)	DRAG ACC. (M/SEC**2)	VELOCITY (M/SEC)
123.250	.15315E -7	2.16756	450.35	.035990	6828.609
123.000	.16472E -7	2.16365	449.55	.035997	6816.320
122.750	.16770E -7	2.16366	449.67	.036652	6816.664
122.500	.17074E -7	2.16368	449.80	.037321	6817.004
122.250	.17383E -7	2.16369	449.92	.038002	6817.344
122.000	.17718E -7	2.16361	449.53	.038737	6817.689
121.750	.18386E -7	2.16199	441.31	.040179	6818.031
121.500	.19192E -7	2.15991	430.80	.041306	6818.371
121.250	.20033E -7	2.15790	420.75	.043707	6818.715
121.000	.20910E -7	2.15596	411.12	.045584	6819.055
120.750	.21825E -7	2.15408	401.91	.047542	6819.395
120.500	.22780E -7	2.15227	393.09	.049582	6819.734
120.250	.23775E -7	2.15051	384.66	.051709	6820.079
120.000	.24814E -7	2.14882	376.58	.053927	6820.414
119.750	.25894E -7	2.14719	368.88	.056233	6820.758
119.500	.26876E -7	2.14603	363.46	.058342	6821.098
119.250	.27806E -7	2.14515	359.38	.060344	6821.438
119.000	.28758E -7	2.14432	355.57	.062393	6821.777
118.750	.29738E -7	2.14353	351.92	.064495	6822.121
118.500	.30749E -7	2.14276	348.43	.066680	6822.457
118.250	.31790E -7	2.14203	345.09	.068921	6822.797
118.000	.32862E -7	2.14133	341.91	.071229	6823.137
117.750	.33966E -7	2.14065	338.86	.073606	6823.477
117.500	.35104E -7	2.14000	335.96	.076053	6823.817
117.250	.36274E -7	2.13939	333.20	.078572	6824.148
117.000	.37479E -7	2.13879	330.56	.081164	6824.484
116.750	.38719E -7	2.13823	328.06	.083831	6824.828
116.500	.39994E -7	2.13769	325.68	.086592	6825.164
116.250	.41305E -7	2.13718	323.43	.089412	6825.504
116.000	.42654E -7	2.13669	321.29	.092322	6825.840
115.750	.44040E -7	2.13623	319.27	.095313	6826.176
115.500	.45465E -7	2.13579	317.35	.098397	6826.512
115.250	.46930E -7	2.13537	315.54	.101546	6826.852
115.000	.48553E -7	2.13480	313.07	.105046	6827.188
114.750	.50392E -7	2.13403	309.71	.108995	6827.520
114.500	.52299E -7	2.13328	306.48	.113087	6827.852
114.250	.54275E -7	2.13256	303.39	.117326	6828.191
114.000	.56286E -7	2.13191	300.61	.121640	6828.527
113.750	.58099E -7	2.13161	299.33	.125552	6828.859
113.500	.60287E -7	2.13095	296.54	.130262	6829.195
113.250	.62687E -7	2.13018	293.25	.135421	6829.527
113.000	.65267E -7	2.12934	289.73	.140959	6829.863
112.750	.68003E -7	2.12849	286.13	.146831	6830.195
112.500	.70567E -7	2.12793	283.80	.152330	6830.527
112.250	.73042E -7	2.12756	282.27	.157661	6830.855
112.000	.75694E -7	2.12712	280.46	.163367	6831.191
111.750	.78481E -7	2.12666	278.58	.169355	6831.516
111.500	.81299E -7	2.12628	277.00	.175412	6831.852
111.250	.84045E -7	2.12604	276.05	.181329	6832.176
111.000	.87490E -7	2.12536	273.24	.188711	6832.508

Table D4. The Hypersonic Sphere Results From XONICS Analysis Using The Lin
 $[T_W/T_\infty = 3]$ Drag Coefficient (Cont.)

ALTITUDE (KM)	DENSITY (KG/M**3)	DRAG COEFFICIENT	TEMPERATURE (DEG.K)	DRAG ACC. (M/SEC**2)	VELOCITY (M/SEC)
110.750	.91266E -7	2.12457	270.00	.196917	6832.876
110.500	.95258E -7	2.12377	266.74	.205385	6833.164
110.250	.99416E -7	2.12300	263.64	.214307	6833.468
110.000	.10384E -6	2.12221	260.47	.223794	6833.816
109.750	.10859E -6	2.12126	257.12	.233960	6834.145
109.500	.11361E -6	2.12072	253.82	.244666	6834.469
109.250	.11878E -6	2.11925	250.82	.255703	6834.789
109.000	.12404E -6	2.11839	248.23	.266936	6835.113
108.750	.12934E -6	2.11764	246.12	.278251	6835.430
108.500	.13468E -6	2.11696	244.43	.289643	6835.750
108.250	.14038E -6	2.11611	242.57	.301792	6836.065
108.000	.14639E -6	2.11525	240.69	.314630	6836.387
107.750	.15259E -6	2.11444	238.96	.327302	6836.707
107.500	.15882E -6	2.11376	237.66	.341222	6837.020
107.250	.16546E -6	2.11303	236.18	.355441	6837.332
107.000	.17256E -6	2.11226	234.56	.370562	6837.648
106.750	.18003E -6	2.11149	232.89	.386503	6837.961
106.500	.18795E -6	2.11069	231.14	.403399	6838.270
106.250	.19658E -6	2.10979	229.05	.421730	6838.578
106.000	.20596E -6	2.10882	226.67	.441694	6838.887
105.750	.21490E -6	2.10814	225.30	.463720	6839.184
105.500	.22356E -6	2.10756	224.66	.479176	6839.496
105.250	.23156E -6	2.10736	225.00	.495313	6839.797
105.000	.23831E -6	2.10749	226.75	.510857	6840.094
104.750	.24252E -6	2.10336	230.99	.520122	6840.395
104.500	.24541E -6	2.10960	236.47	.526662	6840.695
104.250	.25119E -6	2.11003	239.16	.539303	6840.997
104.000	.26468E -6	2.16846	235.06	.568276	6841.289
103.750	.29091E -6	2.10410	221.94	.624227	6841.578
103.500	.32406E -6	2.09690	206.83	.692489	6841.859
103.250	.34377E -6	2.09698	202.96	.733784	6842.141
103.000	.35613E -6	2.09635	202.90	.764195	6842.426
102.750	.37006E -6	2.09629	204.48	.789642	6842.699
102.500	.43130E -6	2.08840	183.26	.917992	6842.969
102.250	.47512E -6	2.08457	174.15	1.009053	6843.227
102.000	.50045E -6	2.08368	173.34	1.061915	6843.477
101.750	.50959E -6	2.08490	178.43	1.081770	6843.730
101.500	.51332E -6	2.08674	185.36	1.090706	6843.977
101.250	.52254E -6	2.08767	190.24	1.111131	6844.223
101.000	.53501E -6	2.08860	193.98	1.138024	6844.465
100.750	.54573E -6	2.08953	198.33	1.161536	6844.711
100.500	.56610E -6	2.08936	199.31	1.204943	6844.945
100.250	.59420E -6	2.08343	137.94	1.264242	6845.180
100.000	.63196E -6	2.08670	194.11	1.343432	6845.418
99.750	.67036E -6	2.08521	191.02	1.424454	6845.637
99.500	.68976E -6	2.08566	193.78	1.465769	6845.848
99.250	.70594E -6	2.08368	197.50	1.498963	6846.055
99.000	.72443E -6	2.07954	200.61	1.535273	6846.266
98.750	.75393E -6	2.07210	200.86	1.592463	6846.477
98.500	.79778E -6	2.06131	197.87	1.676760	6846.672

Table D4. The Hypersonic Sphere Results From XONICS Analysis Using The Lin
 $[T_W/T_\infty = 3]$ Drag Coefficient (Cont.)

ALTITUDE (KM)	DENSITY (KG/M**3)	DRAG COEFFICIENT	TEMPERATURE (DEG.K)	DRAG ACC. (M/SEC**2)	VELOCITY (M/SEC)
98.250	.85165E -6	2.04900	193.34	1.779382	6846.859
98.000	.90506E -6	2.03794	189.93	1.880190	6847.047
97.750	.94024E -6	2.03165	190.93	1.947142	6847.211
97.500	.96452E -6	2.02735	194.29	1.994091	6847.383
97.250	.10040E -5	2.02149	194.75	2.063906	6847.543
97.000	.10435E -5	2.01542	195.47	2.144196	6847.699
96.750	.10875E -5	2.00899	195.67	2.227646	6847.852
96.500	.11361E -5	2.00225	195.39	2.319597	6847.992
96.250	.11854E -5	1.99586	195.35	2.412596	6848.125
96.000	.12358E -5	1.98753	195.49	2.504811	6848.245
95.750	.12792E -5	1.97772	196.98	2.580008	6848.363
95.500	.13150E -5	1.96753	199.78	2.638645	6848.477
95.250	.13679E -5	1.95315	200.14	2.725159	6848.578
95.000	.14278E -5	1.93735	199.85	2.822063	6848.676
94.750	.14804E -5	1.92521	200.87	2.906317	6848.762
94.500	.15250E -5	1.91502	203.14	2.978557	6848.844
94.250	.15936E -5	1.90018	202.48	3.089096	6848.918
94.000	.16617E -5	1.88638	202.29	3.197540	6848.977
93.750	.17207E -5	1.87507	203.48	3.291090	6849.031
93.500	.17760E -5	1.86501	205.29	3.378592	6849.078
93.250	.18350E -5	1.85479	206.83	3.471843	6849.113
93.000	.19076E -5	1.84286	207.07	3.586443	6849.145
92.750	.20000E -5	1.82858	205.59	3.730900	6849.160
92.500	.20939E -5	1.81503	204.46	3.876800	6849.160
92.250	.21882E -5	1.80231	203.73	4.022726	6849.152
92.000	.22785E -5	1.79093	203.78	4.162231	6849.129
91.750	.23846E -5	1.77835	202.81	4.325770	6849.094
91.500	.24815E -5	1.76759	203.00	4.474150	6849.043
91.250	.25824E -5	1.75704	203.18	4.623457	6848.977
91.000	.27013E -5	1.74535	202.34	4.809625	6848.902
90.750	.28262E -5	1.73243	201.49	4.994431	6848.805
90.500	.29235E -5	1.72151	202.93	5.133080	6848.695
90.250	.29944E -5	1.71331	206.30	5.233848	6848.570
90.000	.31124E -5	1.70163	206.61	5.401874	6848.441
89.750	.32878E -5	1.68474	203.65	5.849318	6848.293
89.500	.35087E -5	1.66525	198.84	5.959415	6848.117
89.250	.37240E -5	1.64733	195.40	6.259240	6847.906
89.000	.39172E -5	1.63360	193.83	6.525945	6847.680
88.750	.41095E -5	1.62036	192.86	6.790186	6847.426
88.500	.43240E -5	1.60663	191.37	7.084033	6847.148
88.250	.45490E -5	1.59325	189.98	7.389697	6846.844
88.000	.47398E -5	1.58269	190.45	7.646329	6846.512
87.750	.48888E -5	1.57497	192.81	7.847093	6846.160
87.500	.50642E -5	1.56629	194.28	8.082836	6845.789
87.250	.52635E -5	1.55687	194.87	8.356213	6845.395
87.000	.54769E -5	1.54745	195.59	8.633980	6844.977
86.750	.56725E -5	1.53930	196.99	8.894239	6844.535
86.500	.58220E -5	1.53342	200.11	9.092138	6844.070
86.250	.60228E -5	1.52579	201.59	9.358603	6843.586
86.000	.62775E -5	1.51659	201.53	9.694906	6843.074

Table D4. The Hypersonic Sphere Results From XONICS Analysis Using The Lin
 $[T_w/T_\infty = 3]$ Drag Coefficient (Cont.)

ALTITUDE (KM)	DENSITY (KG/M**3)	DRAG COEFFICIENT	TEMPERATURE (DEG.K)	DRAG ACC. (M/SEC**2)	VELOCITY (M/SEC)
85.750	.65550E -5	1.50714	201.12	10.058795	6842.531
85.500	.68388E -5	1.49809	200.89	10.429211	6841.957
85.250	.71288E -5	1.48940	200.84	10.806156	6841.348
85.000	.74285E -5	1.48097	200.87	11.194180	6840.703
84.750	.77572E -5	1.47227	200.47	11.617399	6840.027
84.500	.81118E -5	1.46346	199.82	12.073290	6839.305
84.250	.84747E -5	1.45506	199.38	12.576354	6838.539
84.000	.88773E -5	1.44631	198.45	13.053594	6837.734
83.750	.92472E -5	1.43882	198.64	13.523273	6836.987
83.500	.96094E -5	1.43195	199.30	13.982242	6835.908
83.250	.99851E -5	1.42573	199.94	14.456758	6835.059
83.000	.10361E -4	1.41887	200.83	14.929549	6834.078
82.750	.10685E -4	1.41376	202.93	15.334043	6833.063
82.500	.10957E -4	1.40937	206.08	15.672358	6832.016
82.250	.11365E -4	1.40160	206.84	16.161377	6830.926
82.000	.11816E -4	1.39236	207.09	16.685745	6829.801
81.750	.12310E -4	1.38283	206.92	17.259505	6828.617
81.500	.12803E -4	1.37387	207.08	17.829285	6827.375
81.250	.13282E -4	1.36567	207.78	18.377945	6826.086
81.000	.13863E -4	1.35650	207.20	19.047562	6824.746
80.750	.14534E -4	1.34670	205.74	19.819214	6823.344
80.500	.15270E -4	1.33676	203.93	20.660373	6821.853
80.250	.16076E -4	1.32664	201.81	21.575409	6820.309
80.000	.16938E -4	1.31649	199.62	22.546402	6818.668
79.750	.17805E -4	1.30658	198.00	23.509911	6816.941
79.500	.18625E -4	1.29727	197.40	24.401276	6815.133
79.250	.19474E -4	1.28827	196.93	25.321715	6813.234
79.000	.20397E -4	1.27911	196.14	26.320663	6811.246
78.750	.21368E -4	1.27013	195.35	27.363770	6809.168
78.500	.22163E -4	1.26325	196.50	28.200359	6807.009
78.250	.23048E -4	1.25571	197.11	29.147395	6804.762
78.000	.24127E -4	1.24678	196.42	30.271989	6802.426
77.750	.25326E -4	1.23746	195.24	31.515856	6799.900
77.500	.26586E -4	1.22835	194.10	32.813614	6797.422
77.250	.27827E -4	1.21998	193.56	34.081116	6794.750
77.000	.28849E -4	1.21357	194.88	35.115875	6791.969
76.750	.29964E -4	1.20694	195.79	36.241135	6789.098
76.500	.31090E -4	1.20109	196.86	37.338397	6786.105
76.250	.32279E -4	1.19590	197.77	38.616486	6783.012
76.000	.33700E -4	1.19008	197.57	40.086533	6779.785
75.750	.35197E -4	1.18433	197.31	41.623596	6776.430
75.500	.36710E -4	1.17889	197.33	43.168411	6772.934
75.250	.38216E -4	1.17383	197.70	44.697006	6769.257
75.000	.39661E -4	1.16928	198.67	46.152786	6765.523
74.750	.41032E -4	1.16523	200.21	47.527573	6761.617
74.500	.42512E -4	1.16102	201.42	49.006210	6757.594
74.250	.44489E -4	1.15519	200.61	50.963333	6753.406
74.000	.46544E -4	1.14832	199.88	52.930756	6749.031
73.750	.48548E -4	1.14207	199.79	54.877372	6744.469
73.500	.50704E -4	1.13575	199.44	56.863358	6737.949

Table D4. The Hypersonic Sphere Results From XONICS Analysis Using The Lin
 $[T_W/T_\infty = 3]$ Drag Coefficient (Cont.)

ALTITUDE (KM)	DENSITY (KG/M**3)	DRAG COEFFICIENT	TEMPERATURE (DEG.K)	DRAG ACC. (M/SEC**2)	VELOCITY (M/SEC)
73.250	.52714E -4	1.13025	200.00	53.746292	6733.262
73.000	.54735E -4	1.12509	200.78	60.702057	6736.160
72.750	.56903E -4	1.11985	201.30	62.799850	6740.000
72.500	.59247E -4	1.11448	201.50	65.023633	6740.820
72.250	.61756E -4	1.10905	201.47	67.375122	6736.797
72.000	.64517E -4	1.10341	201.00	69.917816	6733.891
71.750	.67629E -4	1.09732	199.88	72.741929	6727.098
71.500	.70726E -4	1.09127	199.27	75.503693	6720.531
71.250	.73619E -4	1.08540	199.08	78.238708	6715.379
71.000	.76986E -4	1.07978	199.05	81.028961	6710.414
70.750	.80768E -4	1.07346	197.86	84.371231	6705.992
70.500	.84734E -4	1.06722	196.62	87.920532	6703.250
70.250	.88632E -4	1.06166	196.24	91.312495	6702.352
70.000	.92854E -4	1.05538	195.46	94.982893	6698.617
69.750	.96790E -4	1.05102	195.66	98.330322	6692.750
69.500	1.0018E -3	1.04707	197.24	101.139932	6685.844
69.250	1.0366E -3	1.04329	198.93	103.527902	6676.379
69.000	1.0769E -3	1.03892	199.55	107.197525	6662.059
68.750	1.1229E -3	1.03425	199.55	110.778336	6642.781
68.500	1.1641E -3	1.03034	200.67	113.872879	6622.082
68.250	1.1975E -3	1.02742	203.31	116.317429	6604.961
68.000	1.2323E -3	1.02444	205.78	118.935029	6592.660
67.750	1.2664E -3	1.02167	208.47	121.507767	6582.664
67.500	1.3112E -3	1.01806	209.54	124.398734	6574.094
67.250	1.3557E -3	1.01472	210.86	128.418686	6565.414
67.000	1.4043E -3	1.01120	211.77	132.106415	6554.766
66.750	1.4504E -3	1.00807	213.24	135.499054	6541.930
66.500	1.4921E -3	1.00540	215.50	138.440897	6526.883
66.250	1.5319E -3	1.00300	218.14	141.161636	6510.766
66.000	1.5744E -3	1.00053	220.49	144.093135	6495.655
65.750	1.6264E -3	.99756	221.64	147.835963	6483.559
65.500	1.6879E -3	.99417	221.76	152.316772	6472.414
65.250	1.7517E -3	.99083	221.38	156.581500	6459.650
65.000	1.8136E -3	.98780	222.51	161.160858	6444.105
64.750	1.8732E -3	.98506	223.65	165.135483	6426.172
64.500	1.9310E -3	.98252	225.09	169.950180	6407.512
64.250	1.9922E -3	.98032	226.48	172.861649	6389.176
64.000	2.0533E -3	.97763	227.37	176.770721	6371.434
63.750	2.1157E -3	.97529	229.47	180.739602	6354.055
63.500	2.1801E -3	.97300	230.92	184.733789	6337.195
63.250	2.2428E -3	.97090	232.70	188.677872	6320.609
63.000	2.3045E -3	.96895	234.71	192.443466	6304.074
62.750	2.3700E -3	.96694	236.46	196.400543	6287.434
62.500	2.4438E -3	.96474	237.54	200.875458	6270.734
62.250	2.5274E -3	.96256	237.90	206.033127	6252.684
62.000	2.6047E -3	.96084	239.07	210.577408	6231.430
61.750	2.6841E -3	.95916	240.23	215.061295	6207.238
61.500	2.7650E -3	.95754	241.44	219.473816	6180.870
61.250	2.8538E -3	.95580	242.15	224.326706	6153.547
61.000	2.9387E -3	.95427	243.39	228.789673	6126.617

Table D4. The Hypersonic Sphere Results From XONICS Analysis Using the Lin
 $[T_w/T_\infty = 3]$ Drag Coefficient (Cont.)

ALTITUDE (KM)	DENSITY (KG/M**3)	DRAG COEFFICIENT	TEMPERATURE (DEG.K)	DRAG ACC. (M/SEC**2)	VELOCITY (M/SEC)
60.750	.30324E -3	.95262	244.09	233.759781	6099.337
60.500	.31335E -3	.95090	244.44	239.124008	6072.066
60.250	.32315E -3	.94936	245.26	244.185043	6046.289
60.000	.33322E -3	.94786	246.08	249.371017	6021.918
59.750	.34353E -3	.94641	246.43	254.601868	5997.930
59.500	.35517E -3	.94478	247.06	260.543945	5972.566
59.250	.36721E -3	.94319	247.19	266.709473	5950.020
59.000	.37846E -3	.94186	248.08	272.242920	5928.453
58.750	.38869E -3	.94080	249.80	276.938232	5906.598
58.500	.39406E -3	.94070	254.74	278.217773	5883.102
58.250	.40820E -3	.93907	254.10	284.969238	5854.441
58.000	.42537E -3	.93708	252.03	293.274414	5824.363
57.750	.43835E -3	.93592	252.82	298.740723	5794.973
57.500	.44998E -3	.93504	254.53	303.204834	5766.160
57.250	.46376E -3	.93332	255.21	308.832031	5737.375
57.000	.47902E -3	.93268	255.32	315.075684	5707.219
56.750	.49572E -3	.93136	254.94	321.663086	5671.930
56.500	.51459E -3	.92939	253.31	329.057861	5632.965
56.250	.53426E -3	.92844	252.68	336.612793	5594.457
56.000	.55373E -3	.92715	252.01	343.795654	5557.344
55.750	.57086E -3	.92625	252.69	349.377930	5521.230
55.500	.58289E -3	.92599	255.77	351.949951	5487.324
55.250	.59764E -3	.92551	257.73	355.543457	5448.285
55.000	.61541E -3	.92477	258.54	360.379150	5406.789
54.750	.63110E -3	.92434	260.38	363.730225	5364.465
54.500	.64544E -3	.92410	262.87	366.164063	5322.750
54.250	.66346E -3	.92357	263.99	370.317871	5281.582
54.000	.68462E -3	.92281	264.08	375.734619	5239.855
53.750	.70349E -3	.92236	265.26	379.356689	5194.484
53.500	.72535E -3	.92177	265.52	383.995850	5147.051
53.250	.74923E -3	.92109	265.30	389.168213	5099.012
53.000	.77423E -3	.92047	264.97	394.369629	5049.777
52.750	.80016E -3	.92014	264.63	399.483154	4998.543
52.500	.82290E -3	.92025	265.58	402.676514	4946.746
52.250	.84802E -3	.92027	265.97	406.593018	4895.641
52.000	.88257E -3	.91979	263.78	414.259033	4844.918
51.750	.92080E -3	.91921	261.03	422.822754	4794.508
51.500	.95315E -3	.91914	260.41	428.041504	4742.434
51.250	.97990E -3	.91953	261.57	429.939941	4685.621
51.000	.10031E -2	.92020	263.82	429.901123	4628.488
50.750	.10293E -2	.92079	265.36	430.580078	4569.816